CREEP OF CIRCULAR PLATES SEALING AN INCOMPRESSIBLE FLUID

K.J. Chang and R.H. Lance

Department of Theoretical and Applied Mechanics

Cornell University
Ithaca, N.Y. 14853

ERDA Report No. COO-2733-09

April 1977

DISCLAIMER

ABSTRACT

Creep of a symmetrically loaded clamped circular plate sealing an incompressible fluid is analyzed using a new constitutive relation for inelastic deformation behavior of metals proposed by Hart and Li. The problems are solved numerically for several cases at different temperatures and loading conditions. The salient features of the theory are critically examined. It is concluded that the results obtained are qualitatively similar to the results of creep reported in the literature.

INTRODUCTION

The problem of creep in metallic structures has been the subject of many investigations in recent years. Since creep behavior is nonlinear and hereditary, in order to completely describe the creep deformation of metals it may be necessary to base analysis on a mechanical equation of state relating the variables of stress, strain, time, and temperature [1]. Therefore, great attention in recent literature has been devoted to the development of appropriate constitutive relations for representing time dependent inelastic behavior of metals.

Study of creep-bending of thin circular plates has been extensively treated by many investigators [2-12]. Most of these analyses use either strain hardening laws or time hardening laws. These so-called classical theories are, however, conceptually inadequate to represent some of the experimentally observed phenomena such as recovery since they fail to account for the effect of past history upon creep deformation [13].

Several investigators have proposed modifications to remedy the drawbacks of the classical creep theories. In particular, the state-variable approach proposed by Hart [14] has received much recent attention. In this theory it is shown that each deformation state of the material is a unique state of plastic hardness that can be characterized by a well defined state variable, the hardness σ^*. All states of hardness are shown to be related through an analytical scaling law. The stress-strain rate curves that are characteristic of each state of hardness are expressed in simple analytical terms, and the rate of change of σ^* with strain increments (absolute strain hardening) is also given in simple form [15]. Ellis, Wire and Li [16] have conducted uniaxial constant load creep tests at 250°C on 1100 Aluminum alloy specimens with different initial states.

They have reported that the theoretical results are in good agreement with the experimental data for each case investigated. Also, uniaxial tests to determine parameters for a wide class of metals have been carried out [16,17].

As explained above, Hart's theory has a strong experimental basis. Moreover, the constitutive equations are entirely incremental and have explicit mathematical forms. Therefore the theory was chosen for analysis of creep-bending of beams and plates by Wuang and Lance [18,19], and for analysis of creep in spherical shells and circular cylinders by Kumar and Mukherjee [20,21,22]. It should also be mentioned that Waung and Lance use simple Euler numerical methods, and Kumar and Mukherjee use a Runge-Kutta method of order four, for solving the rate equations with initial values in their analyses.

The problem of a loaded circular plate sealing an incompressible fluid has been treated by some investigators previously. Lance and Robinson [23], and Hodge and Sun [25] discussed the plastic analysis of axisymmetrically loaded circular plates sealing an incompressible fluid. Earlier work by Kerr [26] was concerned with the elastic behavior of plates similarly sealing an incompressible fluid. To the best of the authors' knowledge, creep analyses of similar plate problems have not appeared in literature.

In this paper, a state variable approach to the analysis of creep of an axisymmetric plate is first introduced according to Hart's state variable theory. As an analytical example, we consider the creep of a clamped axisymmetrically loaded thin circular plate sealing an incompressible fluid. In this analysis, the form of Hart's equations determined from uniaxial tests is extended directly to complex stress states. This

serves as a test of the theory and provides a basis for further investigations. It will be shown that solutions of creep-bending problems can be obtained through direct application of Hart's theory and that such solutions have the features of results of creep analyses previously published.

In the present analysis, a predictor-corrector method is utilized for solving numerically the rate equations with initial values by use of IBM 370/168. With this scheme the incremental time steps are controlled by measuring the relative error in the calculations, and we can be confident that the time interval chosen by the computer program for each step of the calculation is justifiable. As a special case, we apply the method directly to the problem of the creep of a regular clamped circular plate. This case is more common and not difficult to study experimentally.

For both cases, analysis have been made for 1100 Aluminum alloy at 22°C and 250°C; the parameters used in Hart's state variable theory have been determiend through experiments [17].

As in previous work [18-22] for creep under steady load, assuming the anelastic components of strain are negligible, the change of hardness σ^* is not significant during creep deformation. Furthermore the creep phenomenon described in terms of the variables such as moment rates, displacement rates, etc., depends strongly on the initial value of hardness. This implies that σ^* accounts for the past history of deformation of the material. If we take into consideration the anelastic components of strain the hardness σ^* should show significant change during creep deformation. This will be considered in a future investigation.

I. THE CONSTITUTIVE RELATIONS OF THE STATE VARIABLE THEORY

Following Hart [14,15], the total strain ε_{ij} at any time can be decomposed into three components:

$$\varepsilon_{ij} = e_{ij} + a_{ij} + P_{ij} \tag{1}$$

where e_{ij} is the elastic strain governed by the laws of classical elasticity; a_{ij} is the anelastic strain, a time dependent strain which is fully recoverable upon release of applied stress; and P_{ij}, deviatoric by definition, is the completely irrecoverable and path dependent permanent strain which includes the time dependent as well as the time independent plastic strains in the classical sense. The anelastic strain rate $\dot{a}_{ij}$, where $\dot{(\ )} = \frac{\partial}{\partial t}$,is appreciable for relatively short times following abrupt change of stress or strain rate, and has vital significance for cyclic loading; however it can be ignored for relatively steady stress cases. Therefore in the present analysis $\dot{a}_{ij}$ is assumed to be zero.

According to the state variable theory, the behavior of an isotropic polycrystalline material is governed by the general Hooke's law for the elastic part, together with the equation of state (2) and the kinetic law (3), and the flow rule used in incremental plasticity. Based on various experiments, Hart et al. [15] have proposed the equation of state and the kinetic law respectively as follows

$$\dot{p} = f(\sigma,\sigma^*T) = (\sigma^*/G)^m F \exp(-Z/RT)\phi(\sigma/\sigma^*) \tag{2}$$

$$\dot{\sigma}^* = g(\sigma,\sigma^*T) = \dot{p}\sigma^*\Gamma(\sigma,\sigma^*) \tag{3}$$

In the above equations, F is an arbitrary coefficient with the dimension of frequency; R is the gas constant; G is the isothermal modulus of

rigidity and is a function of temperature; m is a material constant with value between 3 and 8; Z is a measure of thermal activation energy and is a function of temperature alone; ϕ and Γ are measured functions of their arguments. The explicit form of ϕ and Γ are experimentally determined for each material at hand; those used in the present analysis will be presented later.

Also, in eq's. (2) and (3), σ is the effective stress; $\dot{p}$ is the irrecoverable effective strain rate, defined by Hart [15] as

$$\sigma = \left(\frac{3}{2} S_{ij} S_{ij}\right)^{1/2} , \text{ and} \tag{4}$$

$$\dot{p} = \left(\frac{2}{3} \dot{P}_{ij} \dot{P}_{ij}\right)^{1/2} \tag{5}$$

where

$$S_{ij} = \sigma_{ij} - \frac{1}{3} \sigma_{\ell\ell} \delta_{ij} \tag{6}$$

and $\dot{p}_{ij}$ is itself deviatoric by definition.

A complete description of the constitutive relations can be found in [15].

II. A METHOD OF SOLUTIONS TO THE PROBLEMS OF CREEP OF AXISYMETRIC PLATES

Consider an axisymmetric plate under lateral axisymmetric loading. We propose to determine its deflection as a function of position and time due to a suddenly imposed load which may subsequently vary with time. We shall also study other features of its mechanical response such as distributions of moments, curvatures, stresses and strains at various points as functions of time.

To simplify the problem, the formulation is developed for a thin circular plate under axisymmetric loading as shown in Fig. 1. Let the radius of the plate be 'a' and the thickness be 'h'. The assumptions adopted in the present analysis are:

(i) the deflections $w(r,t)$ are small in comparison with the thickness h of the plate,

(ii) linear elements perpendicular to the central plane before bending remain linear and perpendicular to the central surface after bending,

(iii) in-plane stress resultants or "membrane" forces are neglected,

(iv) the normal stresses in the direction transverse to the plate can be neglected,

(v) following the initial application of load the loading is steady or slowly varying,

(vi) in case there is an incompressible fluid sealed underneath the plate, the reaction of the fluid is assumed to be a constant pressure uniformly distributed throughout the region, i.e. a function of time only.

As creep is a time-dependent process and Hart's constitutive equations are entirely incremental, rate equations must be formulated. With the

assumption that the anelastic strain rate components $\dot{a}_{ij}$ can be ignored at relatively steady or slowly varying loading, equation (1) becomes

$$\dot{\varepsilon}_{ij} = \dot{e}_{ij} + \dot{p}_{ij} \tag{7}$$

In the case of an axisymmetric plate under axisymmetric loading, we use cylindrical coordinates as given in fig. 2, and have

$$\begin{aligned} \dot{\varepsilon}_r(z,r,t) &= \dot{e}_r(z,r,t) + \dot{p}_r(z,r,t) \\ \dot{\varepsilon}_\theta(z,r,t) &= \dot{e}_\theta(z,r,t) + \dot{p}_\theta(z,r,t) \end{aligned} \tag{8}$$

From assumption (ii), it follows that

$$\dot{\varepsilon}_r(z,r,t) = z\dot{K}_r(r,t) \quad , \quad \dot{\varepsilon}_\theta(z,r,t) = z\dot{K}_\theta(r,t) \tag{9}$$

where $\dot{K}_r$ and $\dot{K}_\theta$ are curvature rates of the plate defined by

$$\dot{K}_r(r,t) = -\frac{\partial \dot{V}(r,t)}{\partial r} \quad , \quad \dot{K}_\theta(r,t) = -\frac{\dot{V}(r,t)}{r} \quad , r\varepsilon[0,a], \; t\varepsilon[0,\infty) \tag{10}$$

$\dot{V}$ is the deflection slope rate, i.e.

$$\dot{V}(r,t) = \frac{\partial \dot{w}(r,t)}{\partial r} \quad , \quad r\varepsilon[0,a] \; , \; t\varepsilon[0,\infty) \tag{11}$$

and $\dot{w}$ is the deflection rate.

We shall first formulate the problem of a plate sealing an incompressible fluid, the more general of the two problems considered here; we shall later extract from it, by a simple operation, the problem of a plate without fluid.

We denote the intensity rate of the distributed lateral load at a distance r from the center of the plate as $\dot{q}(r,t)$, the intensity rate of reaction of the fluid against the plate as $\dot{q}^*(t)$, the shearing force rate per unit length as $\dot{Q}(r,t)$, and the bending moment rates per unit length as $\dot{M}_r(r,t)$ and $\dot{M}_\theta(r,t)$. The equilibrium equations and the incompressiblity condition take the following form [23,24]

$$\frac{\partial \dot{M}_r(r,t)}{\partial r} + \frac{\dot{M}_r(r,t)-\dot{M}_\theta(r,t)}{r} + \dot{Q}(r,t) = 0 \ , \ r\varepsilon[0,a], \ t\varepsilon[0,\infty) \tag{12}$$

and

$$\int_0^a \dot{w}(r,t)rdr = 0 \quad , \quad t\varepsilon[0,\infty) \tag{13}$$

where

$$Q(r,t) = \int_0^r 2\pi[\dot{q}(\xi,t)-\dot{q}^*(t)]\xi d\xi/(2\pi r) \ , \tag{14}$$

$$\dot{M}_r(r,t) = \int_{-h/2}^{h/2} \dot{\sigma}_r(z,r,t)zdz \ ,$$

$$\dot{M}_\theta(r,t) = \int_{-h/2}^{h/2} \dot{\sigma}_\theta(z,r,t)zdz \ . \tag{15}$$

In accordance with assumption (iv)

$$\dot{\sigma}_z(z,r,t) = 0 \tag{16}$$

The constitutive relations include the generalized Hooke's law,

$$\dot{e}_{ij} = (\dot{\sigma}_{ij} - \frac{\nu}{1+\nu}\dot{\sigma}_{\ell\ell}\delta_{ij})/2G \tag{17}$$

where ν is the Poisson's ratio, and G the shear modulus; the kinetic equation by Hart given previously in eqs. (2) and (3), can be rewritten as

$$\dot{p} = f(\sigma,\sigma^*,T) \ , \quad \text{and} \tag{18}$$

$$\dot{\sigma}^* = g(\sigma,\sigma^*,T) \ ; \tag{19}$$

The flow rule used in the incremental plasticity, takes the following form

$$\dot{p}_{ij} = \frac{3}{2}(\frac{\dot{p}}{\sigma})S_{ij} \tag{20}$$

In the present case, eq's. (17), (20) are reduced to

$$\dot{e}_r = (\dot{\sigma}_r - \nu\dot{\sigma}_\theta)/E \quad , \quad \dot{e}_\theta = (\dot{\sigma}_\theta - \nu\dot{\sigma}_r)/E \ , \tag{21}$$

$$\dot{p}_r = (\frac{\dot{p}}{\sigma})(\sigma_r - \sigma_\theta/2) \quad , \quad \dot{p}_\theta = (\frac{\dot{p}}{\sigma})(\sigma_\theta - \sigma_r/2) \ , \tag{22}$$

in which σ, from eq's (4) and (6), becomes

$$\sigma = (\sigma_r^2 + \sigma_\theta^2 - \sigma_r\sigma_\theta)^{1/2} \ , \tag{23}$$

Here $E = 2G(1+\nu)$ is the Young's Modulus of the material.

To achieve the aim of obtaining a complete set of evolution equations, we first group eqs. (8), (9) and (21), and get

$$\dot{\sigma}_r = \frac{zE}{1-\nu^2}\left[(\dot{K}_r+\nu\dot{K}_\theta) - (\dot{p}_r+\nu\dot{p}_\theta)\right]$$

$$\dot{\sigma}_\theta = \frac{zE}{1-\nu^2}\left[(\dot{K}_\theta+\nu\dot{K}_r) - (\dot{p}_\theta+\dot{p}_r)\right] \tag{24}$$

substituting eq. (24) into eq. (15) and integrating we obtain

$$\dot{M}_r = D(\dot{K}_r+\nu\dot{K}_\theta) - \Delta\dot{M}_r \quad ,$$

$$\dot{M}_\theta = D(\dot{K}_\theta+\nu\dot{K}_r) - \Delta\dot{M}_\theta \tag{25}$$

where

$$\Delta\dot{M}_r = \frac{E}{1-\nu}\int_{-h/2}^{h/2}(\dot{p}_r+\nu\dot{p}_\theta)z\,dz$$

$$\Delta\dot{M}_\theta = \frac{E}{1-\nu}\int_{-h/2}^{h/2}(\dot{p}_\theta+\nu\dot{p}_r)z\,dz \tag{26}$$

and

$$D = \frac{Eh^3}{12(1-\nu^2)} \tag{27}$$

The rate governing equation is then obtained by substituting eqs. (10), (25) and (26) into the equilibrium equation (12), which reduces to

$$D\frac{\partial}{\partial r}\left\{\frac{1}{r}\frac{\partial}{\partial r}\left[r\dot{V}(r,t)\right]\right\} = \dot{Q}(r,t) - \left[\frac{\partial\Delta\dot{M}_r(r,t)}{\partial r} + \frac{\Delta\dot{M}_r(r,t)-\Delta\dot{M}_\theta(r,t)}{r}\right] \tag{28}$$

Equation (28) together with eq's (12), (13) and the appropriate boundary conditions, form a well defined initial value problem for the creep of an axisymmetric plate.

The initial conditions are the solutions of the corresponding elastic plate problem, which is defined below in terms of the well-defined boundary value problem

$$\frac{d}{dr}\left\{\frac{1}{r}\frac{d}{dr}[rV(r,0)]\right\} = \frac{Q(r,0)}{D} \qquad r\varepsilon[0,a] \tag{29}$$

$$\int_0^a w(r,0)\, r dr = 0 \tag{30}$$

where

$$Q(r,0) = \int_0^r 2\pi[q(\xi,0)-q^*(0)]\xi d\xi/(2\pi r), \tag{31}$$

and

$$\frac{dw(r,0)}{dr} = V(r,0) \qquad r\varepsilon[0,a] \tag{32}$$

together with appropriate boundary conditions. Note that the plastic strain components p_r and p_θ are zero in the initial elastic state.

The reduction of the former formulation to the case in which no fluid is sealed underneath the plate is achieved by simply putting $q^*(t) \equiv 0$, $t\varepsilon[0,\infty)$ in eq's. (14) and (31) and ignoring eq's. (13) and (30).

The following formulas are used for obtaining $K_r(r,t)$, $K_\theta(r,t)$, $\varepsilon_r(z,r,t)$, $\varepsilon_\theta(z,r,t)$, $\sigma_r(z,r,t)$, $\sigma_\theta(z,r,t)$, $M_r(r,t)$ and $M_\theta(r,t)$ after $V(r,t)$ is determined. The same equations are true for the time rate of change of all the appropriate variables.

$$K_r = -\frac{\partial V}{\partial r} \quad , \quad K_\theta = \frac{-V}{r} \tag{33}$$

$$\varepsilon_r = zK_r \quad , \quad \varepsilon_\theta = zK_\theta \tag{34}$$

$$\sigma_r = \frac{E}{1-\nu^2}\left[z(K_r+\nu K_\theta) - (p_r+\nu p_\theta)\right]$$

$$\sigma_\theta = \frac{E}{1-\nu^2}\left[z(K_\theta+\nu K_r) - (p_\theta+\nu p_r)\right] \tag{35}$$

$$M_r = D(K_r+\nu K_\theta) - \Delta M_r$$

$$M_\theta = D(K_\theta+\nu K_r) - \Delta M_\theta \tag{36}$$

where

$$\Delta M_r = \frac{E}{1-\nu^2}\int_{-h/2}^{h/2}(p_r+\nu p_\theta)\,z\,dz \ ,$$

$$\Delta M_\theta = \frac{E}{1-\nu^2}\int_{-h/2}^{h/2}(p_\theta+\nu p_r)\,z\,dz \tag{37}$$

The initial hardness $\sigma^*(z,r,0)$ in actual analysis must be determined experimentally; we shall here assume initial values for σ^* in order to conduct the proposed analysis.

The numerical scheme is summarized as follows

i) solve the corresponding elastic plate problem defined previously by eq's. (29), (30), (31), (32) and determine the expressions in closed form for $V(r,0)$, $w(r,0)$, $q^*(0)$, $K_r(r,0)$, $K_\theta(r,0)$, $\varepsilon_r(z,r,0)$, $\varepsilon_\theta(z,r,0)$, $\sigma_r(z,r,0)$ and $\sigma_\theta(z,r,0)$; these data are then used as the initial conditions for the creep problem, i.e. as solutions at

time $t = 0$; initial values of the plastic strain components $p_r(z,r,0)$ and $p_\theta(z,r,0)$ are zero throughout, and the initial values of the hardness $\sigma^*(z,r,0)$ must be provided in this step,

ii) substitute $\sigma_r(z,r,t)$ and $\sigma_\theta(z,r,t)$ into eq. (23) to obtain the effective stress $\sigma(z,r,t)$ which, together with $\sigma^*(z,r,t)$, give $\dot{p}(z,r,t)$ and $\dot{\sigma}^*(z,r,t)$ by use of Hart's kinetic equations (18) and (19),

iii) $\dot{p}_r(z,r,t)$ and $\dot{p}_\theta(z,r,t)$ are deduced from eq. (22), from which we obtain $\Delta\dot{M}_r(r,t)$ and $\Delta\dot{M}_\theta(r,t)$ by eq's (26). The spatial integrals involved here and in the following steps are carried out numerically using Simpson's rule,

iv) with $\Delta\dot{M}_r(r,t)$ and $\Delta\dot{M}_\theta(r,t)$, the rate equation (28) together with the condition of sealing incompressible fluid (13) and the appropriate boundary conditions, are then solved numerically to determine $\dot{V}(r,t)$, $\dot{w}(r,t)$ and $\dot{q}^*(t)$; with help of eqs. (10) the curvature rates $\dot{K}_r(r,t)$ and $\dot{K}_\theta(r,t)$ are also obtained,

v) forward integration in time for w, V, K_r, K_θ, σ^*, p_r, p_θ is achieved by use of a predictor-corrector method with an error control on the displacement vector that adjusts and determines the step size Δt for further integration; up to this step, values of w, V, K_r, K_θ, σ^*, p_r and p_θ at time $t + \Delta t$ are obtained,

vi) with new values of w, V, K_r, K_θ, p_r and p_θ at time $t + \Delta t$, the corresponding values of ΔM_r, ΔM_θ, ε_r, ε_θ, σ_r, σ_θ, M_r and M_θ are then obtained using eqs. (33) to (37),

vii) with new values of $\sigma_r(z,r,t)$, $\sigma_\theta(z,r,t)$ and $\sigma^*(z,r,t)$ steps (ii) through (vi) are repeated.

The above mentioned integration in time utilizes a self-starting predictor-corrector method which proceeds as follows. Predicted values of σ^*, V, w, q^*, K_r and K_θ are obtained by means of the expression

$$\tilde{u}_{n+1} = u_n + \dot{u}_n \Delta t \tag{38}$$

where u represents the variable under consideration. From these new values of K_r and K_θ we obtain predicted values of σ_r and σ_θ, using eqs. (35). These predicted values are then used in steps (ii), (iii) and (iv) to obtain $\dot{\tilde{V}}_{n+1}$, $\dot{\tilde{w}}_{n+1}$, $\dot{\tilde{q}}_{n+1}$, $\dot{\tilde{K}}_{r_{n+1}}$ and $\dot{\tilde{K}}_{\theta_{n+1}}$. Before proceeding to determine the values of all these quantities at a new time, the process of error control is carried out by calculating first

$$w_{c\ n+1} = w_n + \frac{1}{2}\left[\dot{w}_n + \dot{\tilde{w}}_{n+1}\right]\Delta t \tag{39}$$

Then a check is conducted to determine if the following expression is satisfied

$$e_{min} \leq \left| \left| w_{c_{n+1}} \right| - \left| \tilde{w}_{n+1} \right| \right| \leq e_{max} \tag{40}$$

where e_{min} and e_{max} are given small values; and

$$|w| = \sum_{i=1}^{N} |w_i| \tag{41}$$

where N is the number of radial modes. When eq. (40) is satisfied, values of V, w, q^*, K_r and K_θ at time $t + \Delta t$ are readily obtained by

$$u_{n+1} = u_n + \frac{1}{2}(\dot{u}_n + \tilde{\dot{u}}_{n+1})\Delta t \tag{42}$$

Otherwise an adjusted value of Δt is given and the process restarts from step (ii) until eq. (40) is satisfied. With this scheme, we are sure that the integration step size of time we used at each step of calculation are reasonable and justifiable.

III. ANALYSIS OF A CLAMPED CIRCULAR ALUMINUM PLATE UNDER AXISYMMETRIC LATERAL LOAD

As an example of explicit calculation of the creep problem described above, consider a clamped circular plate under constant uniform axisymmetric lateral load, fig. (1), of the type

$$q(r,t) = \begin{cases} q_o & r\varepsilon[0,\eta a] \\ & t\varepsilon[0,\infty) \\ 0 & r\varepsilon[\eta a, a] \end{cases} \quad , \qquad (43)$$

where q_o and η (≤ 1) are positive constants.

For 1100 Aluminum alloy, eq's. (18) and (19) assume the special forms

$$\dot{p} = (\sigma^*/D_1)^m [\ell n(\sigma^*/\sigma)]^{-1/\lambda}$$

$$\dot{\sigma}^* = \dot{p}\Lambda\sigma^\delta/(\sigma^*)^{\beta-1} \qquad (44\ a,b)$$

where $m = 5$, $\lambda = 0.11$, $\delta = 7.82$, $\beta = 12.5$ and $\Lambda = 1.17 \times 10^{20}$ for both 22°C and 250°C [23]; D_1, the only strongly temperature dependent parameter has the value $10^{7.025}$ at 22°C and $10^{5.03}$ at 250°C. It should be noted that the terms f and $\exp(-Z/RT)$ in eq. (2) do not appear in the above equations since they are absorbed in D_1. Furthermore, the Young's modulus E and the Poisson's ratio ν for this material are [24]:

At 22°C $\quad E = 9.975 \times 10^6$ psi , $\quad \nu = 0.33$.

At 250°C $\quad E = 8.784 \times 10^6$ psi , $\quad \nu = 0.358$.

In the following analysis, referring to fig's (1) and (2), all quantities involved in the calclations are made dimensionless by introducing

the following quantities, noting that σ_r is a function of "z", "y" and "t".

$$\sigma_o = \sigma_r(\frac{h}{2},0,0) \quad , \quad \varepsilon_o = \frac{\sigma_o}{E}(1-\nu) \quad ,$$

$$Q_o = \frac{64D}{a^3} \quad , \quad K_o = \frac{2(1-\nu)}{Eh}\sigma_o \quad , \quad M_o = DK_o \tag{45}$$

$$t_o = (\frac{\sigma_o^*}{D_1})^{-m} \varepsilon_o [\ell n(\frac{\sigma_o^*}{\sigma_o})]^{-1/\lambda} \frac{1}{3600}$$

where σ_o^* is a constant representing the initial reference hardness; t_o has unit of hours. We then define the following dimensionless quantities:

$$\bar{\sigma}_r = \sigma_r/\sigma_o \quad , \quad \bar{\sigma}_\theta = \sigma_\theta/\sigma_o \quad , \quad \bar{\sigma}^* = \sigma^*/\sigma_o \quad , \quad \bar{\sigma}_o^* = \sigma_o^*/\sigma_o \quad ,$$

$$\bar{q} = q_o/Q_o \quad , \quad \bar{q}^* = q^*/Q_o \quad , \quad \bar{\varepsilon}_r = \varepsilon_r/\varepsilon_o \quad , \quad \bar{\varepsilon}_\theta = \varepsilon_\theta/\varepsilon_o \quad ,$$

$$\bar{p}_r = p_r/\varepsilon_o \quad , \quad \bar{p}_\theta = p_\theta/\varepsilon_o \quad , \quad \bar{\Lambda} = \Lambda\varepsilon_o\sigma_o^{\delta-\beta} \quad ,$$

$$\bar{K}_r = K_r/K_o \quad , \quad \bar{K}_\theta = K_\theta/K_o \quad , \quad \bar{V} = V \quad , \tag{46}$$

$$\bar{M}_r = M_r/M_o \quad , \quad \bar{M}_\theta = M_\theta/M_o \quad , \quad \Delta\bar{M}_r = \Delta M_r/M_o \quad , \quad \Delta M_\theta = \Delta M_\theta/M_o \quad ,$$

$$\bar{z} = z/h \quad , \quad \bar{r} = r/a \quad , \quad \bar{\xi} = \xi/a \quad ,$$

$$\bar{t} = t/t_o \quad ,$$

and

$$(\ )' = \frac{\partial(\ )}{\partial \bar{t}} \quad .$$

Henceforth, for simplicity, overbars will no longer be used to denote dimensionless quantities, except where emphasis is necessary.

First , the general relations become

$$\varepsilon_r = e_r + p_r = 2zK_r \quad , \quad \varepsilon_\theta = e_\theta + p_\theta = 2zK_\theta \, , \tag{47}$$

$$K_r = \frac{-1}{aK_o}\frac{\partial V}{\partial r} \quad , \quad K_\theta = \frac{-1}{aK_o}\frac{V}{r} \tag{48}$$

$$\begin{aligned} \sigma_r &= \frac{1}{1+\nu}[2z(K_r+\nu K_\theta) - (p_r+\nu p_\theta)] \\ \sigma_\theta &= \frac{1}{1+\nu}[2z(K_\theta+\nu K_r) - (p_\theta+\nu p_r)] \end{aligned} \tag{49}$$

$$\begin{aligned} M_r &= K_r+\nu K_\theta - \Delta M_r \\ M_\theta &= K_\theta+\nu K_r - \Delta M_\theta \end{aligned} \tag{50}$$

$$\begin{aligned} \Delta M_r &= 6\int_{-1/2}^{1/2} (p_r+\nu p_\theta)z\,dz \\ \Delta M_\theta &= 6\int_{-1/2}^{1/2} (p_\theta+\nu p_r)z\,dz \quad , \end{aligned} \tag{51}$$

The rate forms of these equations also hold true and can be obtained by applying $(\ )'$ to each of them.

Second , the initial conditions of the present problem are obtained by solving the following boundary value problem

$$\frac{d}{dr}\left[\frac{1}{r}\frac{d}{dr}\{rV(r,0)\}\right] = \begin{cases} 32(q-q_o^*)r & r\varepsilon[0,\eta] \\ -32q_o^* r+32\eta^2 q\frac{1}{r} & r\varepsilon[\eta,1] \end{cases} \tag{52}$$

with B.C.

$$V(0,0) = V(1,0) = 0 \quad ,$$

with C.C.

$$V(\eta^-,0) = V(\eta^+,0) \quad ,$$

q_o^* represents the reaction pressure of the fluid against the plate at $t = o$, which is obtained through the condition of incompressibility

$$\int_o^1 w(r,0)rdr = 0 \tag{53}$$

and the auxiliary boundary value problem

$$\frac{dw(r,0)}{dr} = V(r,0) \qquad r\varepsilon[0,1] \tag{54}$$

with B.C.

$$w(1,0) = 0 \quad .$$

Furthermore, other quantities such as $K_r(r,0)$, $K_\theta(r,0)$, $\varepsilon_r(z,r,0)$, $\varepsilon_\theta(z,r,0)$, $\sigma_r(z,r,0)$, $\sigma_\theta(z,r,0)$, $M_r(r,0)$ and $M_\theta(r,0)$ are obtained through equations (47) to (51) providing that $p_r(z,r,0) = p_\theta(z,r,0) = 0$.

Third, the incremental initial value problem is completed by solving the rate equations which can be written as

$$\frac{\partial}{\partial r}\left[\frac{1}{r}\frac{\partial}{\partial r}\{rV'(r,t)\}\right] = -32q'^*(t)r-2\left(\frac{a}{h}\right)\varepsilon_o\left[\frac{\partial\Delta M_r'(r,t)}{\partial r}+\frac{\Delta M_r'(r,t)-\Delta M_\theta'(r,t)}{r}\right] \tag{55}$$

$$r\varepsilon[0,1] \quad , \quad t\varepsilon[0,\infty)$$

with B.C.

$$V'(0,t) = V'(1,t) = 0$$

in which

$$\Delta M_r'(r,t) = 6 \int_{-1/2}^{1/2} [p_r'(z,r,t) + \nu p_\theta'(z,r,t)]z\,dz \quad ,$$

$$\Delta M_\theta'(r,t) = 6 \int_{-1/2}^{1/2} [p_\theta'(z,r,t) + \nu p_r'(z,r,t)]z\,dz \qquad (56)$$

together with the condition of incompressibility

$$\int_0^1 w'(r,t)r\,dr = 0 \qquad (57)$$

and the auxiliary boundary value problem

$$\frac{dw'(r,t)}{dr} = V'(r,t) \qquad r\varepsilon[0,1], \quad t\varepsilon[0,\infty) \qquad (58)$$

with B.C.

$$w'(1,t) = 0 \quad .$$

After obtaining $V'(r,t)$, $K_r'(r,t)$ and $K_\theta'(r,t)$ are then determined through the rate forms of eq's. (48).

In addition, the equation of state, the kinetic law, and the flow rule become

$$\begin{aligned} p'(z,r,t) &= (\sigma^*/\sigma_o^*)^m [\ell n(\sigma^*/\sigma)/\ell n\sigma_o^*]^{-1/\lambda} \\ \sigma'^*(z,r,t) &= p'A\sigma^\delta/\sigma^{*\beta-1} \\ p_r'(z,r,t) &= \frac{p'}{\sigma}(\sigma_r - \sigma_\theta/2) \\ p_\theta'(z,r,t) &= \frac{p'}{\sigma}(\sigma_\theta - \sigma_r/2) \end{aligned} \qquad (59)$$

in which

$$\sigma(z,r,t) = (\sigma_r^2+\sigma_\theta^2-\sigma_r\sigma_\theta)^{1/2} \tag{60}$$

Solutions of the elastic plate problem defined in eq's (52), (53) and (54) are obtained in closed form as follows

$$V(r,0) = \begin{cases} 4q_o^*(r-r^3)+4q[(4\eta^2\ell n\eta-\eta^4)+r^3] & r\varepsilon[0,\eta] \\ 4q_o^*(r-r^3)+4q[\eta^4(\frac{1}{r}-r)+4\eta^2 r\ell nr] & r\varepsilon[\eta,1] \end{cases} \tag{61}$$

$$\omega(r,0) = \begin{cases} q_o^*(-1+2r^2-r^4)+q[4\eta^4\ell n\eta-3\eta^4+4\eta^2)+(8\eta^2\ell n\eta-2\eta^4)r^2+r^4] & r\varepsilon[0,\eta] \\ q_o^*(-1+2r^2-r^4)+q[(2\eta^4+4\eta^2)(1-r^2)+4\eta^4\ell nr+8\eta^2r^2\ell nr] & , r\varepsilon[\eta,1] \end{cases}$$

$$q_o^* = q(\eta^6-3\eta^4+3\eta^2) \quad .$$

Furthermore, from eq's (47) to (51), keeping $p_r(z,r,0) = p_\theta(z,r,0) = 0$, other quantities such as $K_r(r,0)$, $K_\theta(r,0)$, $\varepsilon_r(z,r,0)$, $\varepsilon_\theta(z,r,0)$, $\sigma_r(z,r,0)$, $\sigma_\theta(z,r,0)$, $M_r(r,0)$ and $M_\theta(r,0)$ are obtained in closed form.

To solve the rate expressions, first calculate $p'(z,r,t)$, $p_r'(z,r,t)$, $p_\theta'(z,r,t)$ and $\sigma^{*}{}'(z,r,t)$ with values of $\sigma_r(z,r,t)$, $\sigma_\theta(z,r,t)$ and $\sigma^*(z,r,t)$ obtained from eqs. (59); next obtain $\Delta M_r'(r,t)$ and $\Delta M_\theta'(r,t)$ from eqs. (46). Then eqs. (55), (57) and (58) can be solved directly in the form of definite integrals as follows

$$V'(r,t) = 4q^{*}{}'(t)(r-r^3)+2\varepsilon_o(\frac{a}{h})[r\{I_1(1,t)+I_2(1,t)\} - \frac{1}{r}\{I_1(r,t)+I_2(r,t)\}]$$

$$W'(r,t) = q^{*}{}'(t)(-1+2r^2-r^4)+\varepsilon_o(\frac{a}{h})[(r^2-1)\{I_1(1,t)+I_2(1,t)\}$$

$$+2\{II_1(1,t)+II_2(1,t)-II_1(r,t)-II_2(r,t)\}]$$

$$q^{*}{}'(t) = 3\varepsilon_o(\frac{a}{h})[-\frac{1}{2}\{I_1(1,t)+I_2(1,t)\}+2\{II_1(1,t)+II_2(1,t)\}-4\{III_1(t)+III_2(t)\}] \qquad (62)$$

where

$$I_1(r,t) = \int_o^r \rho\Delta M_r'(\rho,t)d\rho$$

$$I_2(r,t) = \int_o^r \xi \int_o^\xi \frac{\Delta M_r'(\rho,t)-\Delta M_\theta'(\rho,t)}{\rho} d\rho d\xi$$

$$II_1(r,t) = \int_o^r \frac{1}{\rho} I_1(\rho,t)d\rho$$

$$II_2(r,t) = \int_o^r \frac{1}{\rho} I_2(\rho,t)d\rho$$

$$III_1(t) = \int_o^1 rII_1(r,t)dr \quad , \quad III_2(t) = \int_o^1 rII_2(r,t)dr \ .$$

Finally eq's. (48) gives $K_r'(r,t)$ and $K_\theta'(r,t)$ after $V'(r,t)$ is obtained. Thus all the rate quantities necessary in the analysis are obtained.

As described above solutions are obtained from simple expressions involving only integrals which can be easily integrated numerically. Application of the scheme to the above analysis leads to the numerical results which will be presented in the next sections. It should be noted that the formulas given above are based on the problem of creep of a clamped axisymmetrically loaded circular plate sealing incompressible fluid; solutions of the creep problem of a similar plate without fluid can be obtained directly by setting $q^*(t)$ and $q^{*\prime}(t)$ to zero throughout the calculations. Furthermore, η of eq. (43) appears as a parameter in our analysis, change of values of η in the calculations directly leads to the numerical solution of the appropriate creep problem with different loading range.

Numerical results and discussion of the present problem are presented for several cases in the following sections.

IV. NUMERICAL RESULTS AND DISCUSSION

Based on the above analysis we have performed detailed calculations for five problems of plates under loading, with different initial hardness and temperature conditions, as tabulated in Table 1. Note that throughout this section, an overbar is used to indicate dimensionless quantities. The results of the calculations are collected in Appendices I - V. It is not our intention to discuss in detail all the results given there; rather we shall focus first on the general features of the mechanical response of the plates studied and then on some special features which may be of interest to designers. Note that in Table 1, as well as in all appendices, we use the symbols WF, meaning a plate "with fluid," and NF, meaning "no fluid," referring to the conditions defining the general problem. Table 1 also lists the material constants chosen for our analysis. Note in particular, the initial hardness is assumed uniform in all cases, two values being chosen. The higher value, $\sigma^* = 10{,}617$ psi, corresponds to 10% cold work [16].

As noted above to start the calculations it was necessary to construct elastic solutions on which we based the definition of the dimensionless variables defined in the previous sections. Reference values of the constants derived from the elastic solution are given in Table 2. Because we have based the formulation of the problem and all calculations on dimensionless variables, the results may be applied to plates of any physical dimension, within the customary limits of bending theory. Nevertheless to proceed with the calculations it was necessary to choose a reference plate to establish the values shown on Table 2. Subsequently, all calculations are based on a plate with the following physical dimensions: radius $a = 16"$ and thickness $h = 1"$.

All calculations were started by fixing the value of σ_o (see Table 2), i.e., the value of the tensile stress in the outer fiber at the center of the plate, from which the load and the pertinent constants can be determined. This means that, from eq's. (35) and (36), for any loading condition the same central curvature and moment are obtained. Thus we have the same starting condition for each case: three plates at 250°C; and two plates at 22°C.

As described above, forward integration in time was carried out by a self-starting predictor-corrector scheme with error control on the displacement vector. The trapezoidal rule has been used to evaluate the spatial integrals appearing in the relevant equations, in which the radius a and the thickness h were divided into 50 and 32 equal segments, respectively, to form the integrating mesh. The computations were carried out on an IBM 370/168 digital computer.

All curves were produced on the automatic curve drawing facility associated with the computer. A general attempt was made to produce identical-looking curves, sacrificing therefore identical scales.

Table 3 gives a correlation between the symbols representing the variables introduced in the problem formulation and the names of the same variables used in the computer program, and hence in the computer-generated curves.

As shown in figs. 1, 2, 3, and 8 of each appendix, the magnitudes of the time-rates-of-change of the displacements, the curvatures and the reaction pressure decrease following application of the load and tend to approach asymptotically constant values as time increases. Thus, our model contains the usual features of classical creep models, namely the primary and secondary creep regimes.

Figure 5a of each appendix shows the stress profiles across the thickness of the corresponding plate at the center and clamped edges. We note that at the center of the plate, the radial and the circumferential stress components remain equal for all times implied by equilibrium and symmetry. Also, stresses at the outer fibers decrease with time, while those near the middle fiber ($z = 0$) increase. Stresses tend to approach constant values as shown in figs. 6b and 6d of each appendix. This observation has two implications. The stress redistribution across the thickness does not exhibit the invariant stress point, defined by Marriott and Leckie [28] as the skeletal point. On the other hand, since the stress field tends to a constant distribution, the implication is that the plate reaches the stationary state as defined by Penny and Marriot [10].

Figures 7b and 7d of each appendix show the time dependence of the plastic strain components. It is noted that each curve approaches asymptotically a straight line. This implies that the plastic strain rate fields achieve a stationary state along with the stress fields.

It is interesting to note that, as shown in fig. 1 of each appendix, the points at which the elastic displacements are zero, (in particular in the WF plates at $\frac{r}{a} \cong 0.48$) remain undisplaced during creep. It is also noted that during creep deformation the moment components do not change significantly with time, whereas other variables such as the plastic strains, the curvatures, the stresses and the displacements change considerably with time.

The above mentioned general features of the present analysis are true for all cases considered in our calculations. The general features that we have discussed are those that have been considered in other analyses of

similar problems. Similar conclusions have been reached by Kumar and Mukherjee [20, 21, 22], and Waung and Lance [18, 19] applying the same state variable approach to creep of other types of structures.

Figure 3 shows the effect of initial hardness on displacement and stress at the center of the plate, in the clamped plate sealing a fluid (WF). The plate was assumed to be at 250°C and initially loaded (t = 0) so that the maximum normal stress at the center was 1000 psi. One important result to note in fig. 3a is the trend we have denoted the "cross-over effect", i.e., for a fixed time, say t = 30 hours, the displacement in the plate with high hardness (σ^* = 10,617 which is equivalent to 10% cold work [17]) is greater than that for a plate with low hardness (say σ^* = 2,000 psi). This remarkable result, which is contrary to results expected initially, indicates that the general mechanical behavior of the structure depends not only on hardness, but the stress level and the geometric constraints, for example. The cross-over effect in analysis of structures based on Hart's relation was first noticed by Kumar and Mukherjee [22] and is consistant with the predictions of Hart [15] in his studies of uniaxial tests. The work of Waung and Lance [19] did not show this effect because too few numerical examples were presented. The curves in fig. 3b, showing the values of radial stress ($\sigma_r = \sigma_\theta$) at the outer fibers of the plate center, exbibit a similar cross-over effect.

Another significant feature of the displacement results (fig. 3a) is the intersection of pairs of curves at small time. Note, in particular, that the displacement curve for σ^* = 10,617 psi intersects the curve for σ^* = 2,000 psi at $t \cong 5.5$ hours. A similar intersection occurs between the other pair of displacement curves shown. This phenomenon also has been noted earlier by Kumar and Mukherjee [22], and is consistent with the observations of Hart [15].

The physical significance of the results described above is not yet clear. Certainly, they are the result of using the new constitutive relations introduced above, neglecting the so-called anelastic effect. Such an approximation may be too severe, resulting in the introduction of seemingly paradoxical results in view of the physical motion of "hardness". Indeed the extension of Hart's uniaxial constitutive relations to multiaxial states of stress is still open to further investigation. It is necessary to preceed with caution in interpreting these results, because we do not yet have experimental data obtained from tests on structures under multiaxial states of stress.

The results of analyses of plates without fluid are shown in fig. 4. Similar trends of mechanical behavior appear, particularly in fig. 4a which shows the central displacement history of a clamped plate loaded with uniform lateral pressure over its entire surface. Here again, for fixed time, say $t = 20$ hours, the plate with larger hardness $\sigma^* = 10{,}617$ psi undergoes more displacement than a plate with lower hardness, $\sigma^* = 2{,}500$ psi. The results shown in fig. 4b (stress vs. time) exhibit the same cross-over effect.

It is interesting to note that, as expected, creep rates in plates sealing fluid, case HTA (Appendix I), are less than the rates in identical plate without fluid. This phenomenon is shown in fig. 5.

Although direct comparison between plates identical except for temperature is not possible, with the data given here it is easy to see that temperature effect on the creep of plates is obvious in that creep rates of plates at room temperature are very much lower than those for plates at higher temperature. The variation of corresponding variables has the same tendency if the loading conditions are the same. This can be seen by

comparing corresponding figures in the appendices, e.g., cases HTA and RMA (Table 1). In case HTA (250°C) the time required for the central displacement to become 1.5 times the initial (elastic) displacement is around 20 hours, while the time in case RMA (22°C) is around 15×10^7 hours.

It is, perhaps, worthwhile noting that the method of plate analysis used here can proceed without making any assumptions about the moment distributions. Venkatraman and Hodge [3, 4] for example, found it necessary to assume, within the constraints of the theory they used, based on Trasca's yield criterion, that the moment distribution near the clamped edge took a special form. Here no such special conditions were imposed other than the usual boundary condition of the plate theory. Bentson et al [5] basing their analysis on energy methods, also were able to construct creep solutions without a prior specification of moment distributions.

V. CONCLUSIONS AND REMARKS

In this paper, the equation of state approach proposed by Hart and Li has been applied to analyze creep of an axisymetrically loaded circular plate. It is found that the results obtained here are qualitatively similar to the results of creep obtained by classical theories. Furthermore, an important new feature of this theory is implied, namely the prior deformation history has been taken into account by introducing a state variable called hardness. In the present analysis, the anelastic strain components have been neglected since steady loading is considered; these components must be considered for rapidly varying loading, and will be the subject of a future study.

It should be remarked that Hart's theory has a strong experimental basis and can be written in explicit incremental mathematical form. The scheme used in the present paper applies directly to any kind of structure. Once the initial elastic solution of a structure under creep loading is obtained, the calculations of the creep of the structure are straight forward. Thus, in conjunction with the finite element method, the present scheme can be used to analyze creep of any type of structure.

ACKNOWLEDGEMENTS

This research was supported by Contract No. EY-76-S-02-2733 of the Energy Research and Development Administration, Washington, D.C. with Cornell University, Ithaca, N.Y. 14853.

References

1. J.H. Holloman, "The Mechanical equation of State", AIMME Technical Publications, No. 2034 (1946).

2. N.N. Malinin, "Continuous creep of round symmetrically loaded plates", (in Russian), Moscow, Vysshee Tekhnickeskoe Uchilishche, Trudy. Vol. 26, 221-238 (1953).

3. B. Venkatraman and P.G. Hodge, Jr.,"Creep behavior of Circular Plates", J. Mech. Phys. Solids, Vol. 6, 163-176 (1958).

4. B. Venkatraman and P.G. Hodge, Jr.,"A further note on the creep behavior of circular plates", J. Mech. Phys. Solids., Vol. 12, 191-197 (1964).

5. J. Bentson, S.A. Patel and B. Venkatraman, "Creep analysis of circular plates by energy methods", Int. J. Nonlinear Mech., Vol. 1, 81 (1966).

6. S.A. Patel, F.B. Cozzarelli and B. Venkatraman, "Creep of compressible circular plates", Int. J. Mech. Sci., Vol. 5, 77-85 (1963).

7. S.A. Patel, "Creep of annular plates under symmetric lateral pressure", Proc. Inst. Mech. Engr., 17 Pt 3L, 58-62 (1963-64).

8. F.K.G. Odqvist, "Applicability of elastic analogue in creep problems for plates, membranes and beams", IUTAM Colloquium on creep in structures, Stanford Univ., July 11-15, 1960.

9. F.A. Cozzarelli, "Creep of circular plates with temperature gradients", Int. J. Mech. Sci., Vol. 8, 321-331 (1966).

10. R.K. Penny and D.L. Marriot, "Design for Creep", McGraw-Hill, London (1971).

11. P.T. Tarpgaard, Jr. and Norman Jones, "The influence of finite-deformation upon the creep behavior of circular plates", Int. J. Mech. Sci., Vol. 14, 447-467 (1972).

12. T.M. Hrudey, "A creep bending analysis of plates by the finite element method", Int. J. Solids Structures, Vol. 9, 291-303 (1973).

13. E.T. Onat, and F. Fardshisheh, "Representation of creep of metals", ORNL-4783, Contract # W-7405-eng-26, (1972).

14. Edward W. Hart, "A phenomenological theory for plastic deformation of polycrystalline metals", Acta Metallurgica, Vol. 18, 599-610, (1970).

15. Edward W. Hart, C.Y. Li, H. Yamada, and G.L. Wire, "Phenomenological theory: a guide to constitutive relations and fundamental deformation properties", in 'Constitutive Equations in Plasticity", edited by A. Argon, MIT Press, (1976).

16. F.V. Ellis, G.L. Wire, and C.Y. Li, "Work hardening and mechanical equation of state in some metals in monotonic loading", AEC Report # COO-2172-4, Cornell University (1973).

17. F.V. Ellis, G.L. Wire, and C.Y. Li, "Mechanical properties and mechanical equations of state of 1100 Aluminum alloy in monotonic loading", AEC Report No. COO-2172-5, Cornell University (1974).

18. Y.C. Waung, and R.H. Lance, "Creep of beams using a state-variable approach", ERDA Report # COO-2733-6, Cornell University (1976).

19. Y.C. Waung, and R.H. Lance, "Creep of circular plates using a state-variable approach", ERDA Report # COO-2733-7, Cornell University (1976).

20. V. Kumar, and S. Mukherjee, "Creep analysis of structures using a new equation of state type constitutive relations", Intl. Jl. of Computer and Structures, Vol. 6, 420-437 (1976).

21. V. Kumar, and S. Mukherjee, "Time-Dependent Inelastic Analysis of Metallic Media using Constitutive Relations with State Variables", Nuclear Engineering and Design, Vol. 41, 27-43 (1977).

22. V. Kumar, and S. Mukherjee, "Creep Analysis of Metallic Structures in the Presence of Thermal Gradients using Newer Constitutive Relations", Journal of Pressure Vessel Technology, Trans. ASME (to appear). Vol. 99, series J, 272-280 (1977).

23. R.H. Lance, and D.N. Robinson, "Plastic analysis of a plate sealing a fluid", J. of the Engrg. Mech. Div., Proc. A.S.C.E., 96, EM6, 1183-1194 (1970).

24. P.G., Hodge, Jr., and C-K Sun, "Yield-point load of a circular plate sealing an incompressible fluid", Int. J. of Mech. Sci., Vol. 9, 405-414 (1967).

25. A.D. Kerr, "On plates sealing an incompressible fluid", Int. J. of Mech. Sci., Vol. 8, 295-304 (1966).

26. F.V. Ellis, G.L. Wire, and C.Y. Li, "Effects of cold work and mechanical equation of state in Aluminum Alloy", Journal of Engrg. Material and Technology, Trans. ASME, Vol. 97, 338-342 (1975).

27. G. Simon and H. Wang, "Single crystal elastic constants and calculated aggregate properties", MIT press, London (1971).

28. D.L. Marriot, and F.A. Leckie, "Some observations on the deflection of structures during creep", Conf. on thermal loading and creep in structures and components, Proc. Inst. Mech. Engr., 178, Pt. 3L (1963-64).

Table 1. Configurations and Material Constants Used in Each Case

	Cases / Quantities	H T A (I)	H T B (II)	H T C (III)	R M A (IV)	R M B (V)
Configuration	Temperature (T)	250°C	250°C	250°C	22°C	22°C
	Laod Range (η)	1/2	1	1/2	1/2	1
	Load Condition	WF	NF	WF	WF	NF
	Fluid Reaction (q*, q*')	≠0	=0	≠0	≠0	=0
Material Constants	Initial Hardness σ_o^* (psi)	10,617	10,617	2,000	10,617	10,617
	Poisson's Ratio (ν)	0.358	0.358	0.358	0.330	0.330
	Young's Modulus E (psi)	8.784×10^6	8.784×10^6	8.784×10^6	9.975×10^6	9.975×10^6
	D_1	1.0715×10^5	1.0715×10^5	1.0715×10^5	1.059×10^7	1.059×10^7
Other Constants	$m = 5$, $\lambda = 0.11$, $\delta = 7.82$, $\beta = 12.5$, $\Lambda = 1.17 \times 10^{20}$					

Table 2. Physical Quantities Appearing in Calculations for Each Case (calculations based upon a plate of radius 16" and thickness 1")

Quantities \ Cases	H T A (I)	H T B (II)	H T C (III)	R M A (IV)	R M B (V)
σ_o (psi)	1,000	1,000	1,000	6,000	6,000
Q_o (psi)	1.3119×10^{4}	1.3119×10^{4}	1.3119×10^{4}	1.4575×10^{4}	1.4575×10^{4}
t_o (hrs)	5.268761	5.268761	2.774687	6.745×10^{5}	6.745×10^{5}
q (psi)	43.2092	7.6706	43.2092	264.7133	46.9925
K_o (1/in)	0.1462×10^{-3}	0.1462×10^{-3}	0.1462×10^{-3}	0.8060×10^{-3}	0.8060×10^{-3}
M_o (in-lb)	166.7	166.7	166.7	1,000.0	1,000.0
W_o (in)	0.3219×10^{-2}	0.9355×10^{-2}	0.3219×10^{-2}	1.7751×10^{-2}	5.1585×10^{-2}
ε_o (in/in)	0.7309×10^{-4}	0.7309×19^{-4}	0.7309×10^{-4}	4.0301×10^{-4}	4.0301×10^{-4}

$\sigma_o = \sigma_r(h/2,0,0)$, $Q_o = 64D/a^3$, $D = Eh^3/12(1-\nu^2)$

$t_o = (\sigma_o^*/D_1)^{-m}\varepsilon_o[\ell n(\sigma_o^*/\sigma_o)]^{1/\lambda}\frac{1}{3600}$, $M_o = M(0,0)$

$K_o = K_r(0,0)$, $\varepsilon_o = \varepsilon_r(h/2,0,0)$, $W_o = W(0,0)$

Table 3. Symbols used in the appendixes

Symbols Used in Charts	Corresponding symbols used in equations
R, Z	r, z
A, H	a, h
T	t
TO	t_o
W	w
MR, MQ	M_r, M_θ
KR, KQ	K_r, K_θ
WO, MO, KO	w_o, M_o, K_o
DW, DKR, DKQ	$\frac{dw}{dt}$, $\frac{dK_r}{dt}$, $\frac{dK_\theta}{dt}$
SR, SQ	σ_r, σ_θ
PR, PQ	p_r, p_θ
SO, EPO	σ_o, ε_o
QSTRN	$\bar{q}^*$
DQSTR	$\frac{d\bar{q}^*}{dt}$

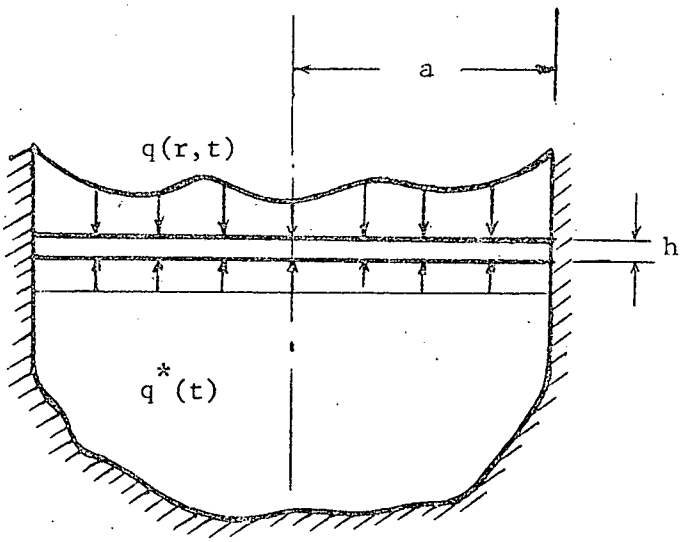

Figure 1. Symmetrically Loaded Circular Plate Sealing a Fluid

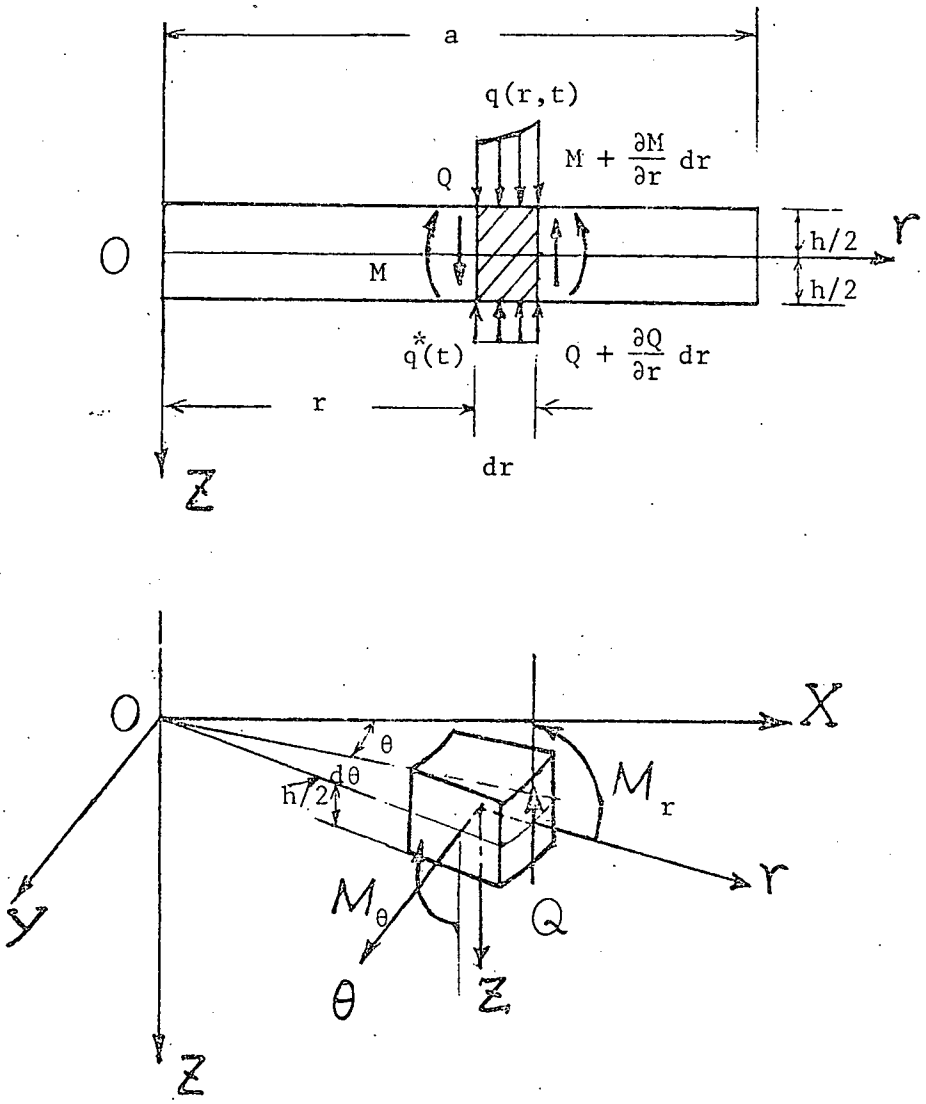

Figure 2. Plate Element and Coordinates

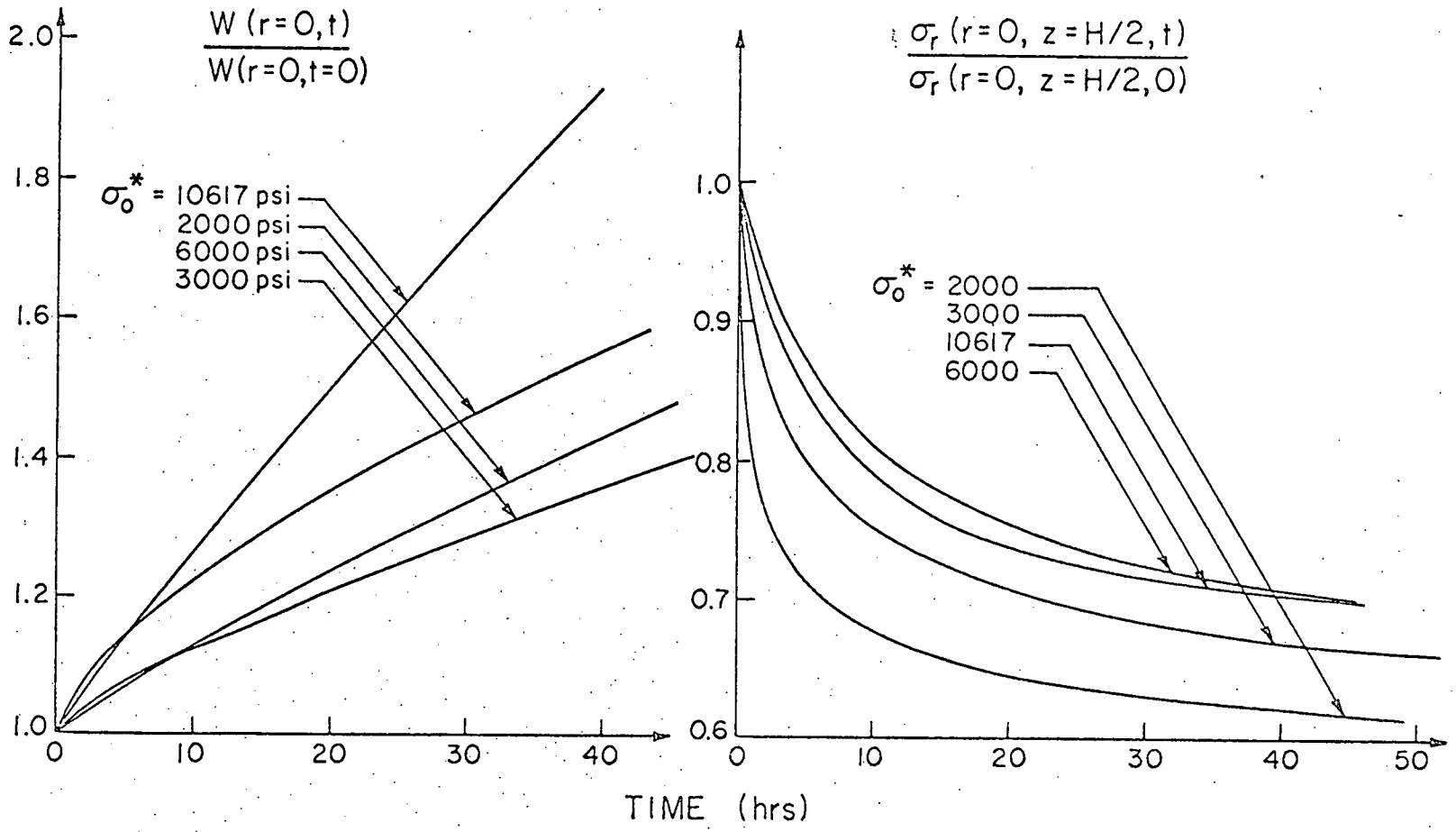

Figure 3. Creep Displacements and Radial Stress Relaxation of Plate With Fluid for Various Values of Initial Hardness. T = 250°C, σ_o = 1,000 psi, $\eta = \frac{1}{2}$ (WF)

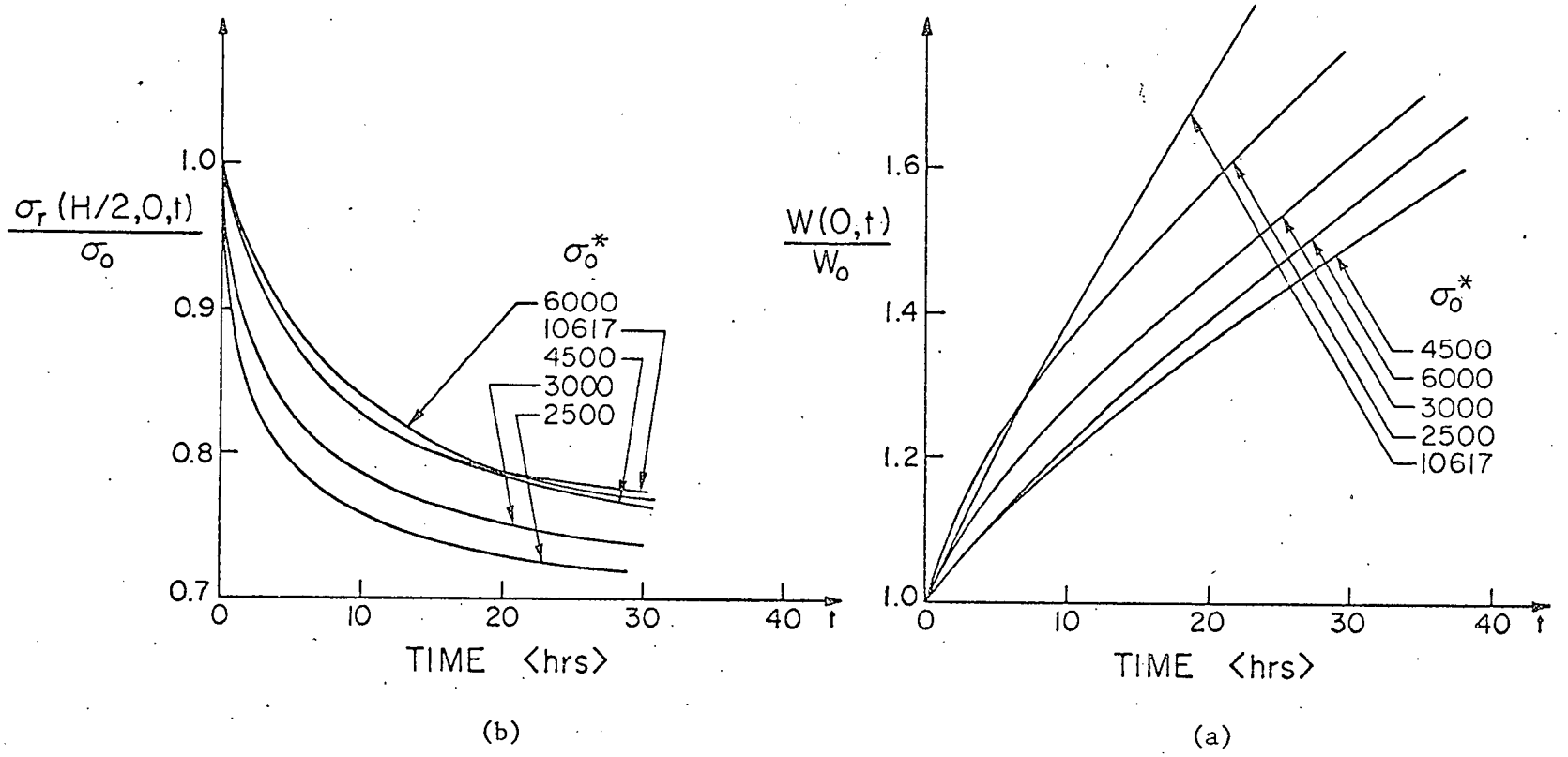

Figure 4. Creep Displacements and Radial Stress Relaxation of Plate Without Fluid for Various Values of Initial Hardness. T = 250°C, σ_o = 1,000 psi, η = 1(NF)

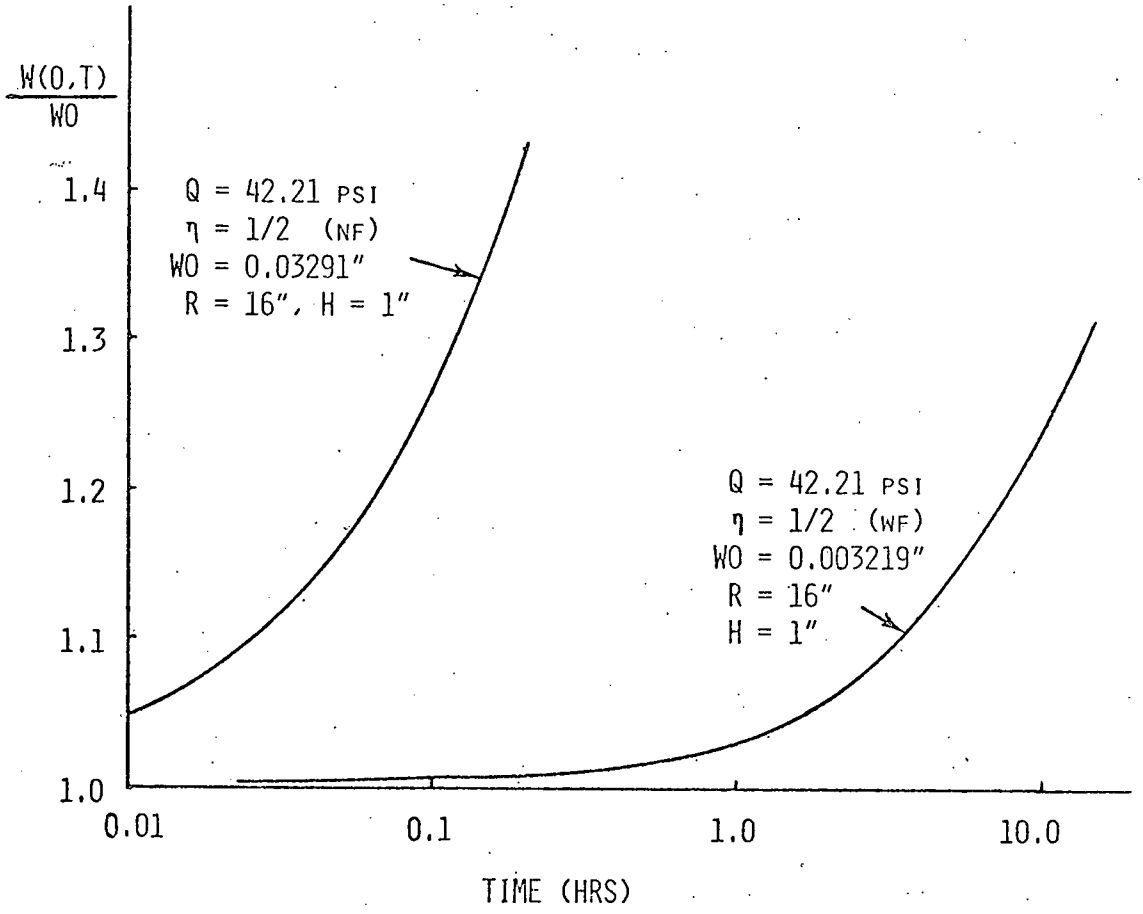

Figure 5. Center Displacements of Plate Sealing Fluid (WF) and Plate Without Fluid (NF) under the Same Creep Loading Condition

APPENDIX I

CLAMPED CIRCULAR

ALUMINUM PLATE

WITH FLUID

T = 250°C

INITIAL HARDNESS = 10,617 psi

(HTA)

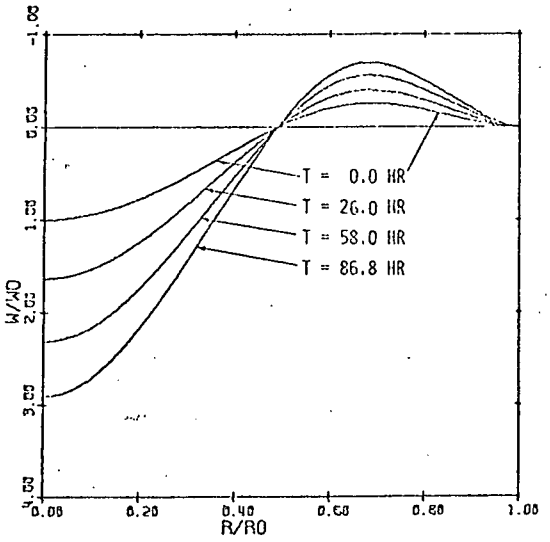

(a) DISPLACEMENT PROFILE

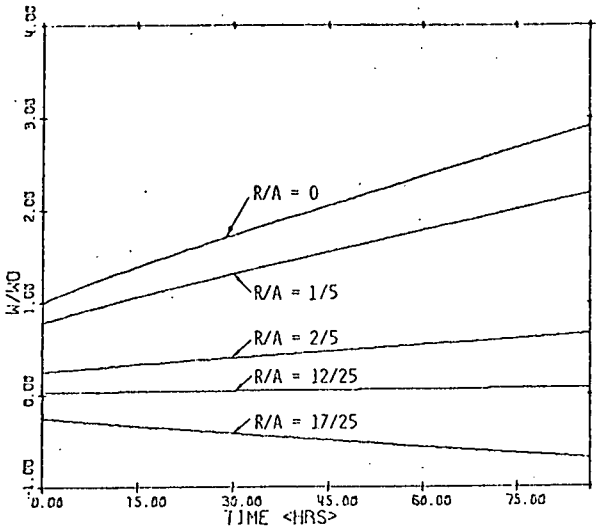

(b) DISPLACEMENT VS TIME

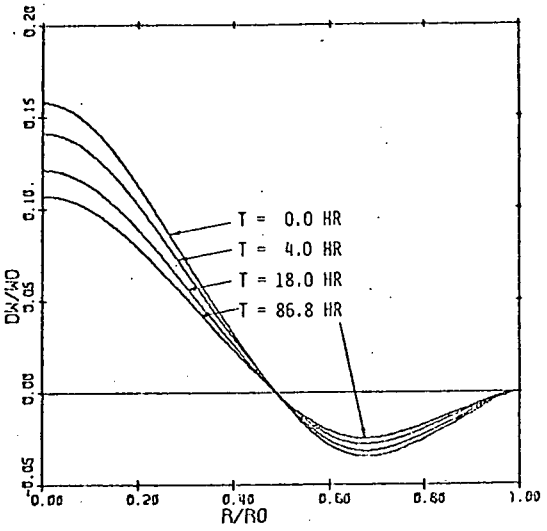

(c) DISPL RATE PROFILE

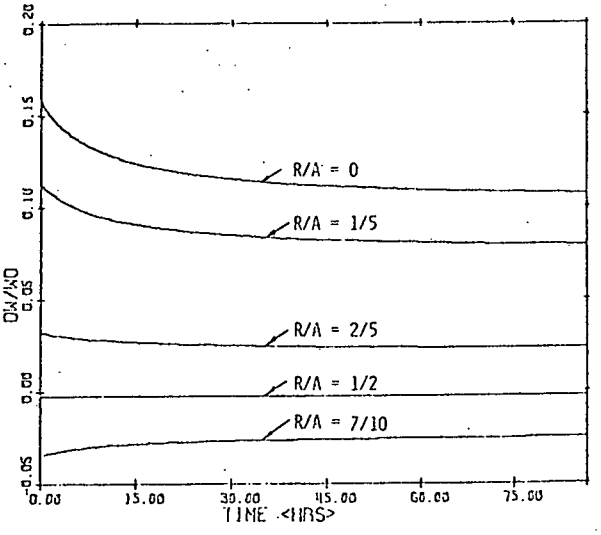

(d) DISP RATE VS TIME

Figure 1. Displacements and Displacement Rates

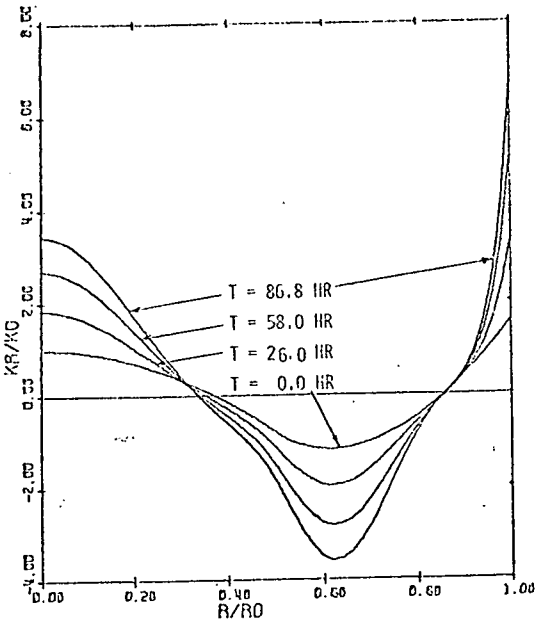

(a) CURVATURE PROFILE <KR>

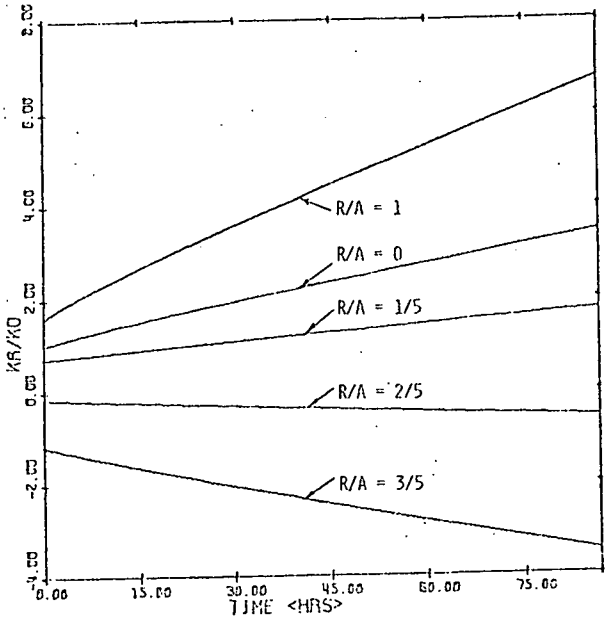

(b) CURVATURE <KR> VS TIME

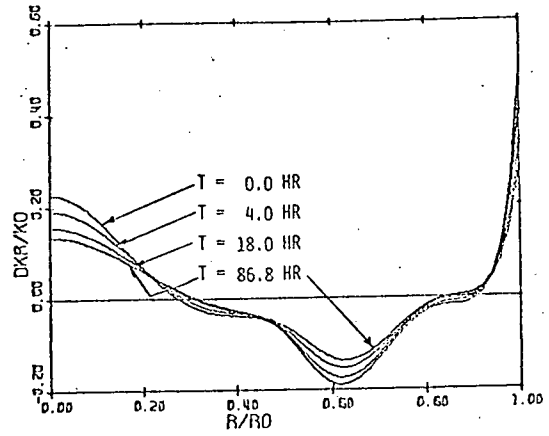

(c) CURVATURE RATE PROFILE <KR>

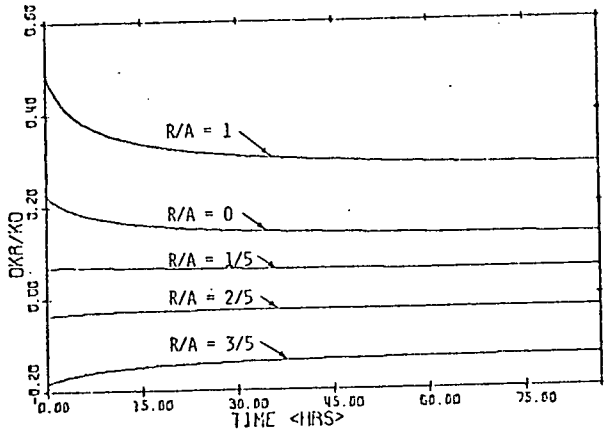

(d) KR RATE VS TIME

Figure 2. Radial Curvatures and Rates

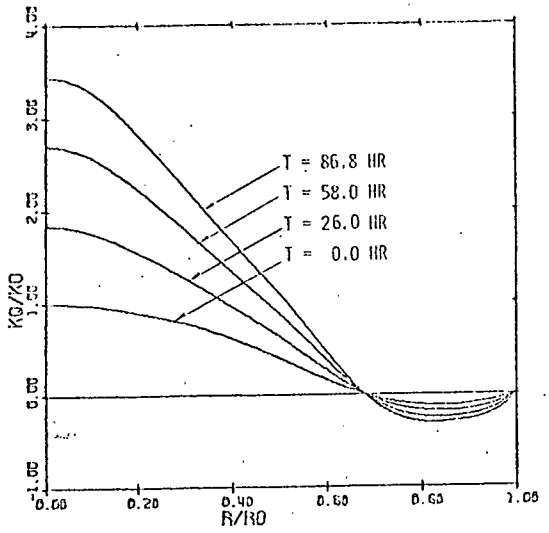

(a) CURVATURE PROFILE <KQ>

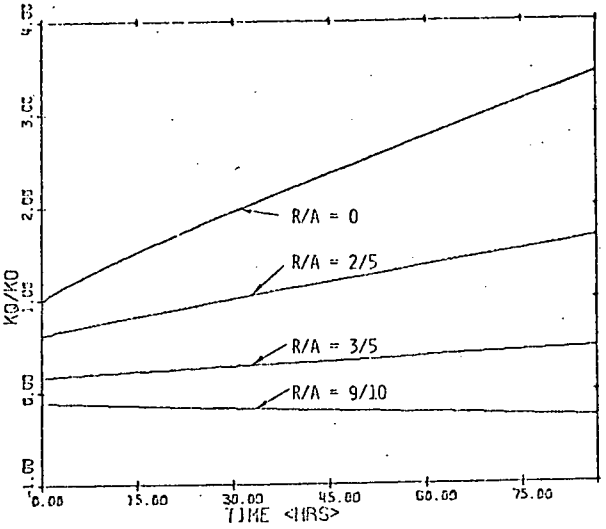

(b) CURVATURE <KQ> VS TIME

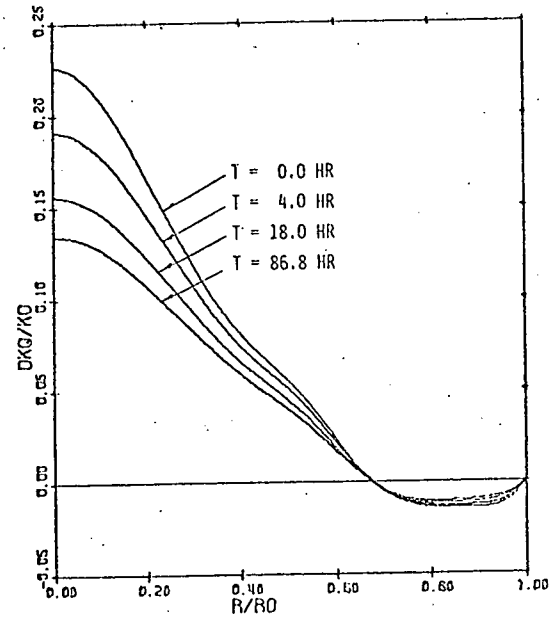

(c) CURVATURE RATE PROFILE <KQ>

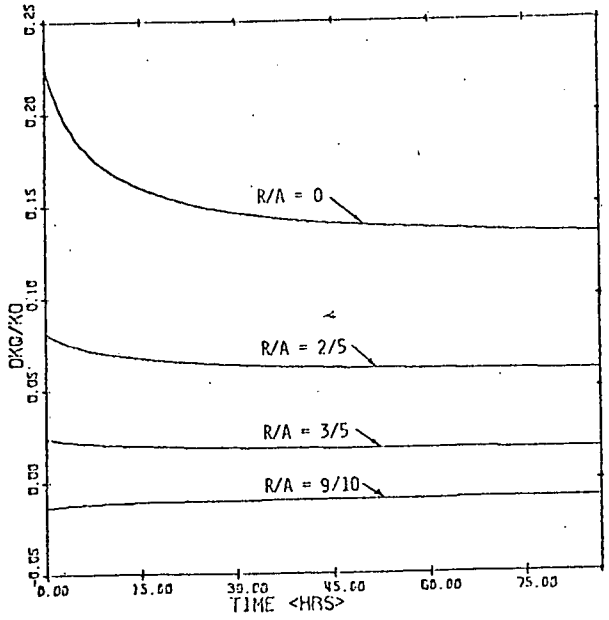

(d) KQ RATE VS TIME

Figure 3. Circumferential Curvatures and Rates

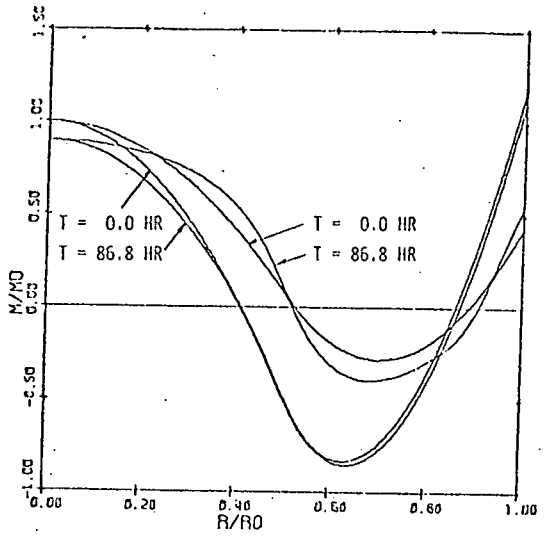

(a) MOMENT PROFILES

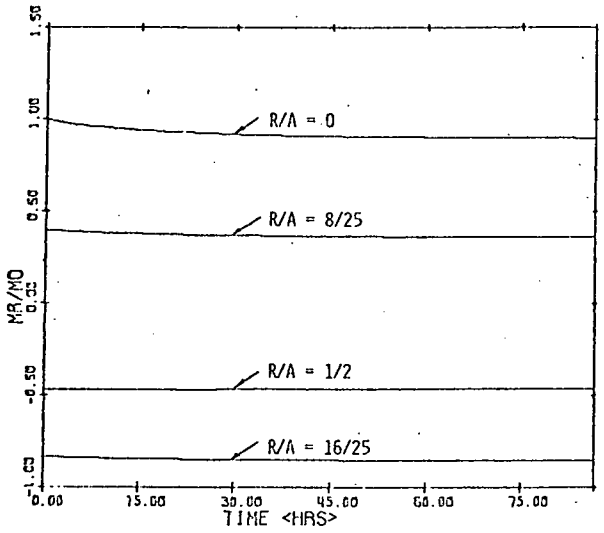

(b) MOMENT <MR> VS TIME

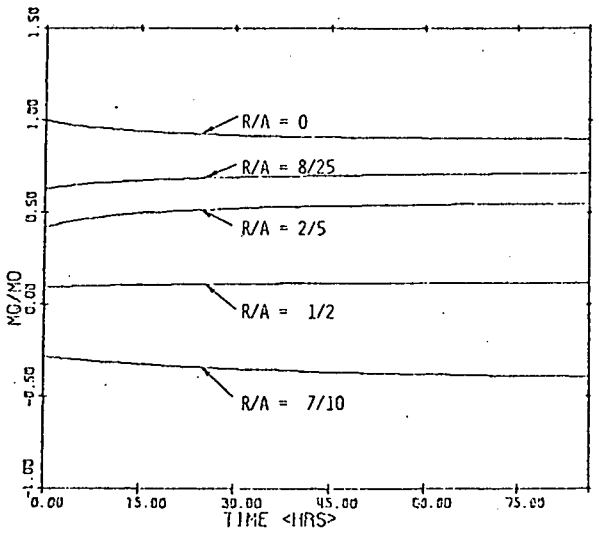

(c) MOMENT <MQ> VS TIME

Figure 4. Moments .

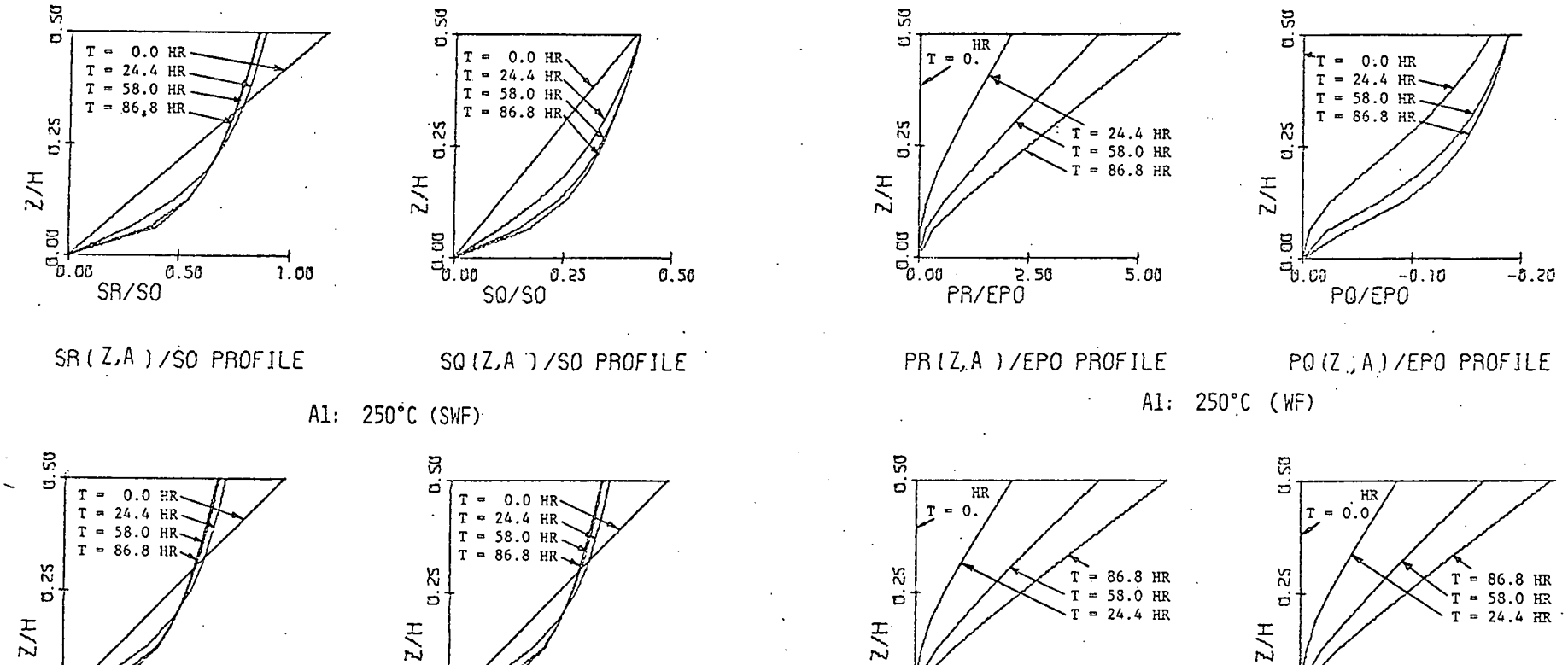

Figure 5. Stress and Plastic Strain Profiles Across Thickness

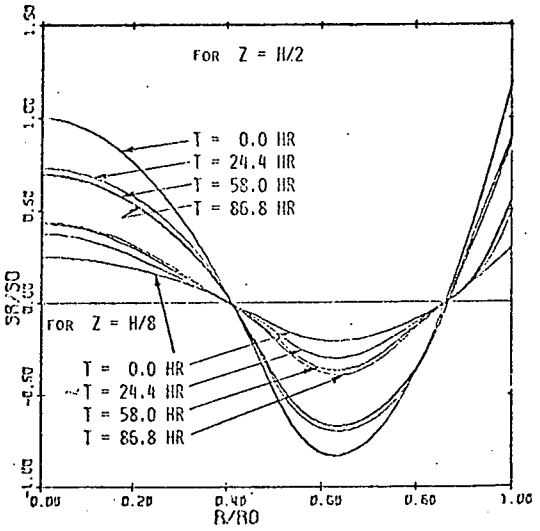

(a) STRESS <RR> PROFILE

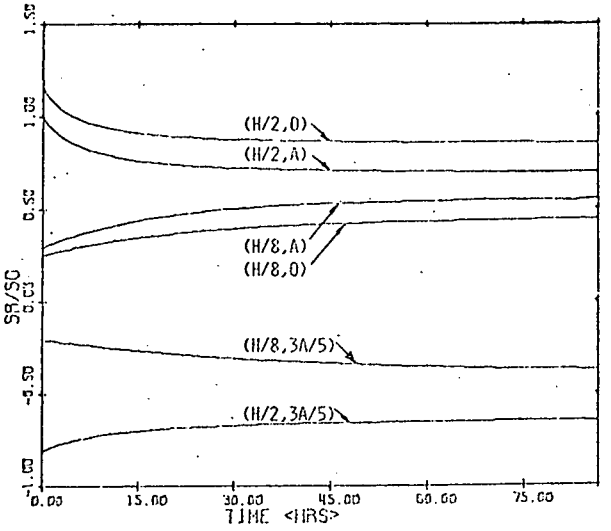

(b) STRESS <SR/SO> VS TIME

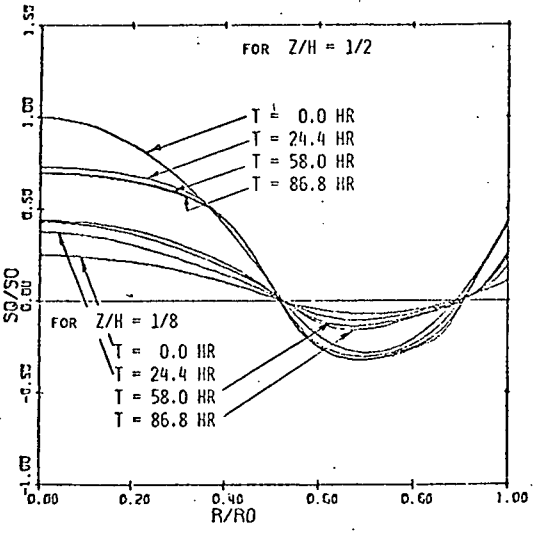

(c) STRESS <QQ> PROFILE

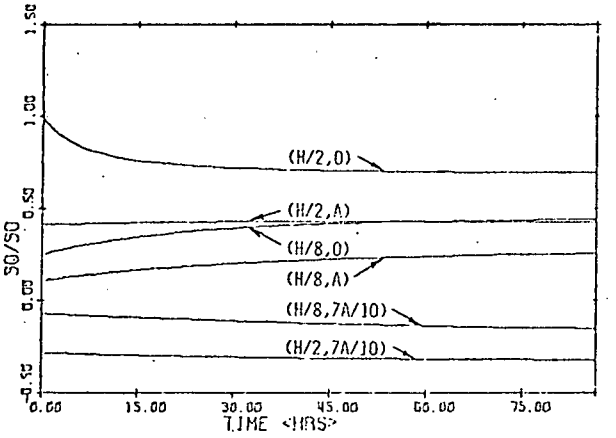

(d) STRESS <SO/SO> VS TIME

Figure 6. Stresses

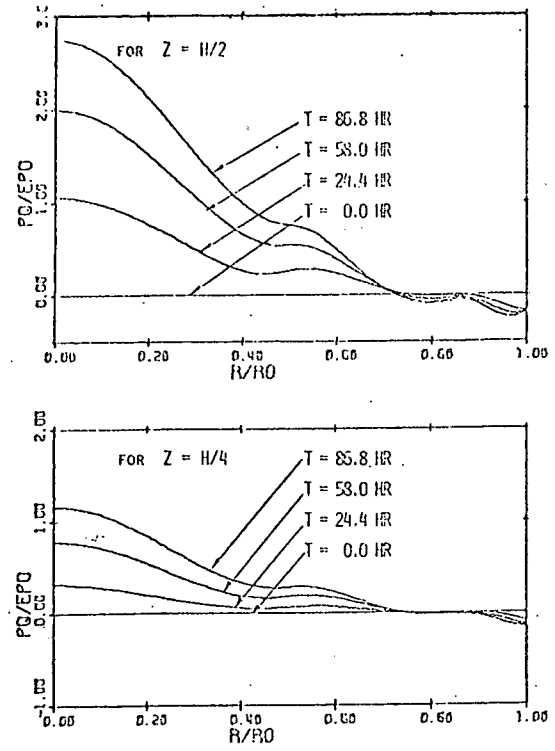

(a) PLASTIC STRAIN <PQ> PROFILE

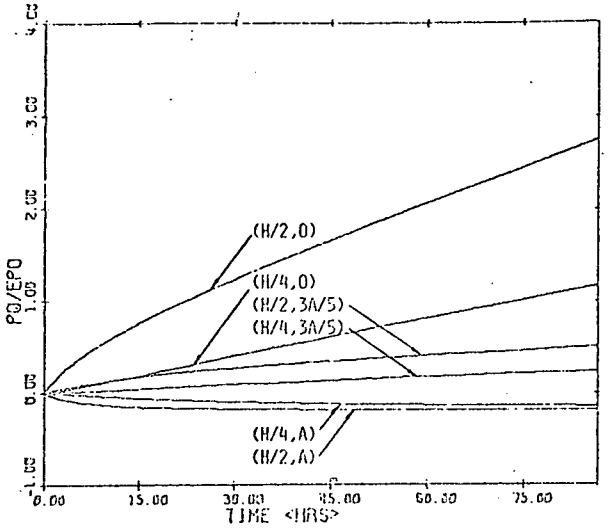

(b) STRAIN <PQ/EPO> VS TIME

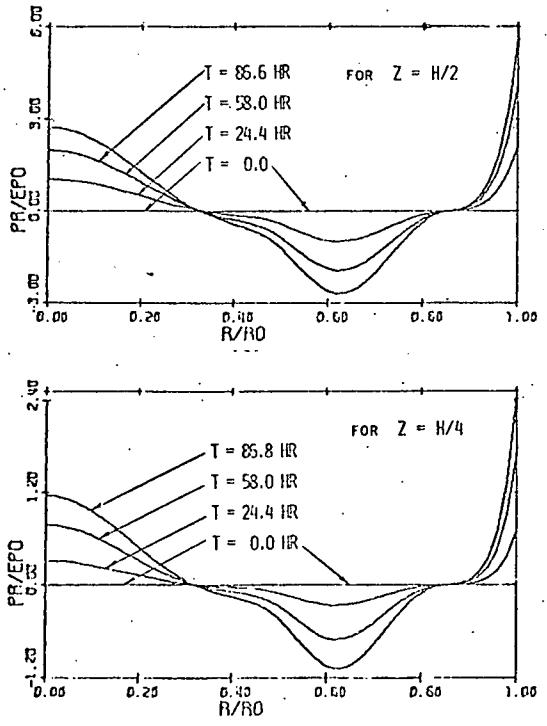

(c) PLASTIC STRAIN <PR> PROFILE

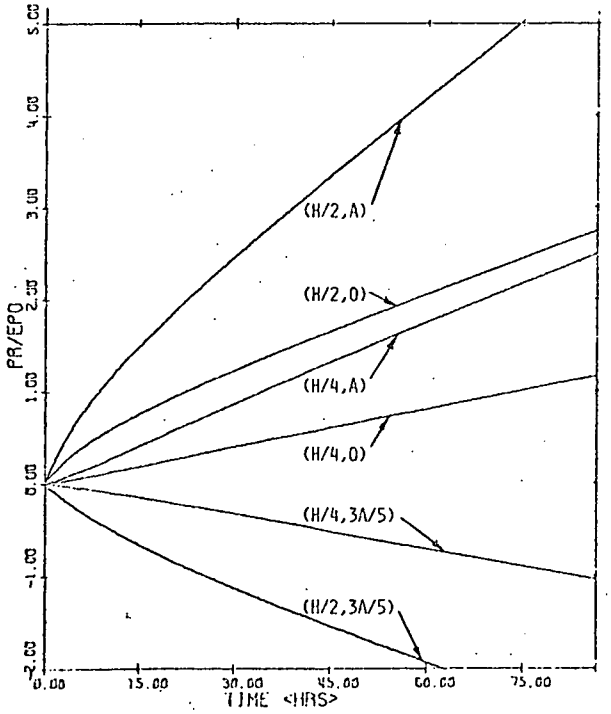

(d) STRAIN <PR/EPO> VS TIME

Figure 7. Plastic Strains

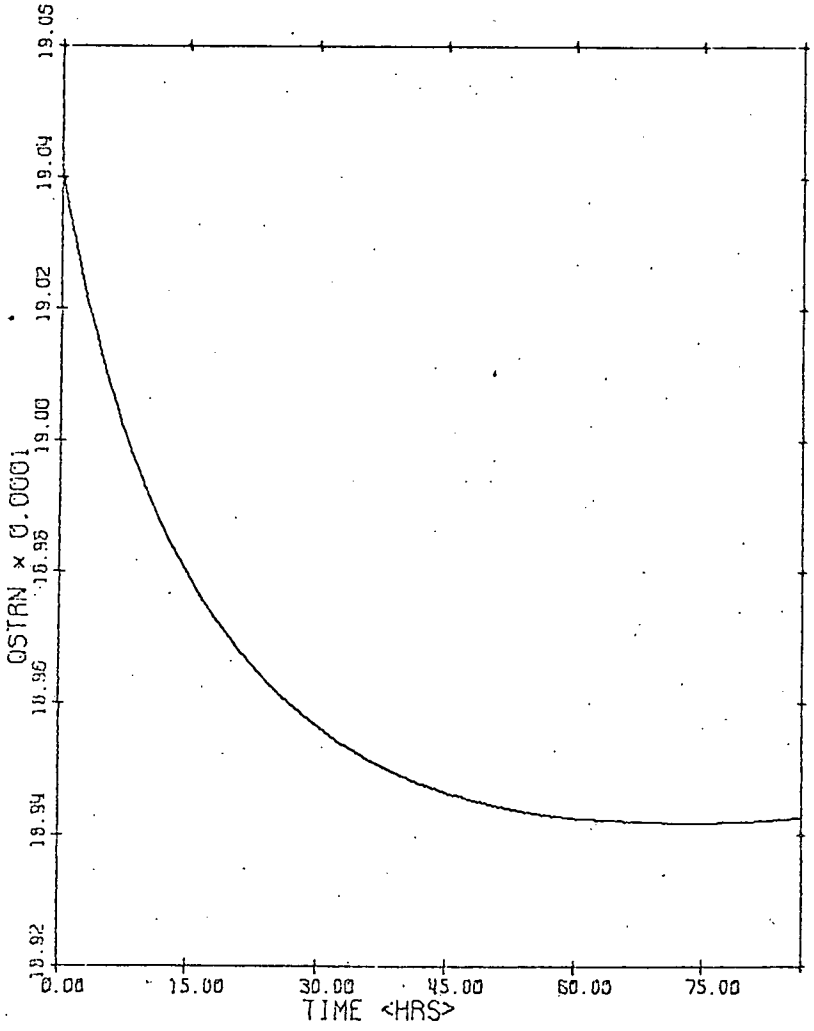

(a) FLUID PRESSURE VS TIME

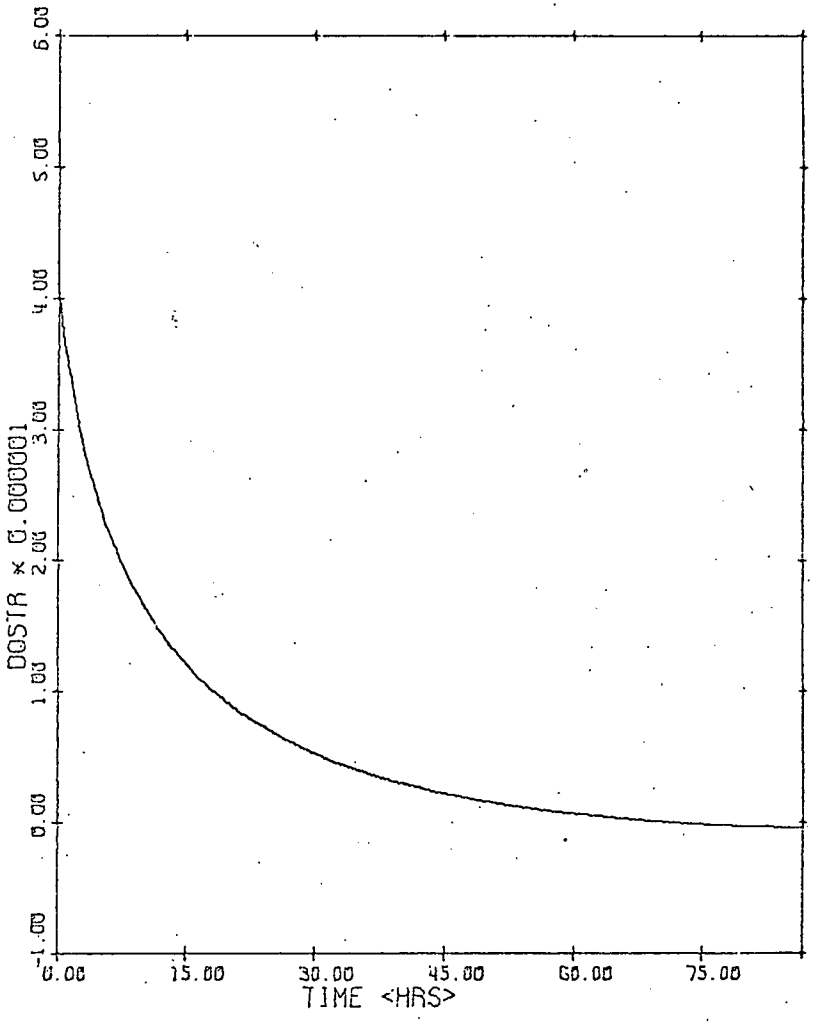

(b) PRESSURE RATE VS TIME

Figure 8. Fluid Pressure and Rate

APPENDIX II

CLAMPED CIRCULAR

ALUMINUM PLATE

WITHOUT FLUID

T = 250°C

INITIAL HARDNESS = 10,617 psi

(HTB)

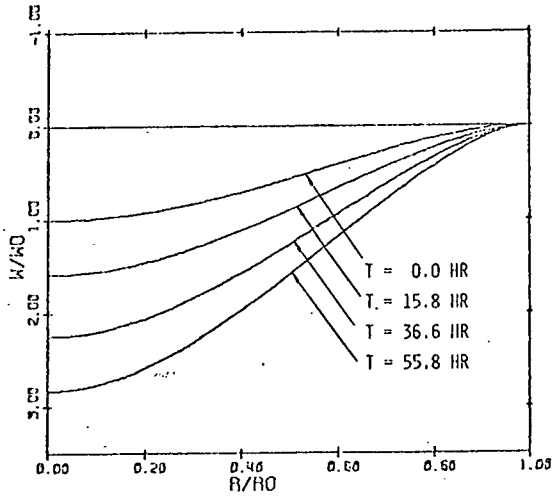

(a) DISPLACEMENT PROFILE

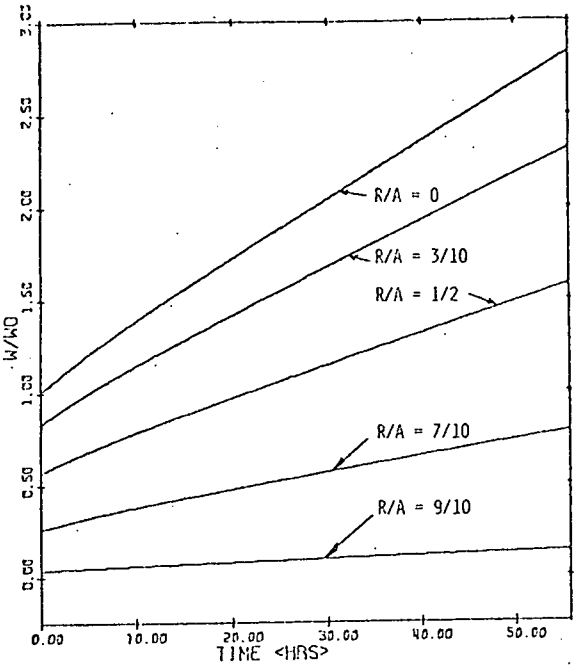

(b) DISPLACEMENT VS TIME

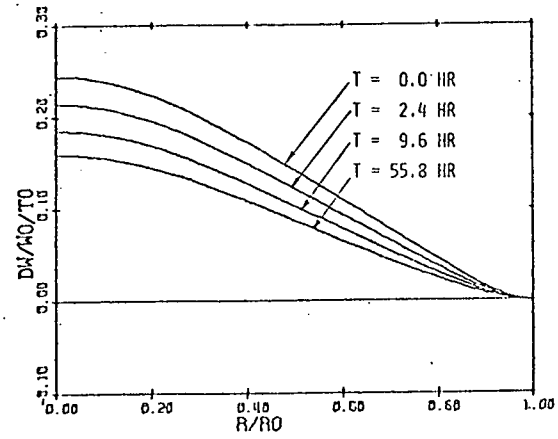

(c) DISPL RATE PROFILE

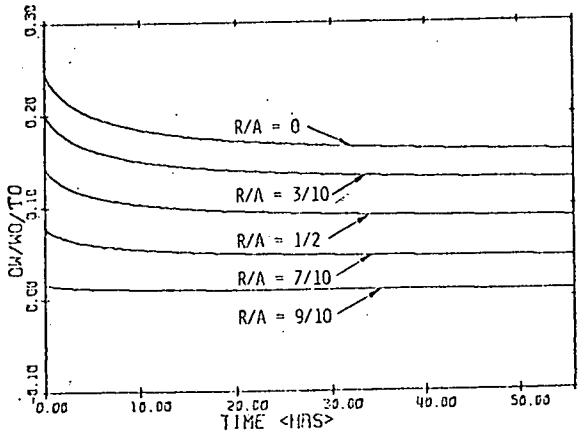

(d) DISP RATE VS TIME

Figure 1. Displacements and Displacement Rates

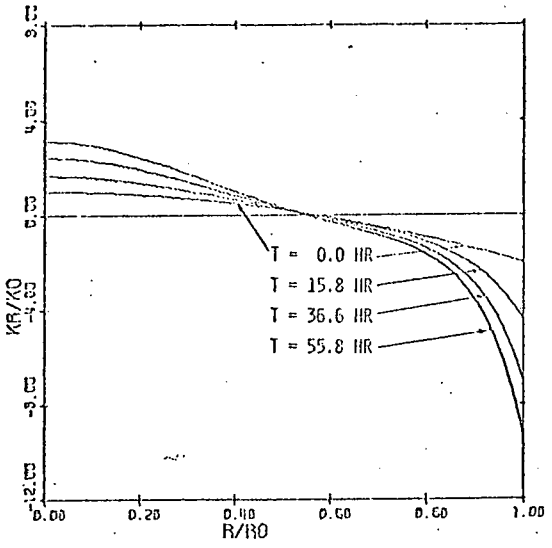

(a) CURVATURE PROFILE <KR>

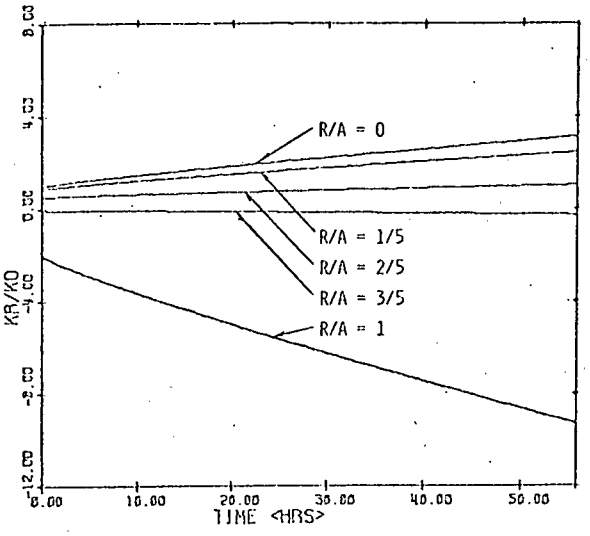

(b) CURVATURE <KR> VS TIME

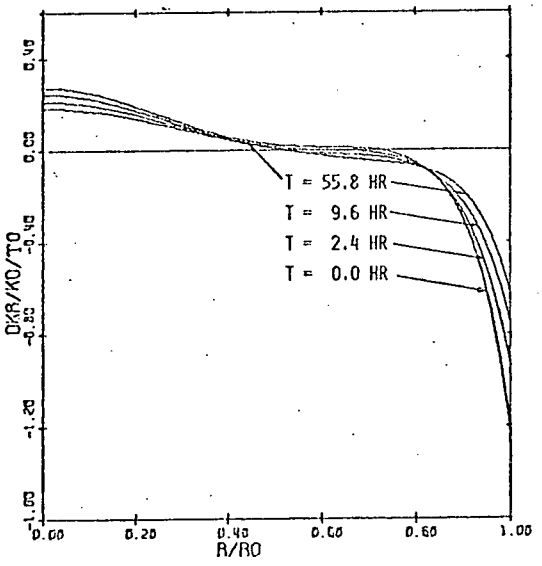

(c) CURVATURE RATE PROFILE <KR>

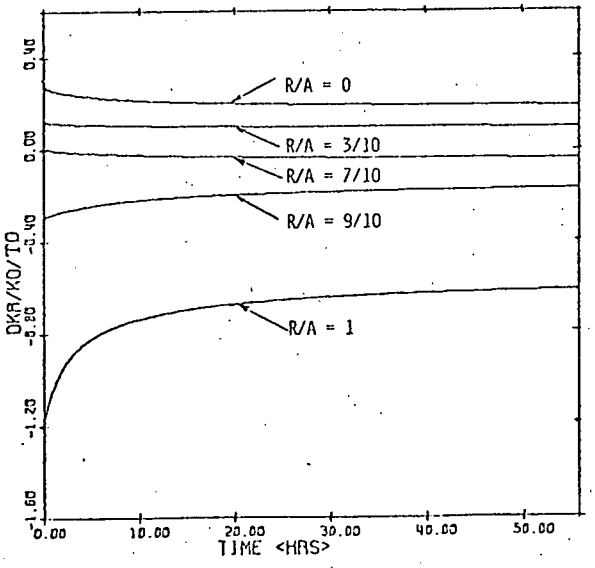

(d) KR RATE VS TIME

Figure 2. Radial Curvatures and Rates

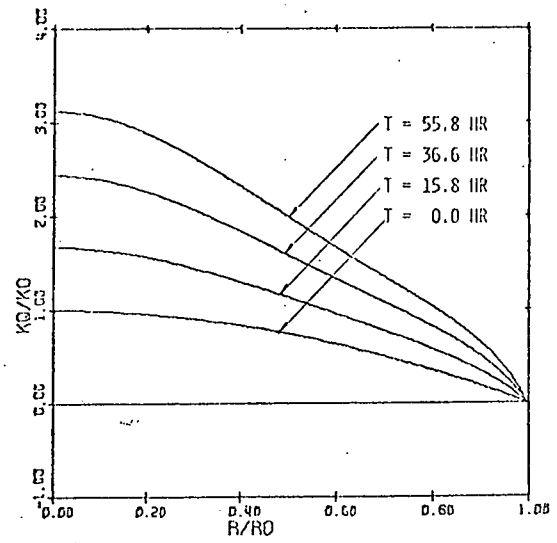

(a) CURVATURE PROFILE <KQ>

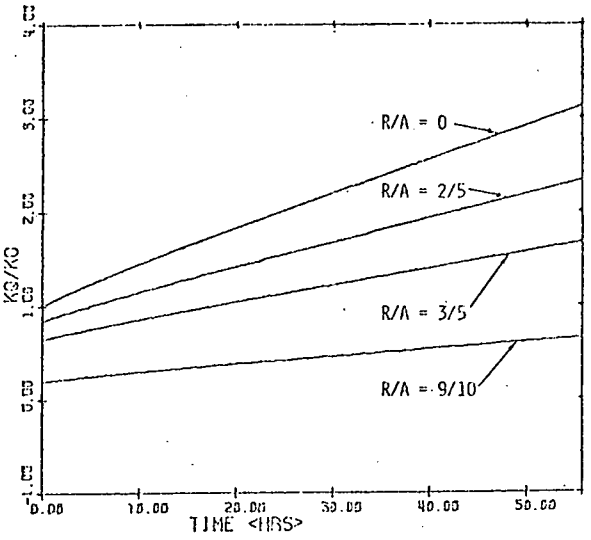

(b) CURVATURE <KQ> VS TIME

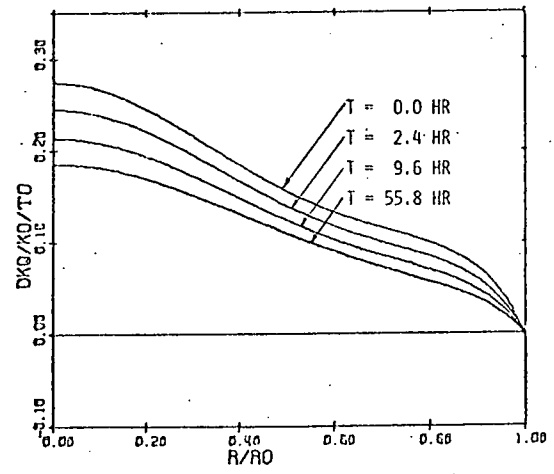

(c) CURVATURE RATE PROFILE <KQ>

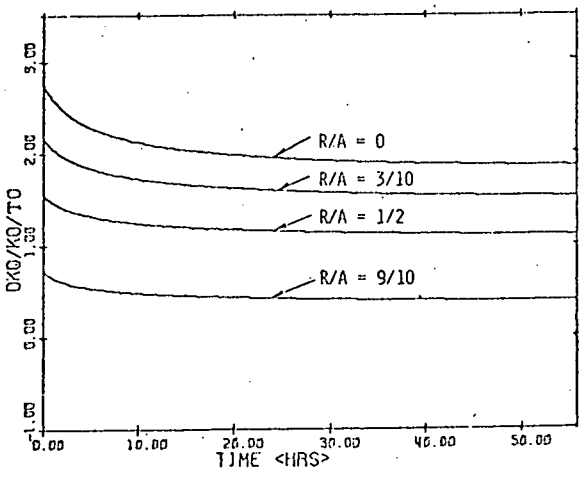

(d) KQ RATE VS TIME

Figure 3. Circumferential Curvatures and Rates

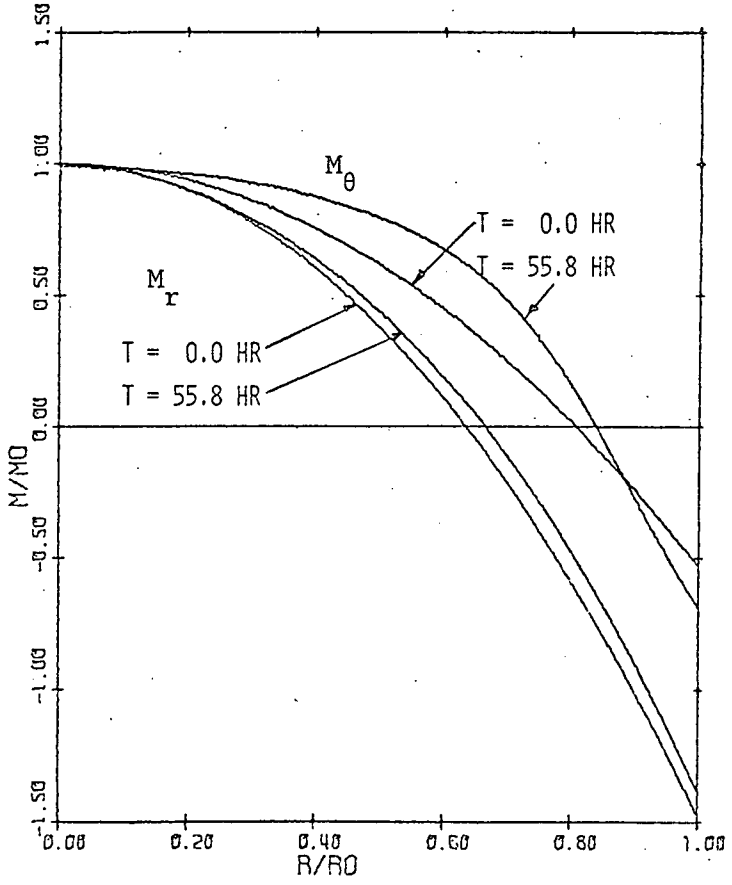

(a) MOMENT PROFILES

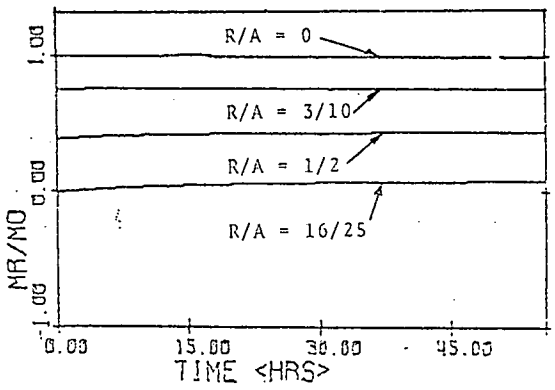

(b) <MR> VS TIME

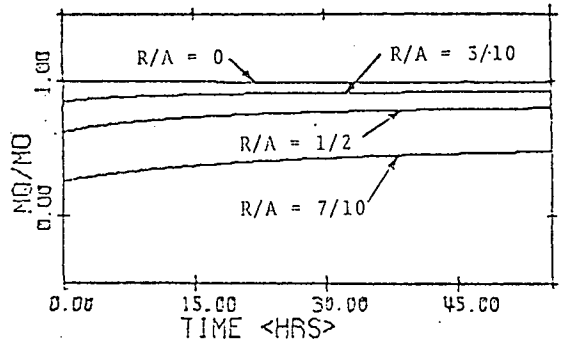

(c) <MQ> VS TIME

Figure 4. Moments

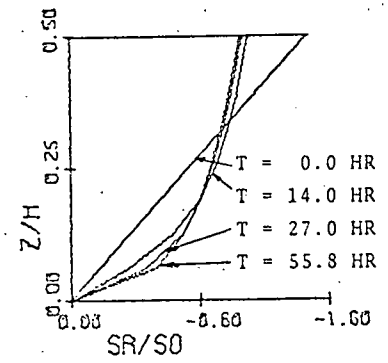

SR(Z,A)/SO PROFILE

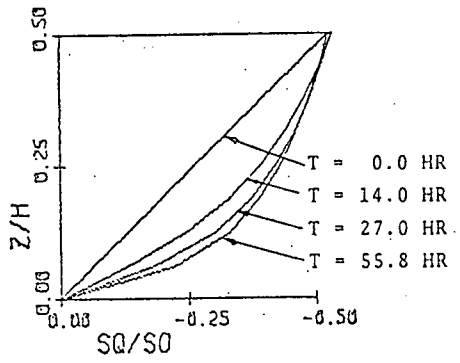

SQ(Z,A)/SO PROFILE

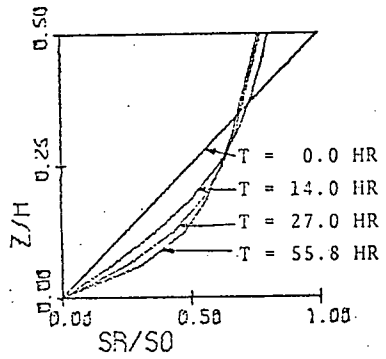

SR(Z,0)/SO PROFILE

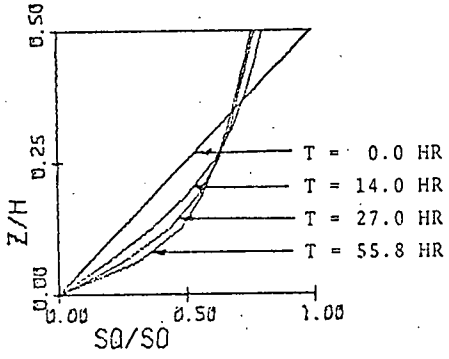

SQ(Z,0)/SO PROFILE

(a) STRESS PROFILES ACROSS THICKNESS

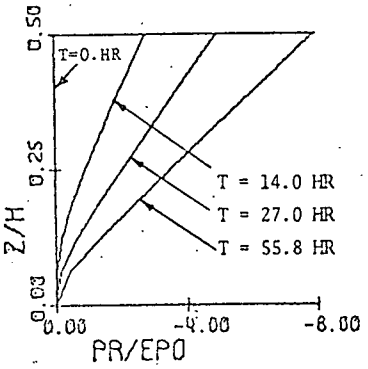

PR(A,Z)/EPO PROFILE

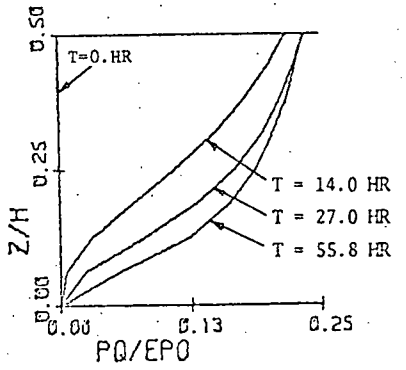

PQ(A,Z)/EPO PROFILE

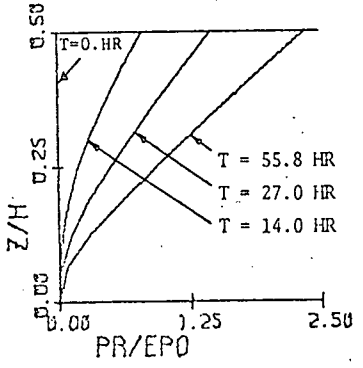

PR(0,Z)/EPO PROFILE

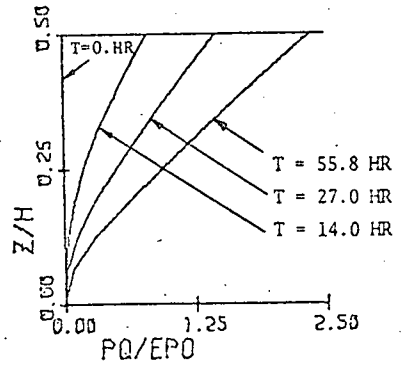

PQ(0,Z)/EPO PROFILE

(b) STRAIN PROFILES ACROSS THICKNESS

Figure 5. Stress and Plastic Strain Profiles Across Thickness

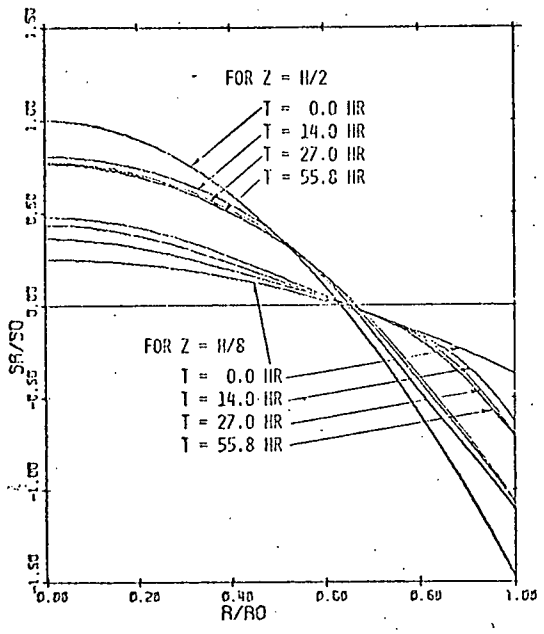

(a) STRESS <RR> PROFILE

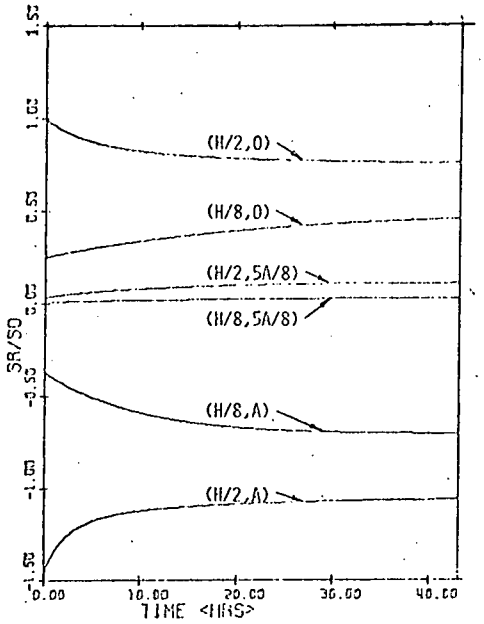

(b) STRESS <SR/SO> VS TIME

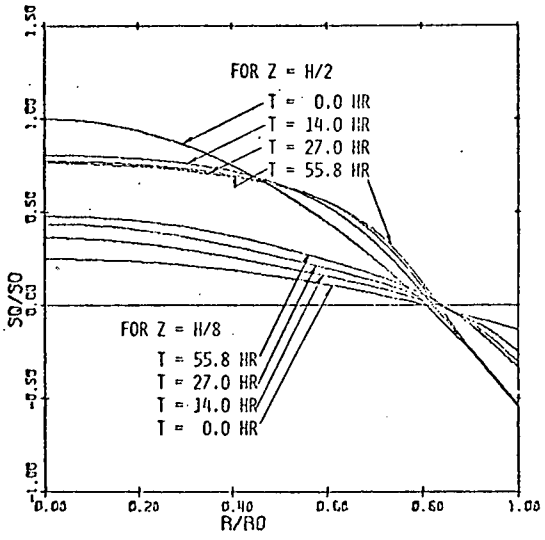

(c) STRESS <QQ> PROFILE

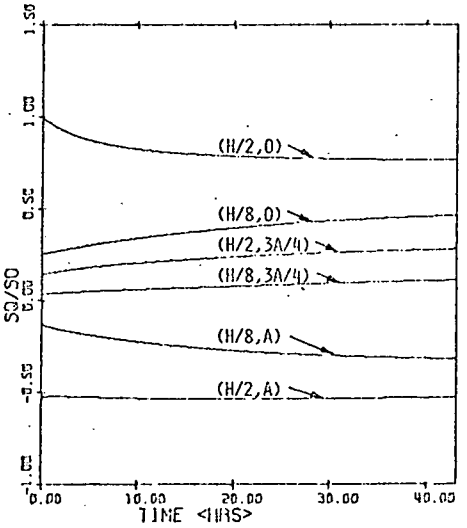

(d) STRESS <SQ/SO> VS TIME

Figure 6. Stresses

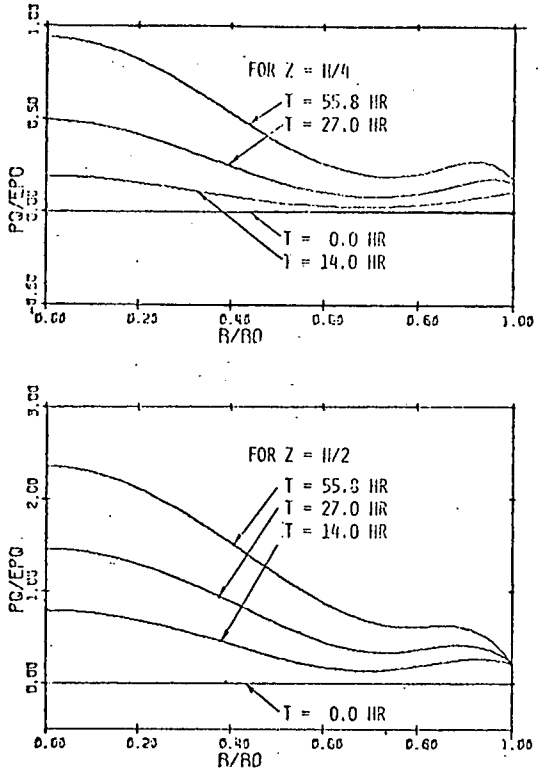

(a) PLASTIC STRAIN <PQ> PROFILE

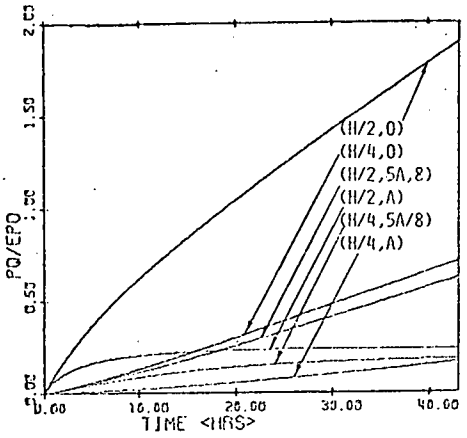

(b) STRAIN <PQ/EPO> VS TIME

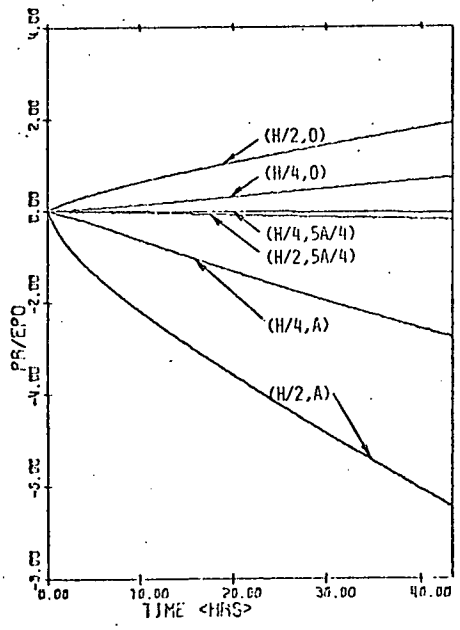

(d) STRAIN <PR/EPO> VS TIME

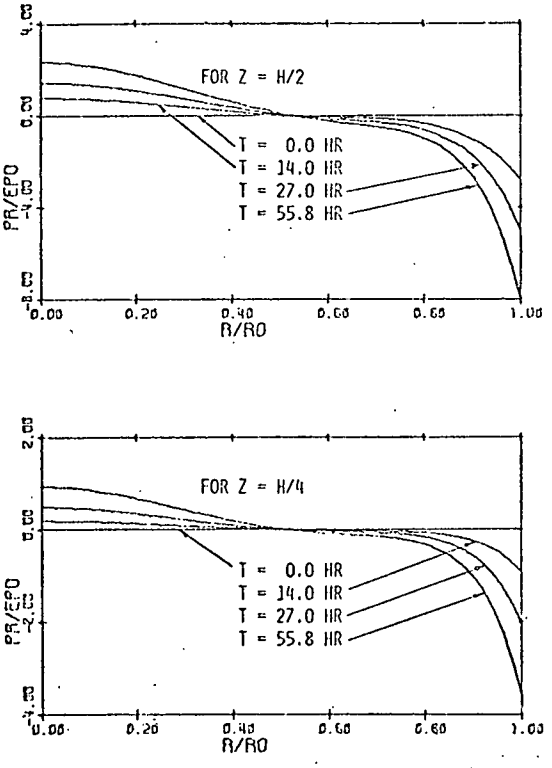

(c) PLASTIC STRAIN <PR> PROFILE

Figure 7. Plastic Strains

APPENDIX III

CLAMPED CIRCULAR

ALUMINUM PLATE

WITH FLUID

T = 250°C

INITIAL HARDNESS = 3,000 psi

(HTC)

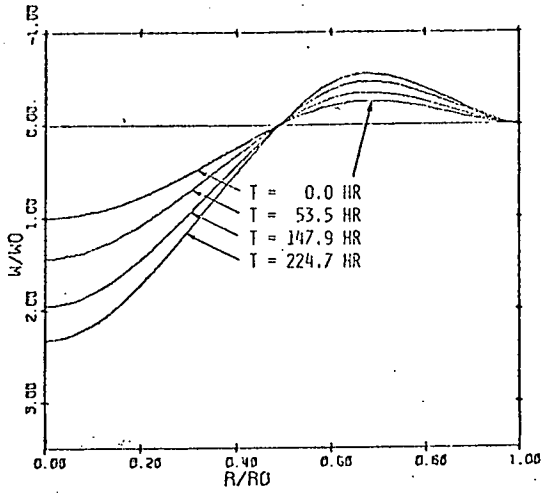

(a) DISPLACEMENT PROFILE

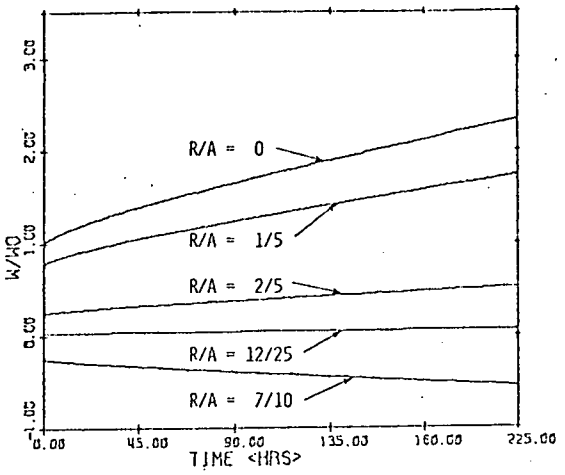

(b) DISPLACEMENT VS TIME

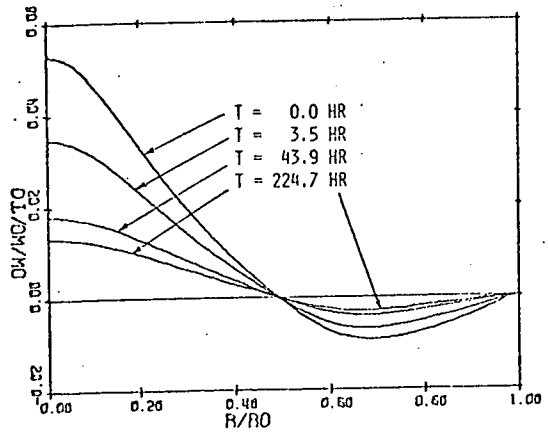

(c) DISPL RATE PROFILE

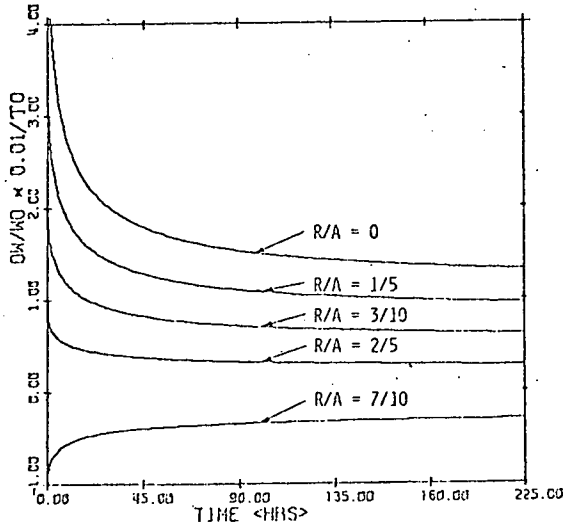

(d) DISP RATE VS TIME

Figure 1. Displacements and Displacement Rates

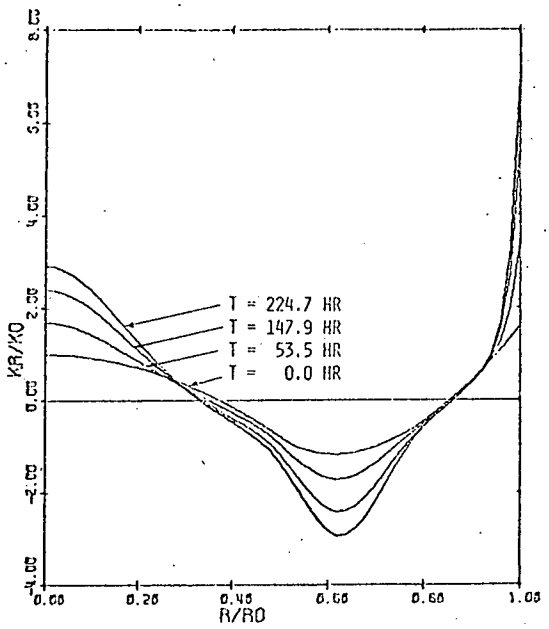

(a) CURVATURE PROFILE <KR>

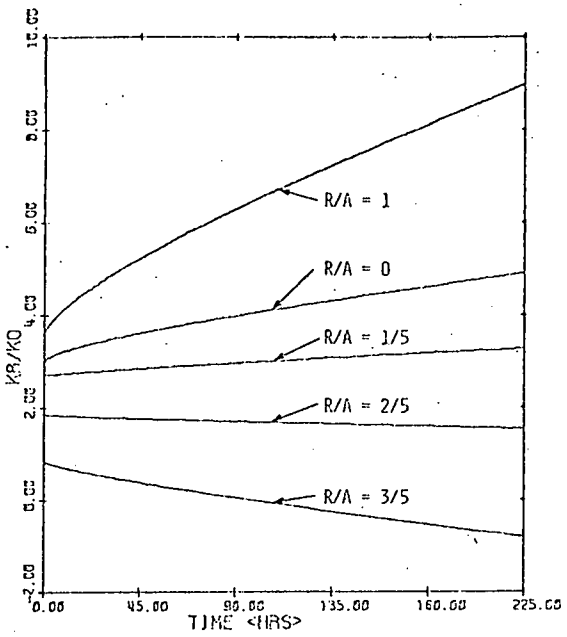

(b) CURVATURE <KR> VS TIME

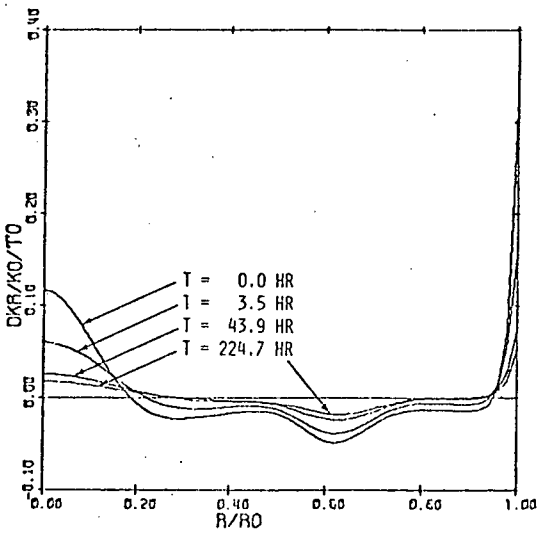

(c) CURVATURE RATE PROFILE <KR>

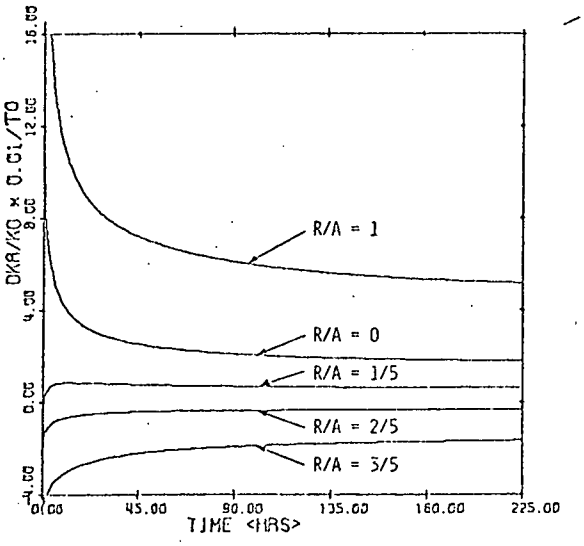

(d) KR RATE VS TIME

Figure 2. Radial Curvatures and Rates

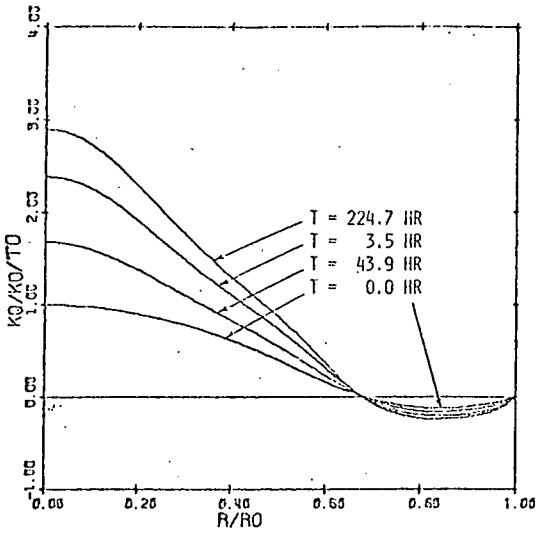

(a) CURVATURE PROFILE <KQ>

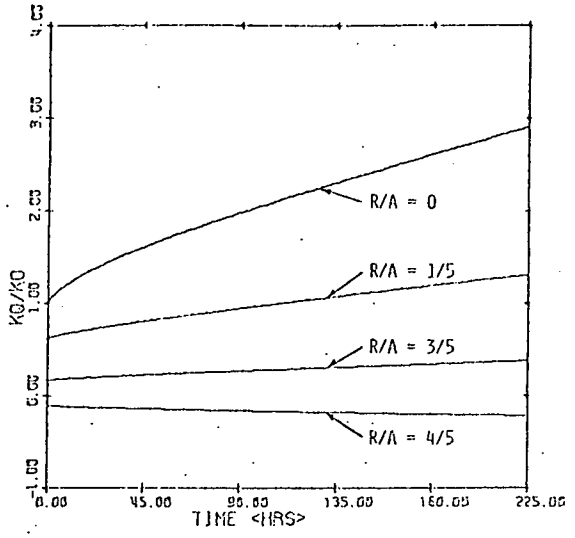

(b) CURVATURE <KQ> VS TIME

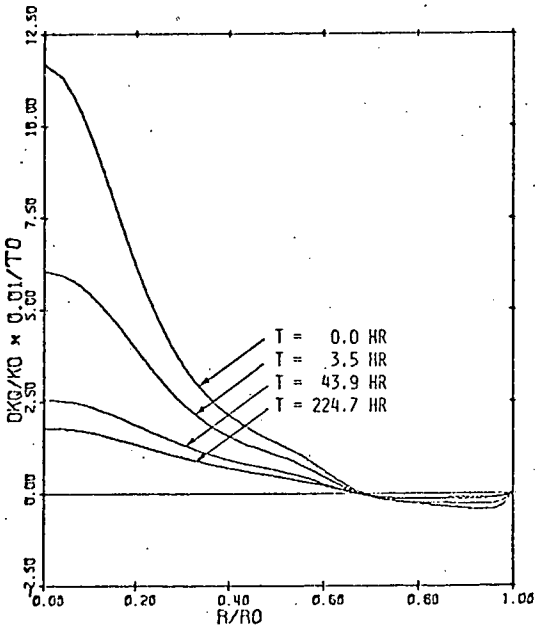

(c) CURVATURE RATE PROFILE <KQ>

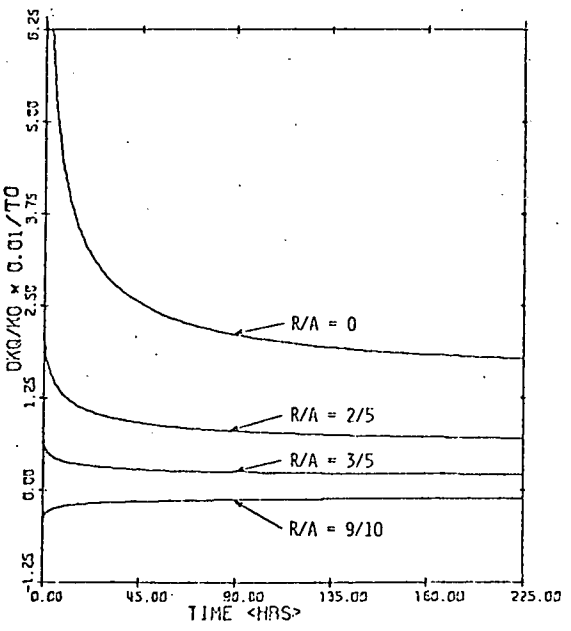

(d) KQ RATE VS TIME

Figure 3. Circumferential Curvatures and Rates

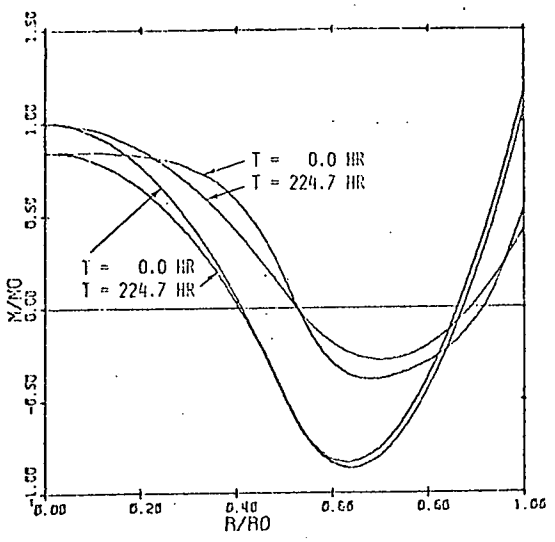

(a) MOMENT PROFILES

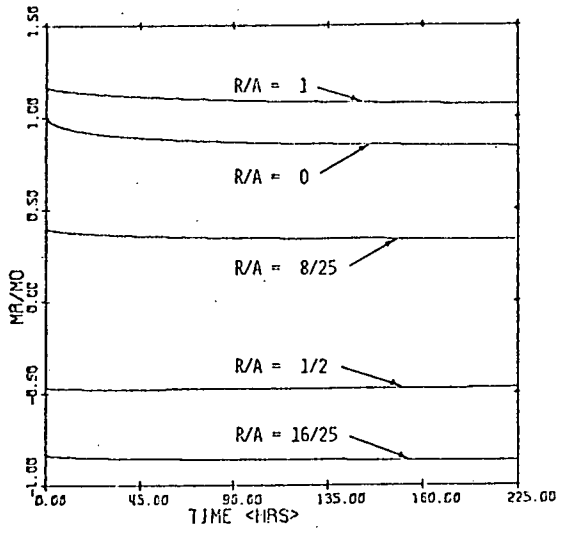

(b) MOMENT <MR> VS TIME

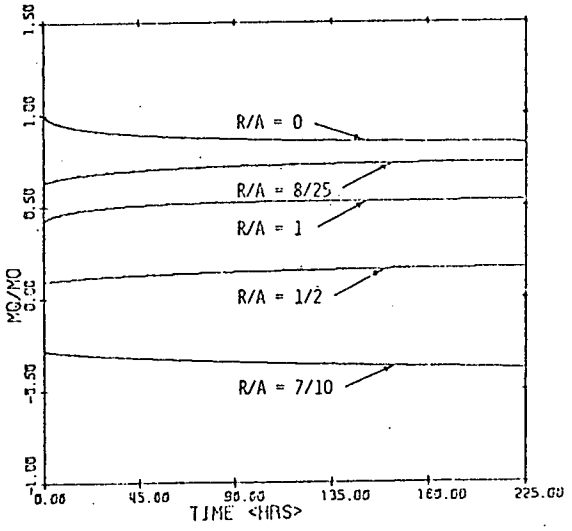

(c) MOMENT <MO> VS TIME

Figure 4. Moments

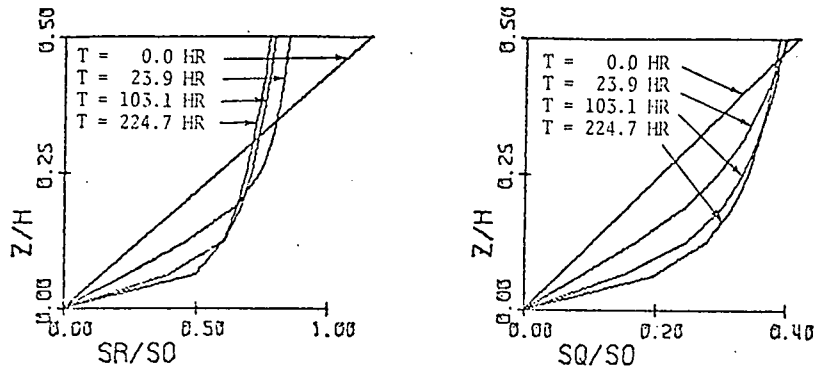

SR(Z,A)/SO PROFILE SQ(Z,A)/SO PROFILE

A1:250°C (WF)

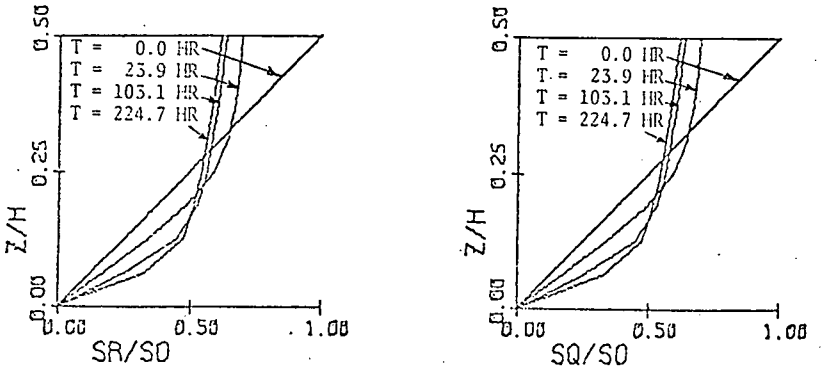

SR(Z,0)/SO PROFILE SQ(Z,0)/SO PROFILE

(a) STRESS PROFILES ACROSS THICKNESS

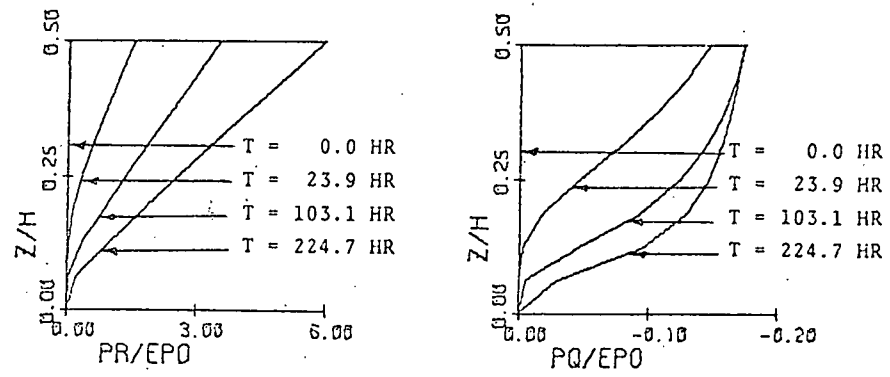

PR(A,Z)/EPO PROFILE PQ(A,Z)/EPO PROFILE

A1: 250°C (WF)

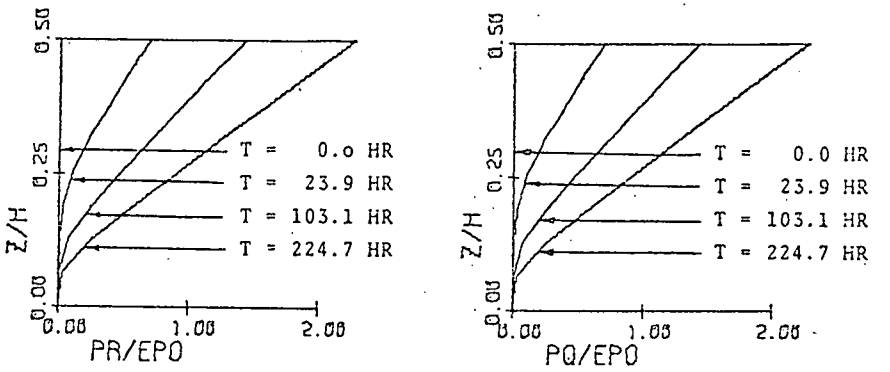

PR(0,Z)/EPO PROFILE PQ(0,Z)/EPO PROFILE

(b) STRAIN PROFILES ACROSS THICKNESS

Figure 5. Stress and Plastic Strain Profiles Across Thickness

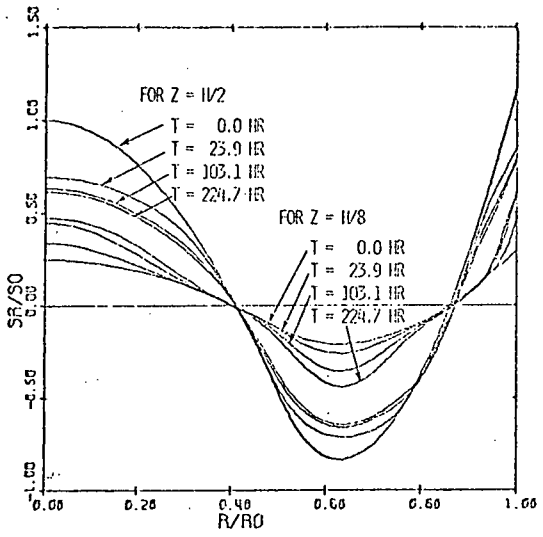

(a) STRESS <RR> PROFILE

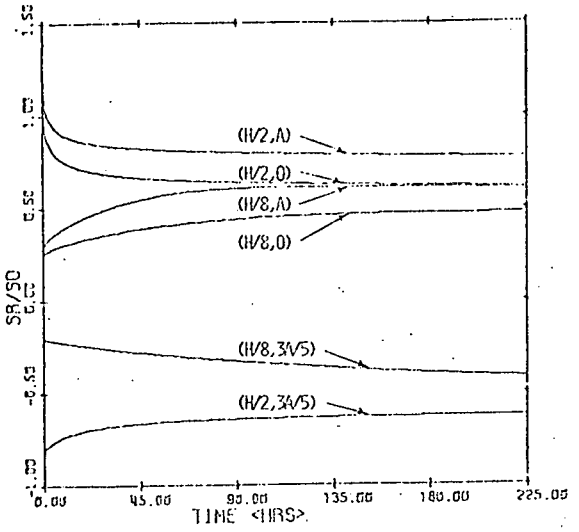

(b) STRESS <SR/SO> VS TIME

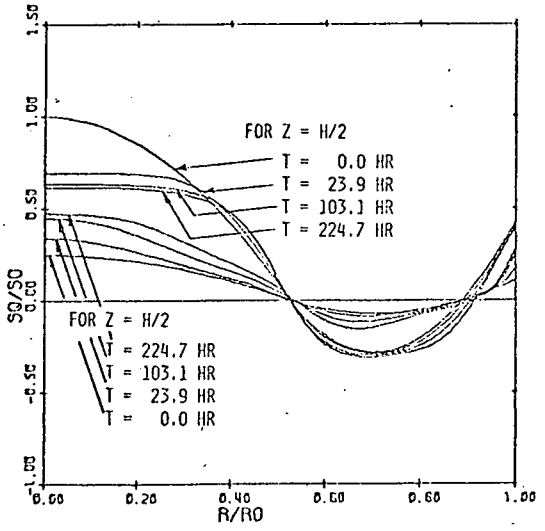

(c) STRESS <QQ> PROFILE

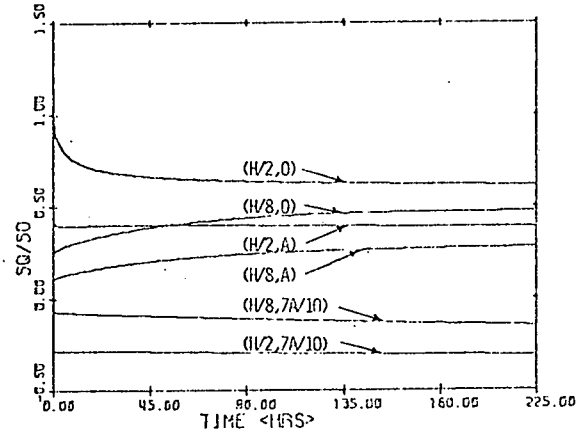

(d)STRESS <SQ/SO> VS TIME

Figure 6. Stresses

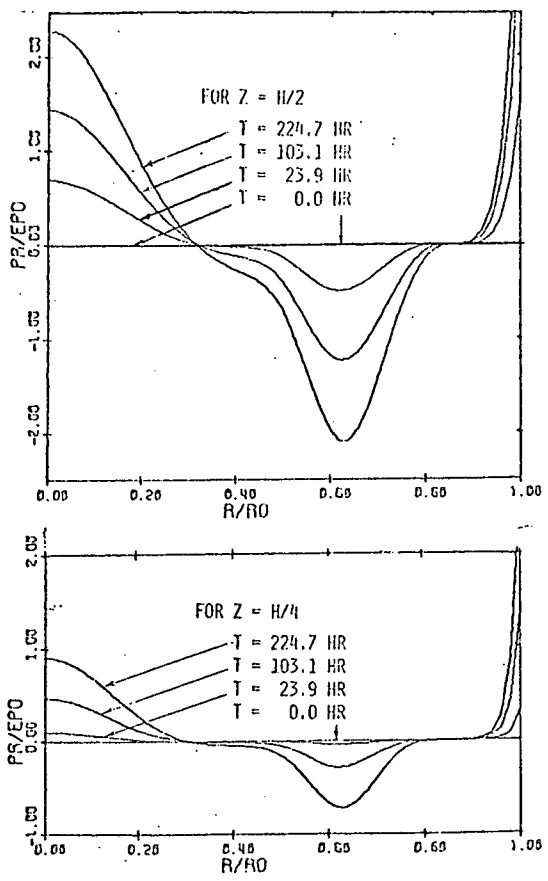

(a) PLASTIC STRAIN <PR> PROFILE

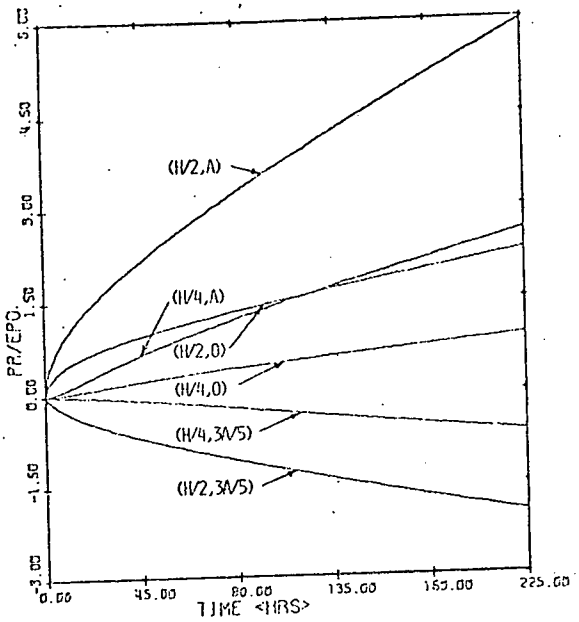

(b) STRAIN <PR/EPO> VS TIME

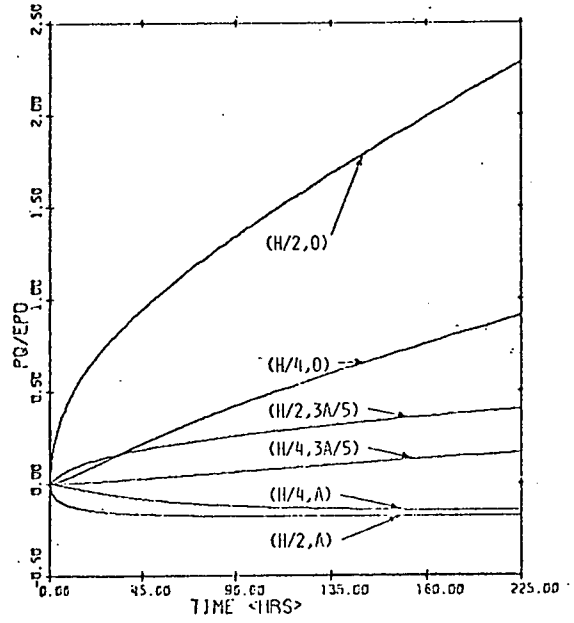

(d) STRAIN <PQ/EPO> VS TIME

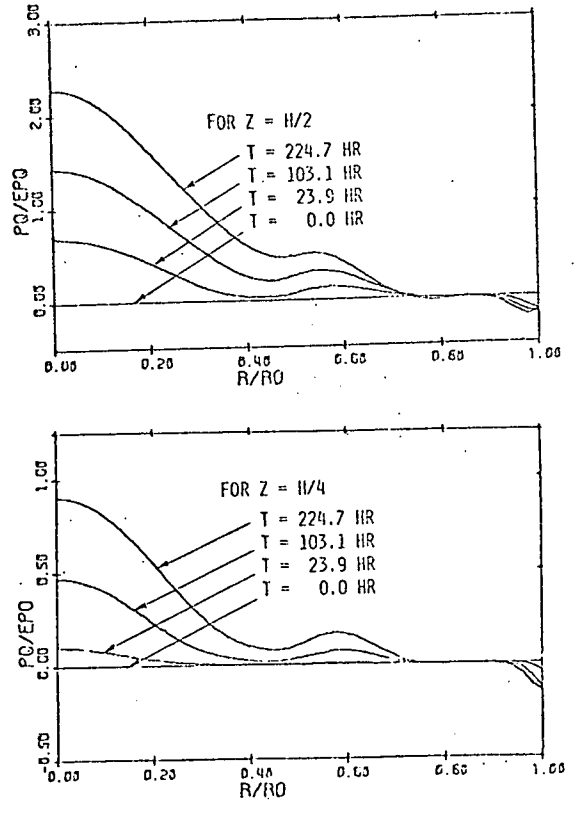

(c) PLASTIC STRAIN <PQ> PROFILE

Figure 7. Plastic Strains

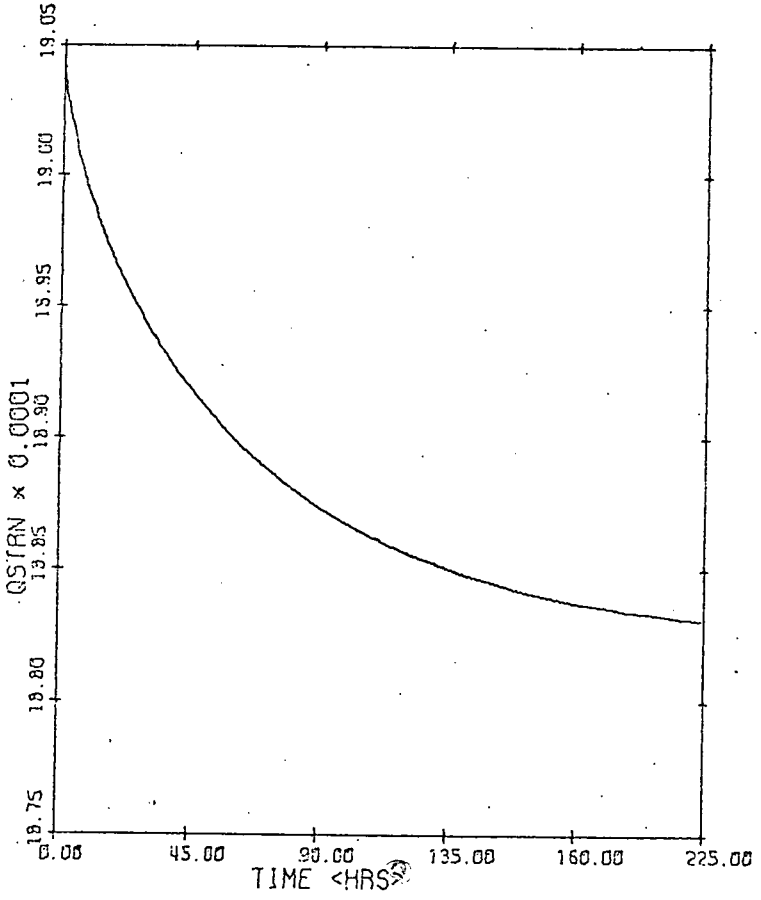

(a) FLUID PRESSURE VS TIME

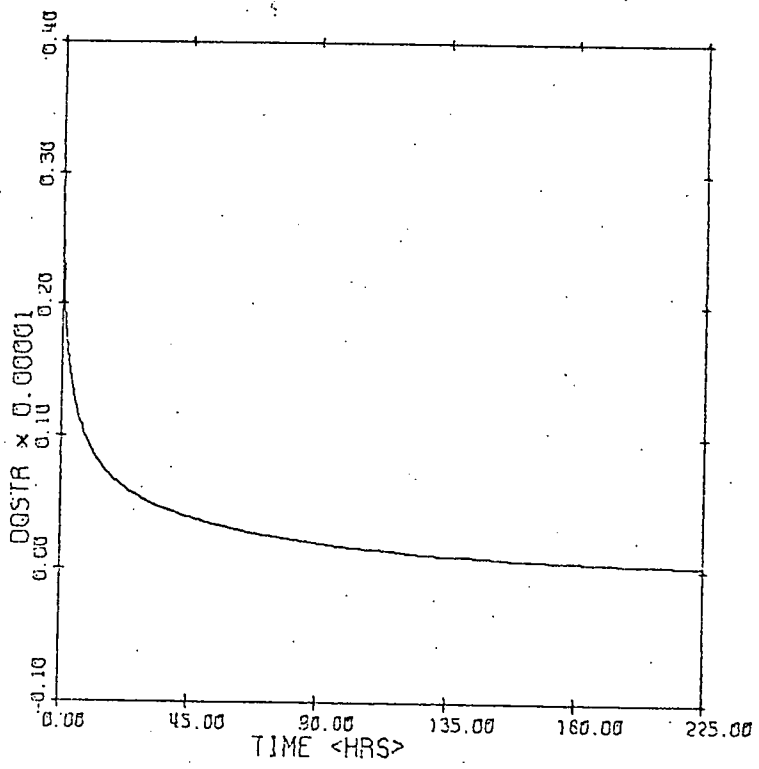

(b) PRESSURE RATE VS TIME

Figure 8. Fluid Pressure and Rate

APPENDIX IV

CLAMPED CIRCULAR

ALUMINUM PLATE

WITH FLUID

T = 22°C

INITIAL HARDNESS = 10,617 psi

(RMA)

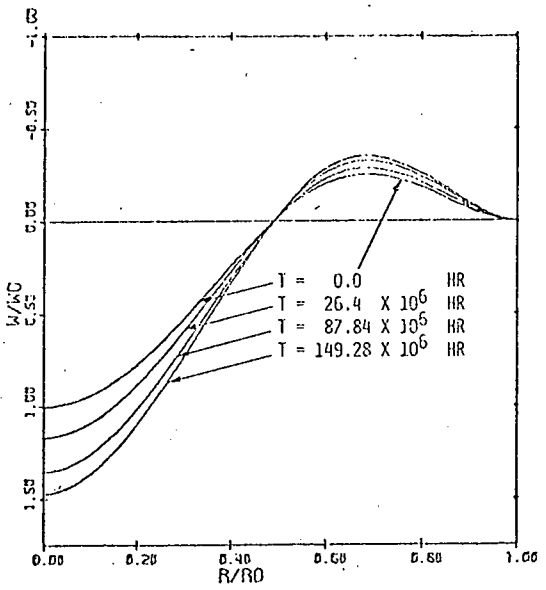

(a) DISPLACEMENT PROFILE

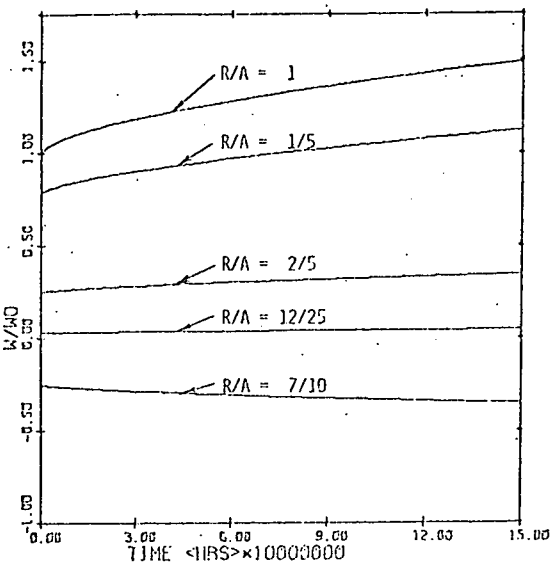

(b) DISPLACEMENT VS TIME

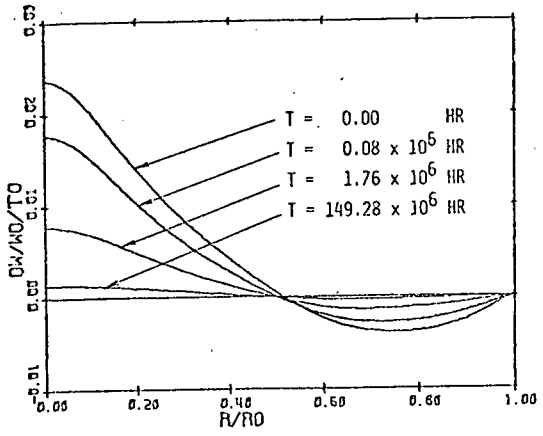

(c) DISPL RATE PROFILE

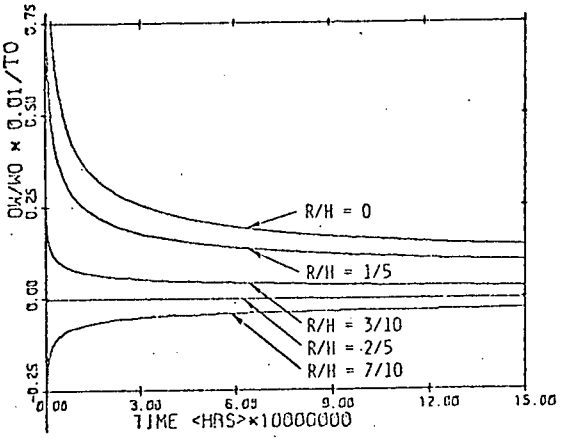

(d) DISP RATE VS TIME

Figure 1. Displacements and Displacement Rates

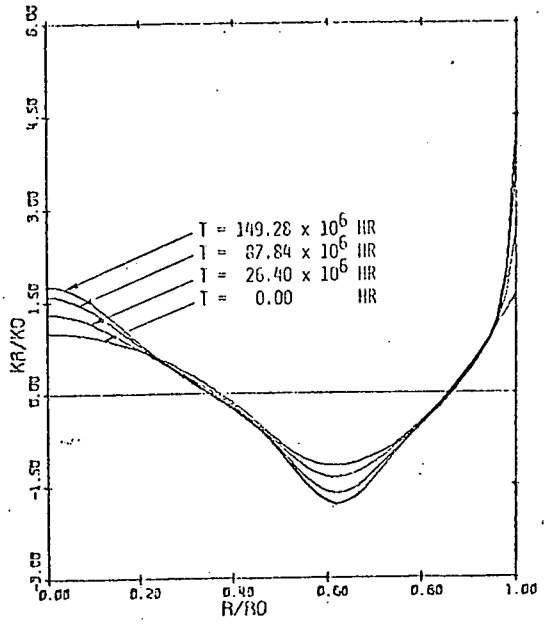

(a) CURVATURE PROFILE <KR>

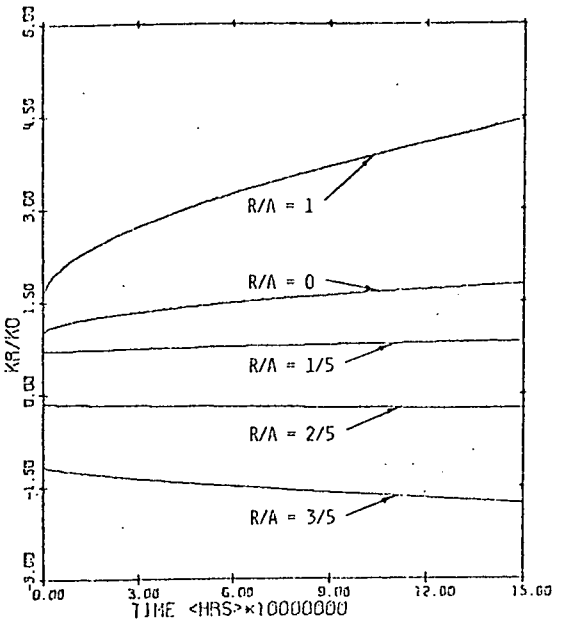

(b) CURVATURE <KR> VS TIME

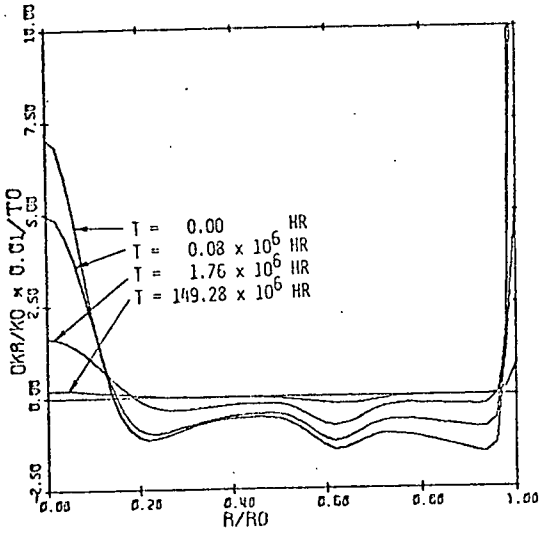

(c) CURVATURE RATE PROFILE <KR>

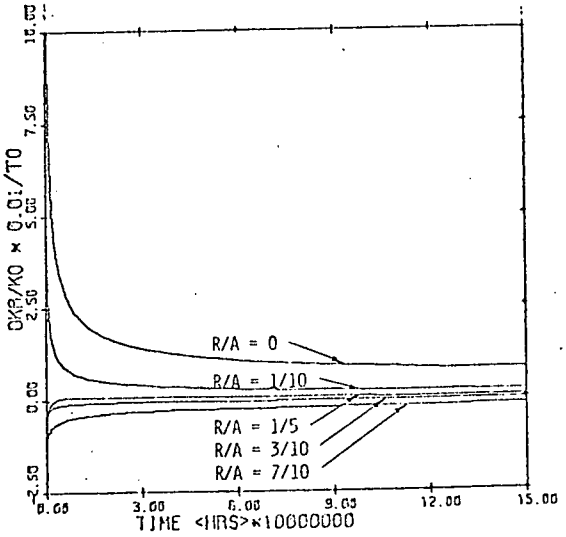

(d) KR RATE VS TIME

Figure 2. Radial Curvatures and Rates

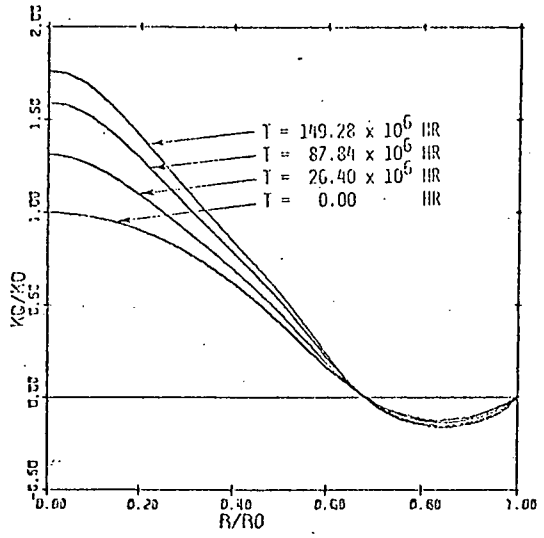

(a) CURVATURE PROFILE <KQ>

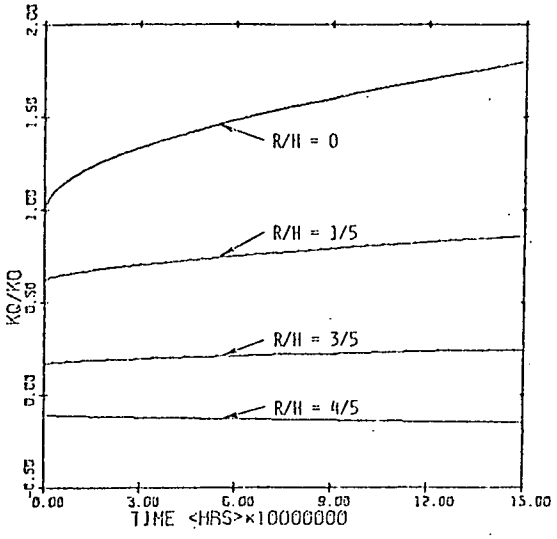

(b) CURVATURE <KQ> VS TIME

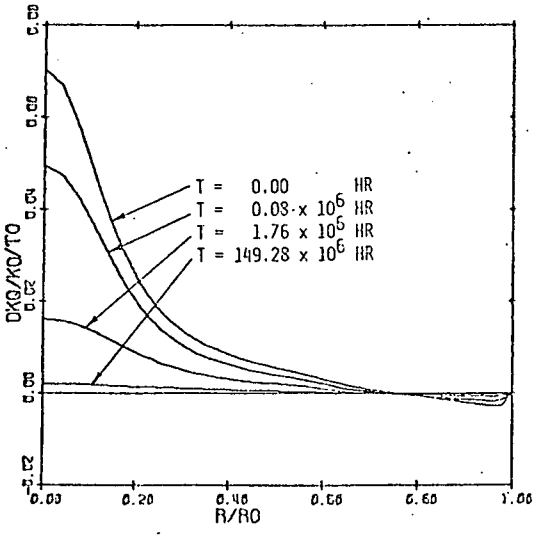

(c) CURVATURE RATE PROFILE <KQ>

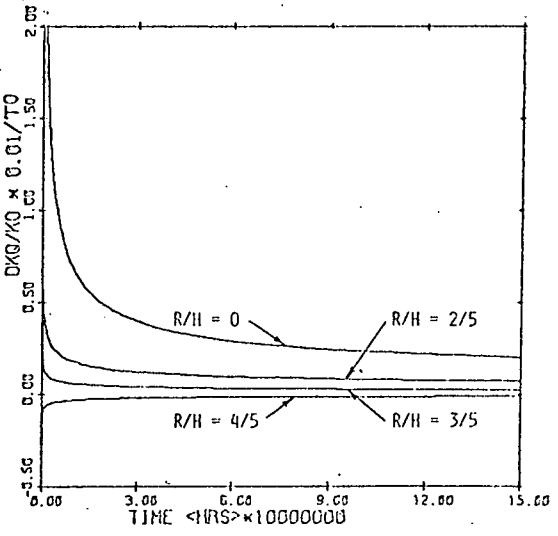

(d) KQ RATE VS TIME

Figure 3. Circumferential Curvatures and Rates

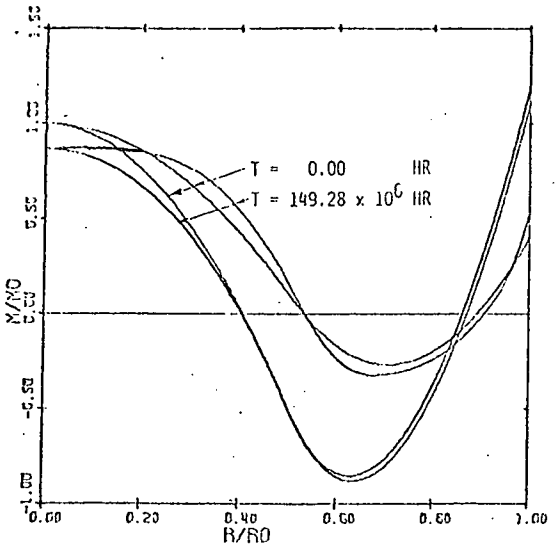

(a) MOMENT PROFILES

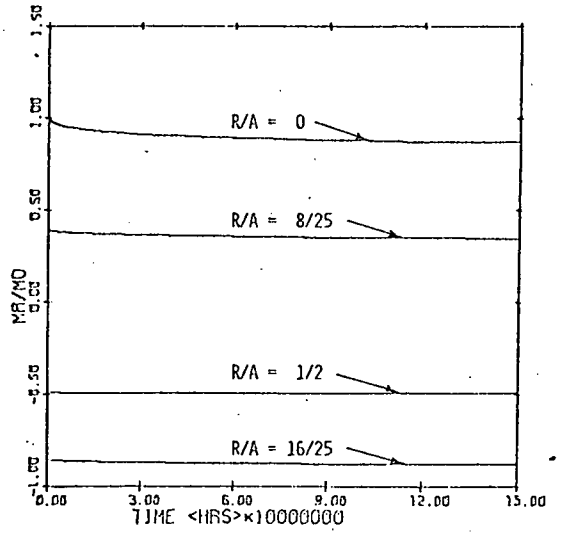

(b) MOMENT <MR> VS TIME

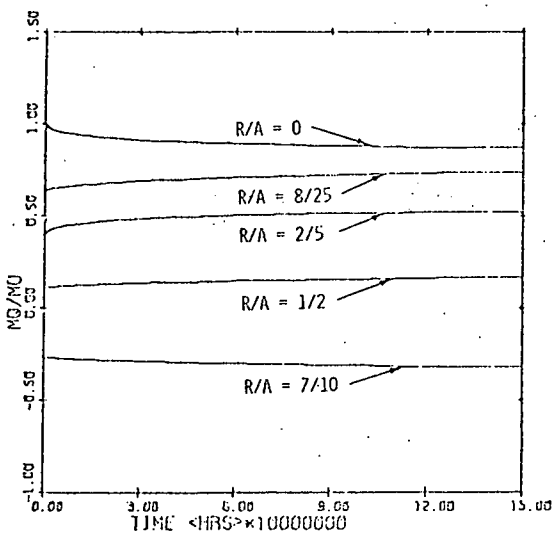

(c) MOMENT <MQ> VS TIME

Figure 4. Moments

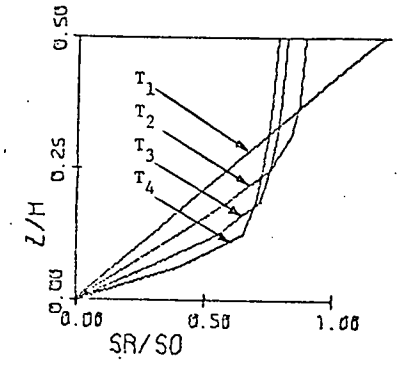

SR(Z,A)/SO PROFILE

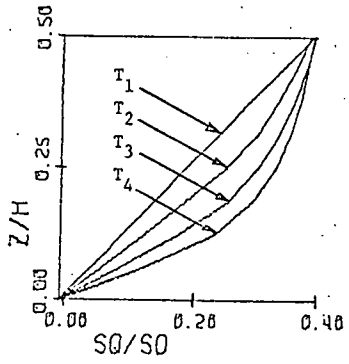

SQ(Z,A)/SO PROFILE

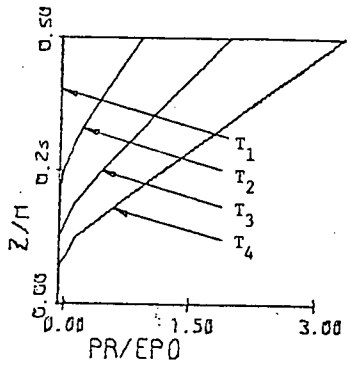

PR(Z,A)/EPO PROFILE

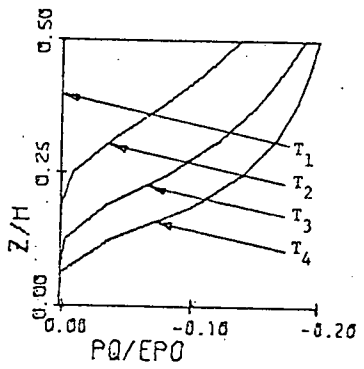

PQ(Z,A)/EPO PROFILE

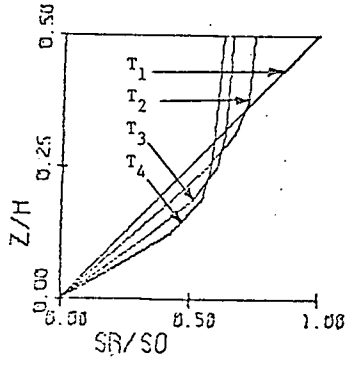

SR(Z,0)/SO PROFILE

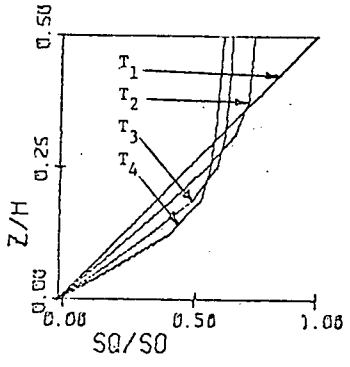

SQ(Z,0)/SO PROFILE

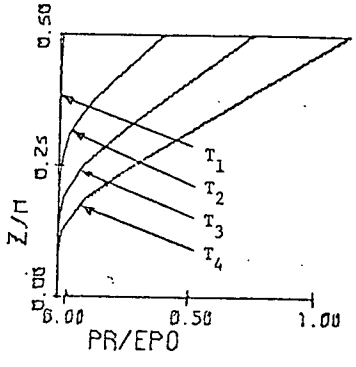

PR(Z,0)/EPO PROFILE

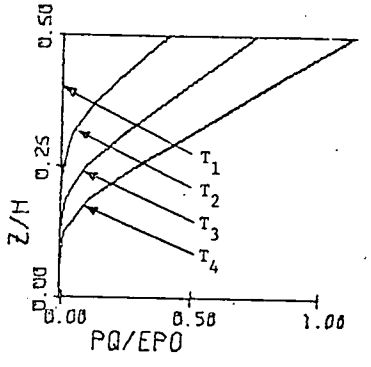

PQ(Z,0)/EPO PROFILE

(a) STRESS PROFILES ACROSS THICKNESS

T_1 = 0.0 HR, T_2 = 7.84 x10^6 HR, T_3 = 46.88 x 10^6 HR, T_4 = 149.28 x 10^6 HR.

(b) STRAIN PROFILES ACROSS THICKNESS

T_1 = 0.0 HR, T_2 = 7.84 x 10^6 HR, T_3 = 7.84 x10^6 HR, T_4 = 149.28 x 10^6 HR.

Figure 5. Stress and Plastic Strain Profiles Across Thickness

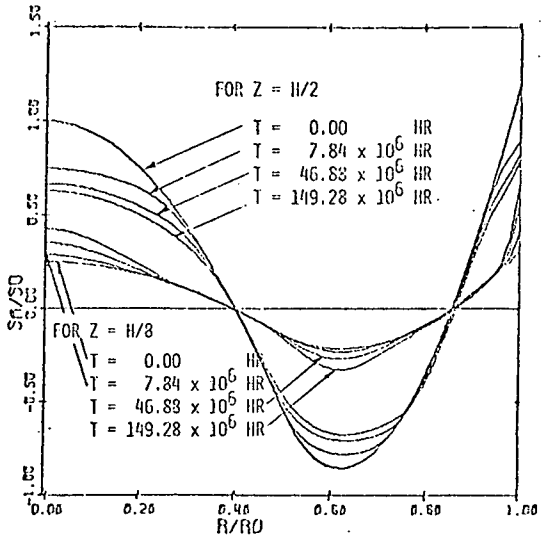

(a) STRESS <RR> PROFILE

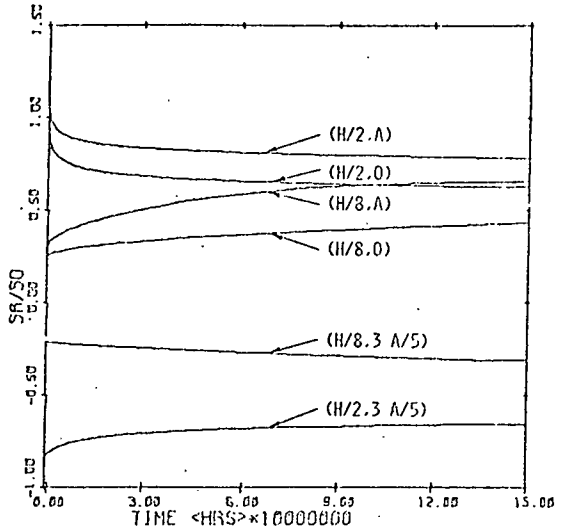

(b) STRESS <SR/SO> VS TIME

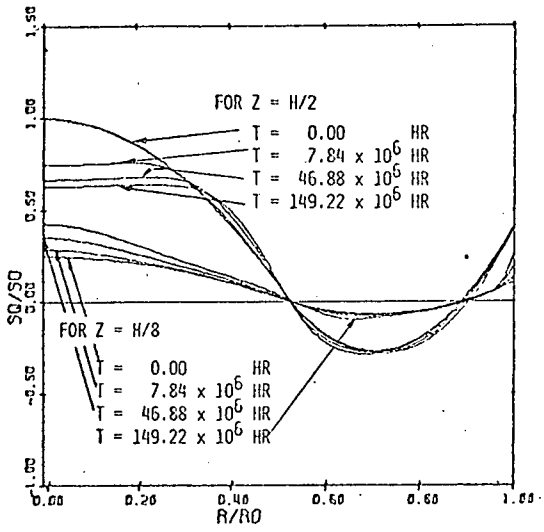

(c) STRESS <QQ> PROFILE

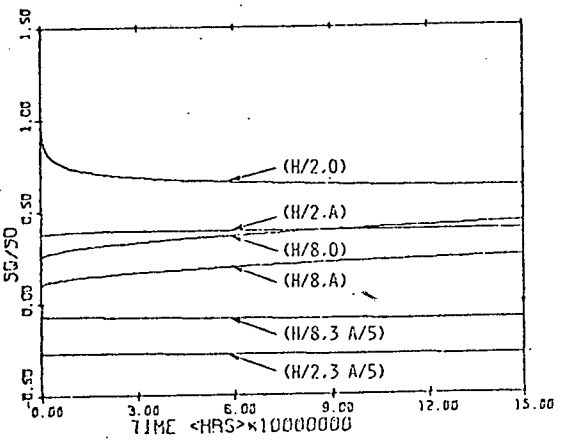

(d) STRESS <SQ/SO> VS TIME

Figure 6. Stresses

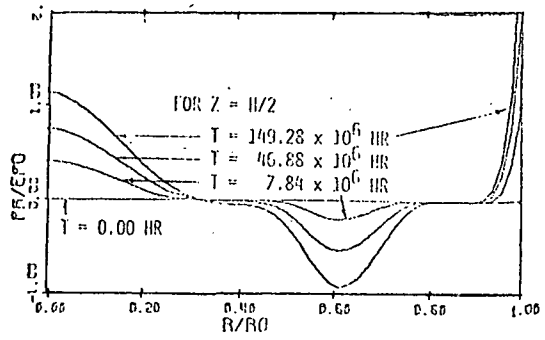

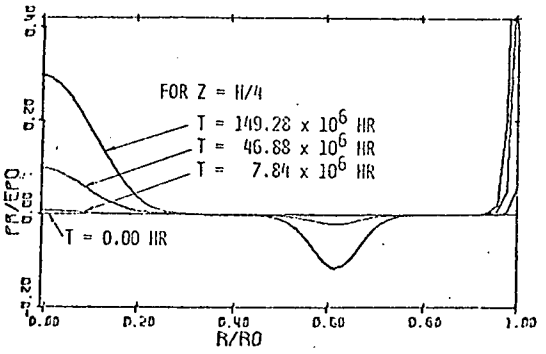

(a) PLASTIC STRAIN <PR> PROFILE

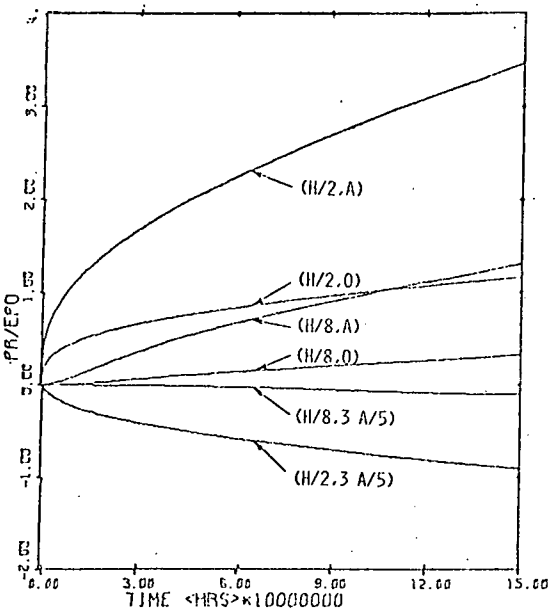

(b) STRAIN <PR/EPO> VS TIME

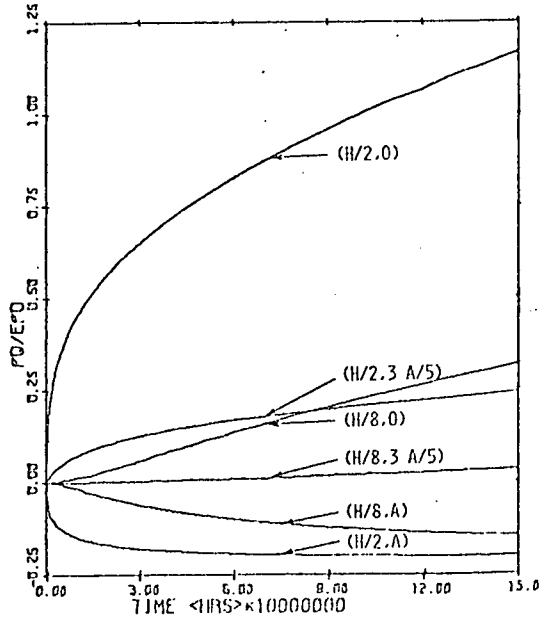

(d) STRAIN <PO/EPO> VS TIME

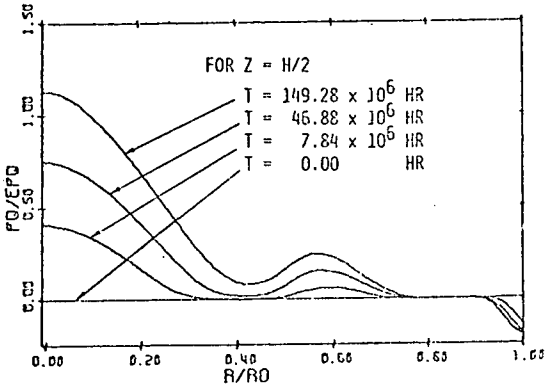

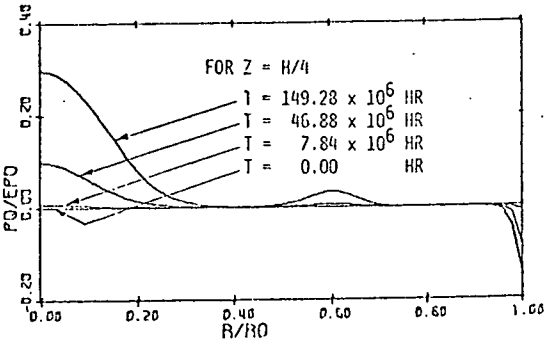

(c) PLASTIC STRAIN <PO> PROFILE

Figure 7. Plastic Strains

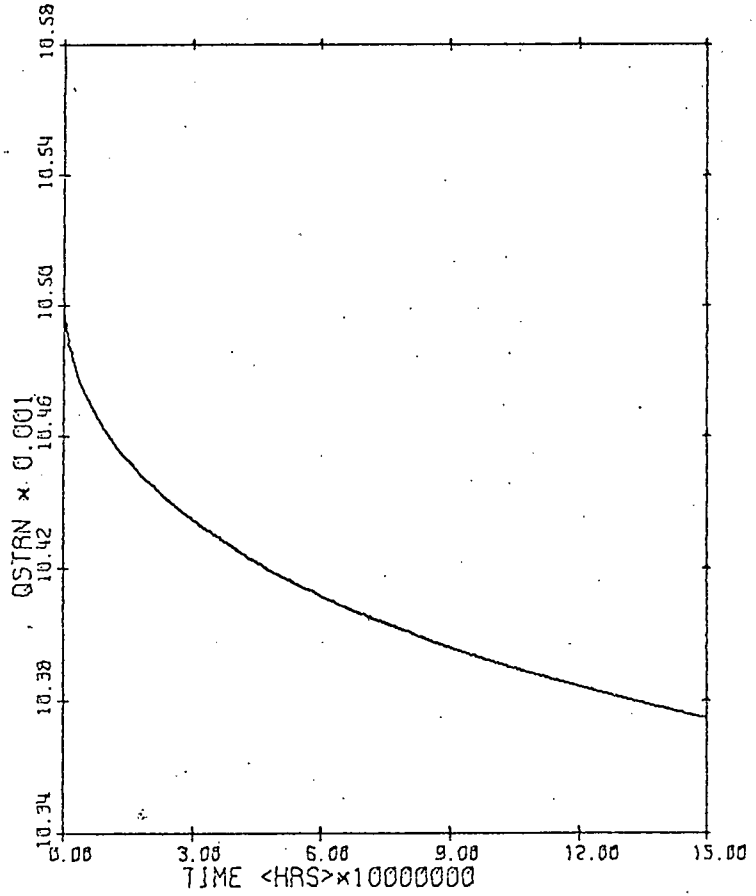

(a) FLUID PRESSURE VS TIME

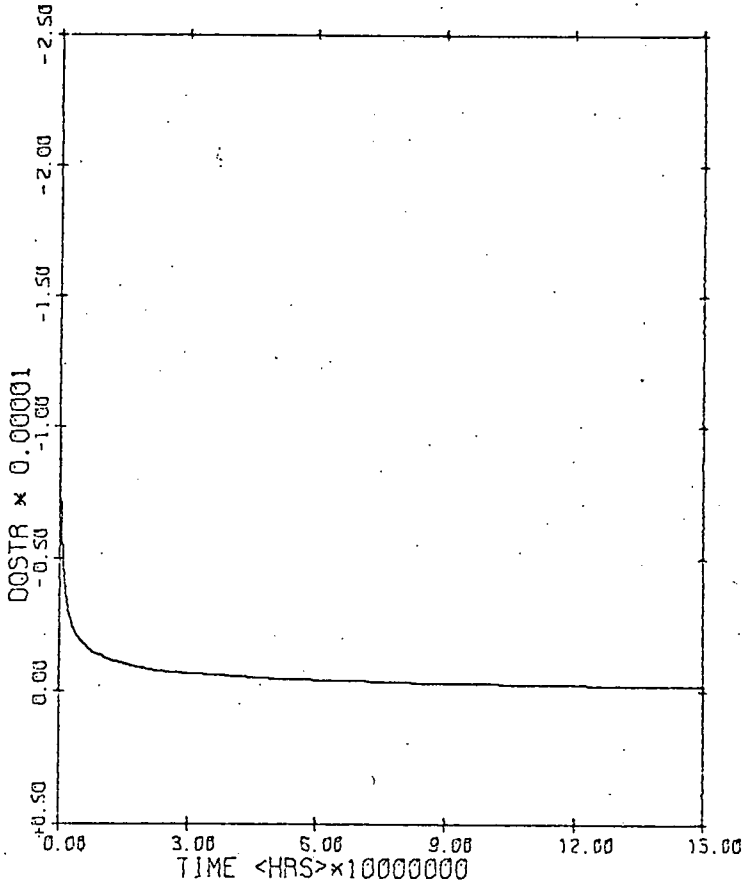

(b) PRESSURE RATE VS TIME

Figure 8. Fluid Pressure and Rate

APPENDIX V

CLAMPED CIRCULAR

ALUMINUM PLATE

WITHOUT FLUID

T = 22°C

INITIAL HARDNESS = 10,617 psi

(RMB)

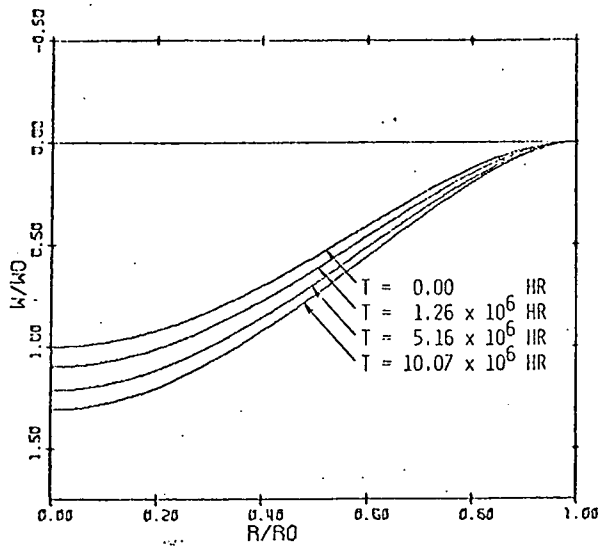

(a) DISPLACEMENT PROFILE

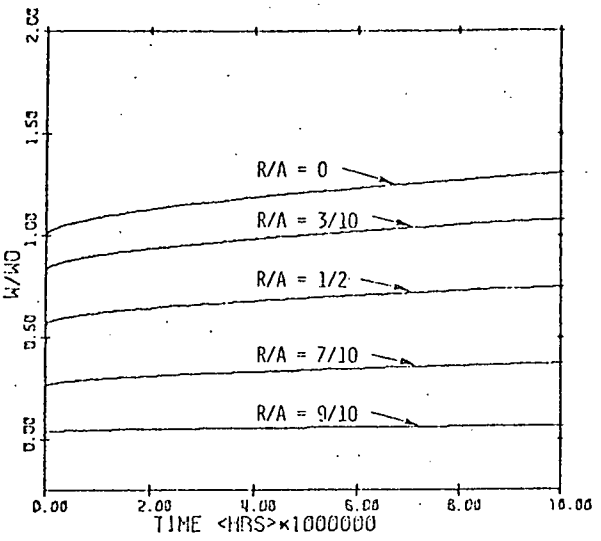

(b) DISPLACEMENT VS TIME

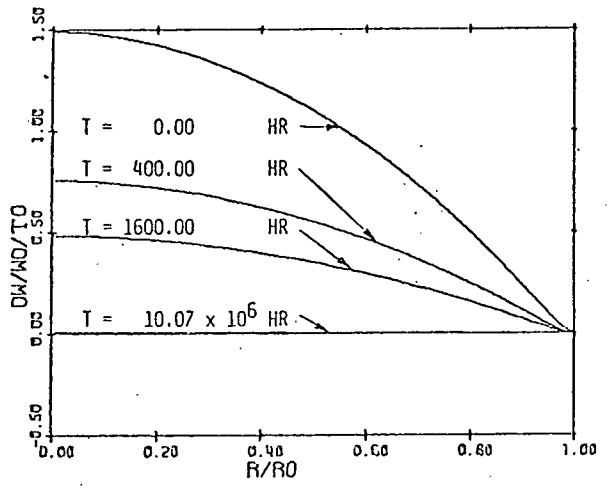

(c) DISPL RATE PROFILE

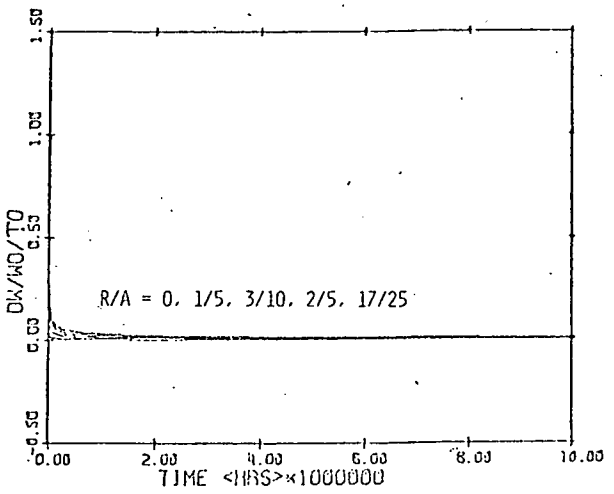

(d) DISP RATE VS TIME

Figure 1. Displacements and Displacement Rates

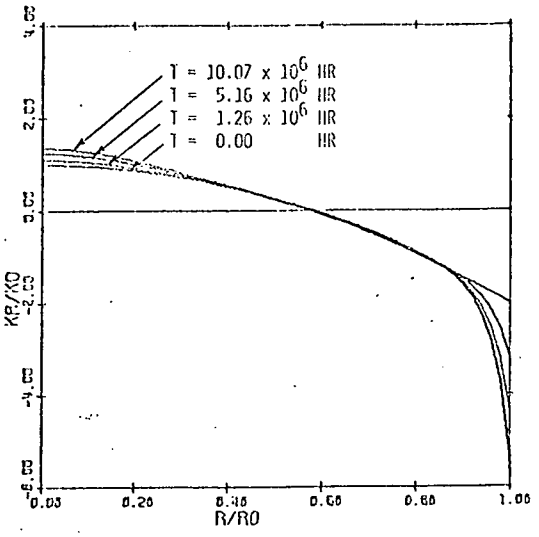

(a) CURVATURE PROFILE <KR>

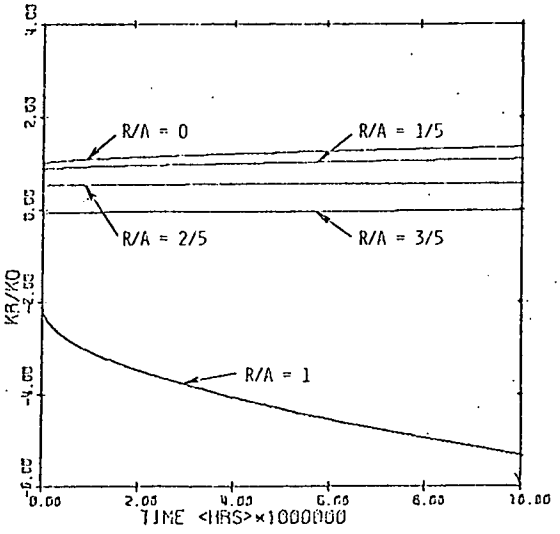

(b) CURVATURE <KR> VS TIME

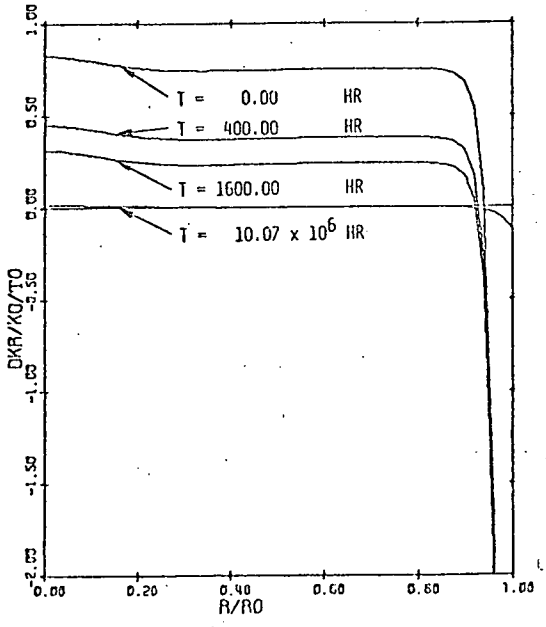

(c) CURVATURE RATE PROFILE <KR>

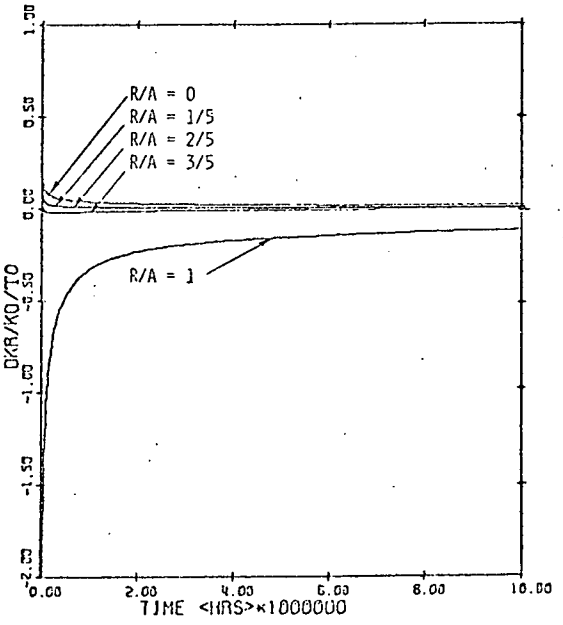

(d) KR RATE VS TIME

Figure 2. Radial Curvatures and Rates

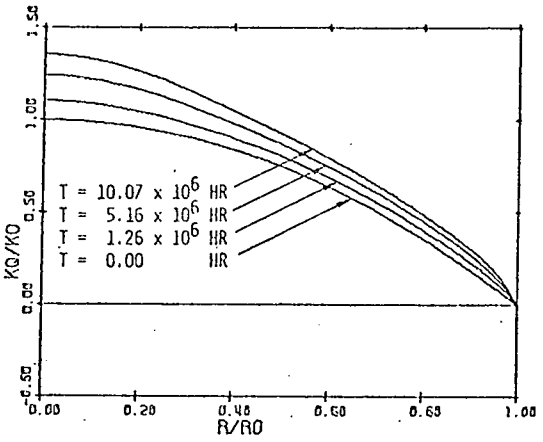

(a) CURVATURE PROFILE <KQ>

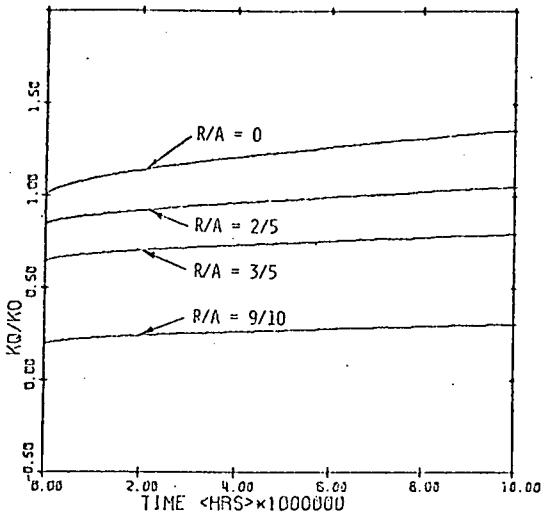

(b) CURVATURE <KQ> VS TIME

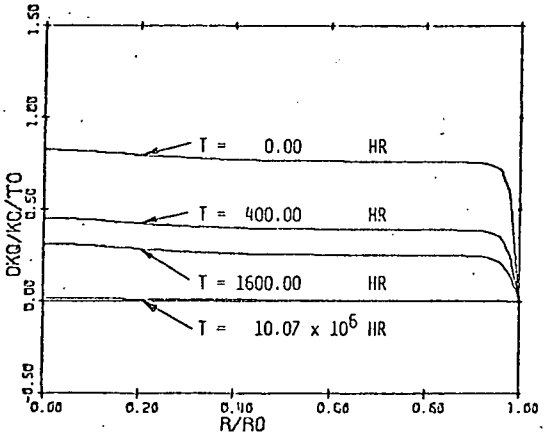

(c) CURVATURE RATE PROFILE <KQ>

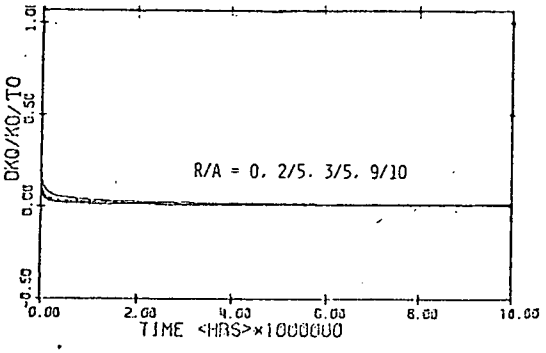

(d) KQ RATE VS TIME

Figure 3. Circumferential Curvatures and Rates

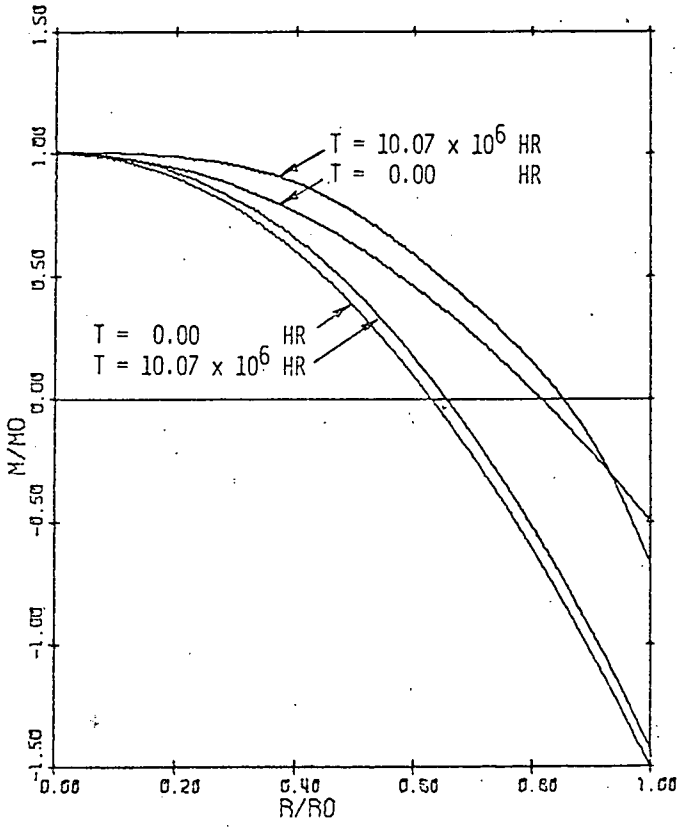

(a) MOMENT PROFILES

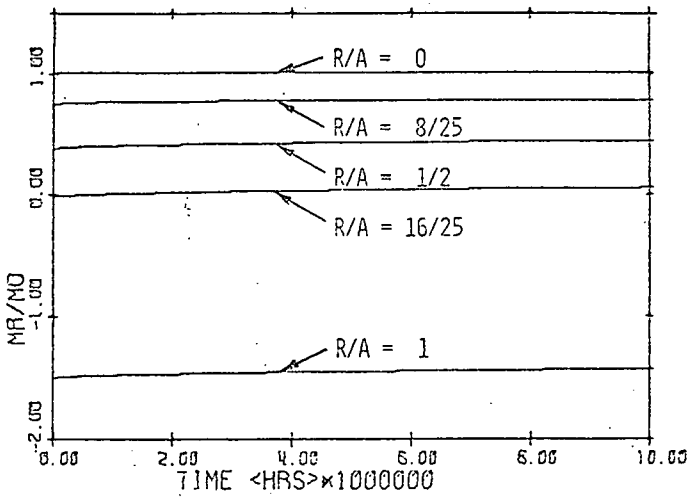

(b) <MR> VS TIME

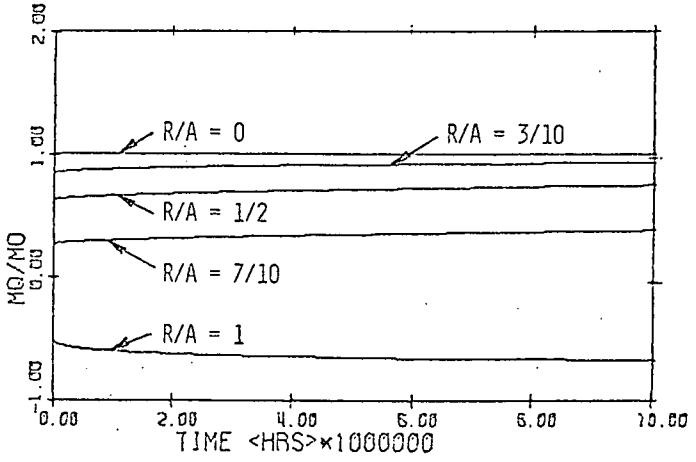

(c) <MQ> VS TIME

Figure 4. Moments

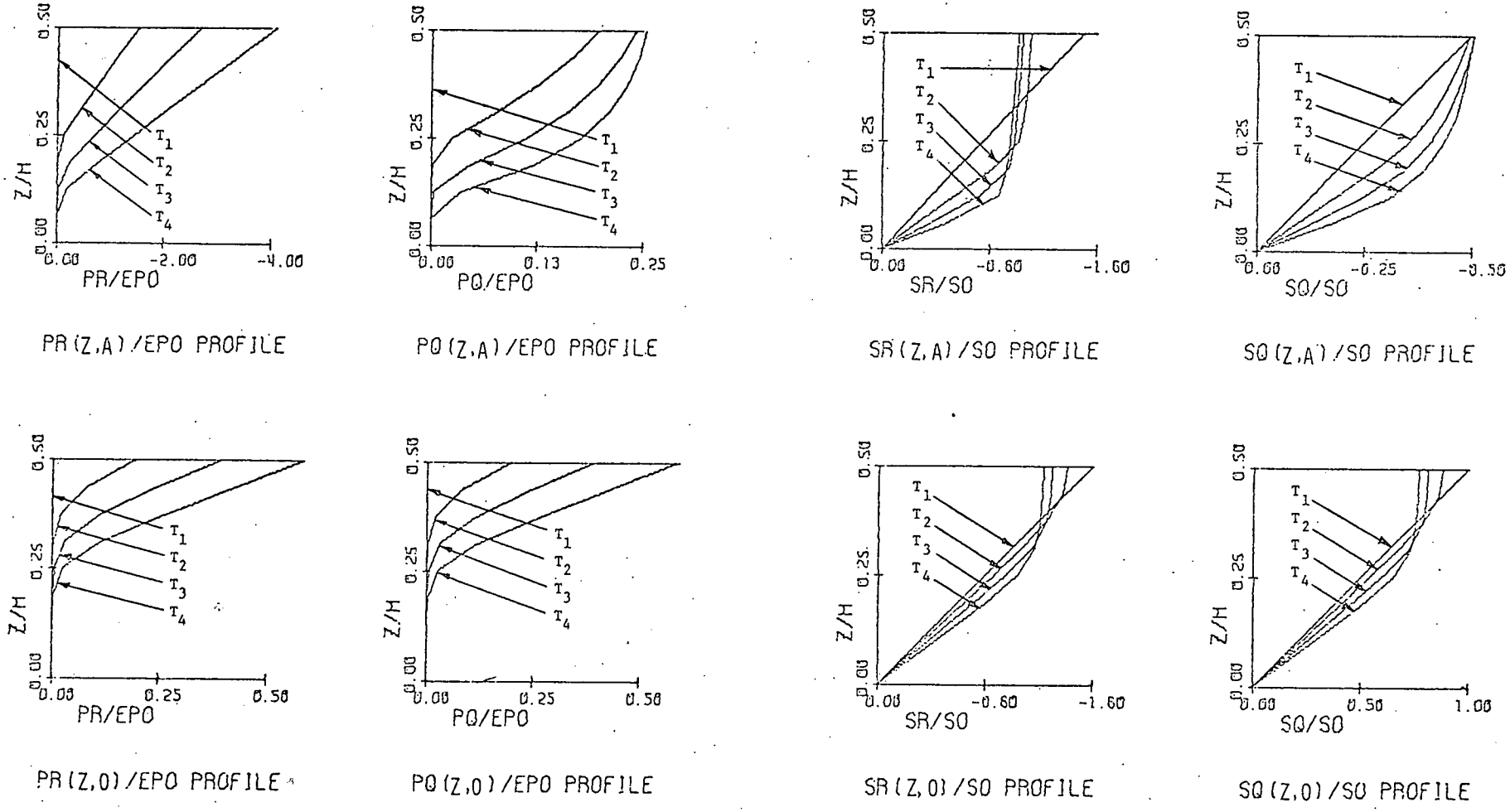

(a) STRAIN PROFILES ACROSS THICKNESS

T_1 = 0.0 HR, T_2 = 0.7788 x 10^6 HR, T_3 = 3.7228 x 10^6 HR, T_4 = 10.0176 x 10^6 HR.

(b) STRESS PROFILES ACROSS THICKNESS

T_1 = 0.0 HR, T_2 = 0.7788 x10^6 HR, T_3 = 3.7228 x 10^6 HR, T = 10.0716 x 10^6 HR.

Figure 5. Stress and Plastic Strain Profiles Across Thickness

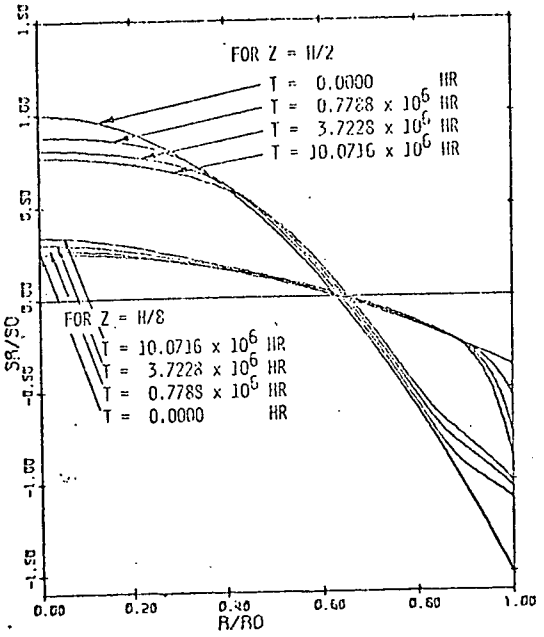

STRESS <RR> PROFILE

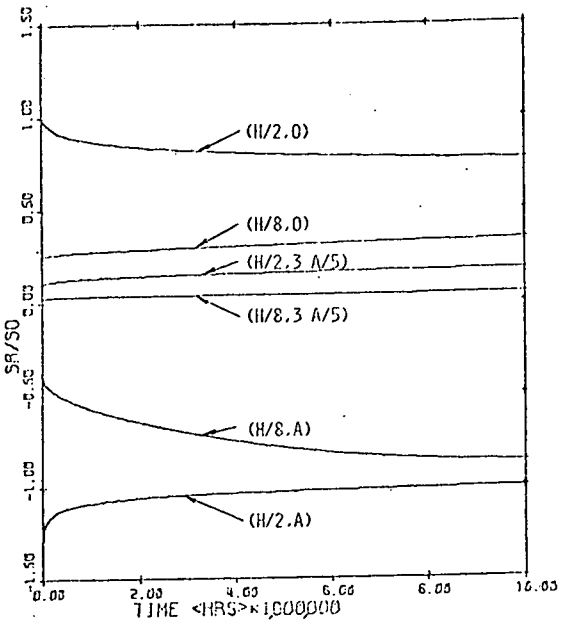

STRESS <SR/SO> VS TIME

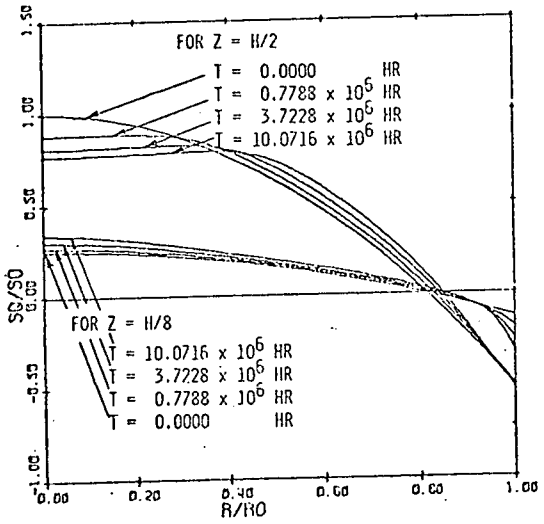

STRESS <QQ> PROFILE

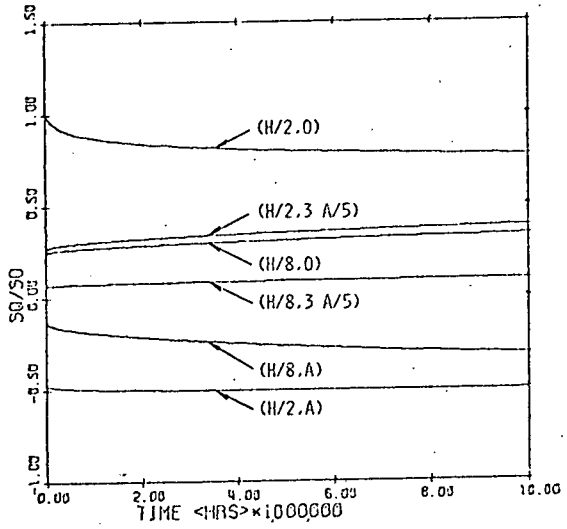

STRESS <SQ/SO> VS TIME

Figure 6. Stresses

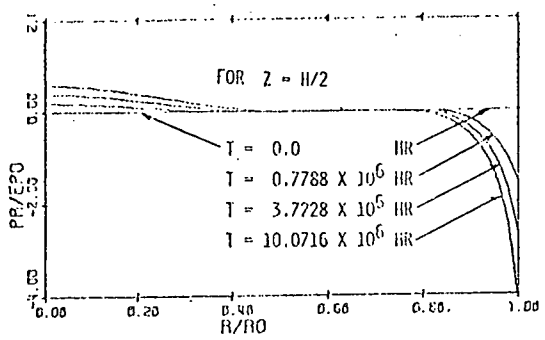

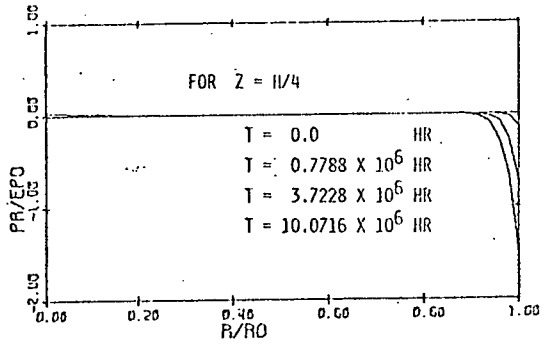

(a) PLASTIC STRAIN <PR> PROFILE

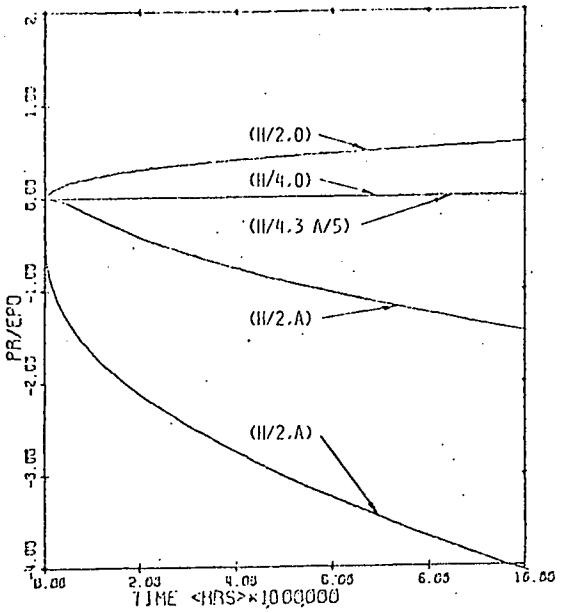

(b) STRAIN <PR/EPO> VS TIME

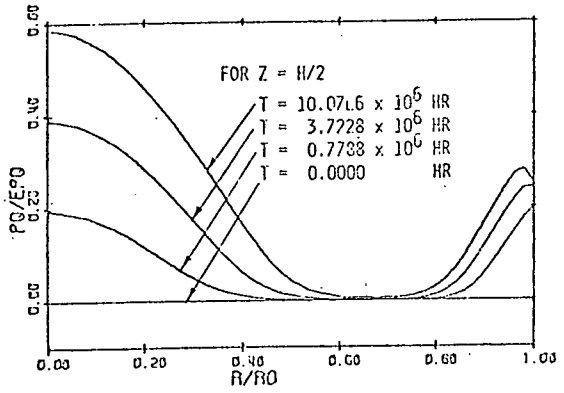

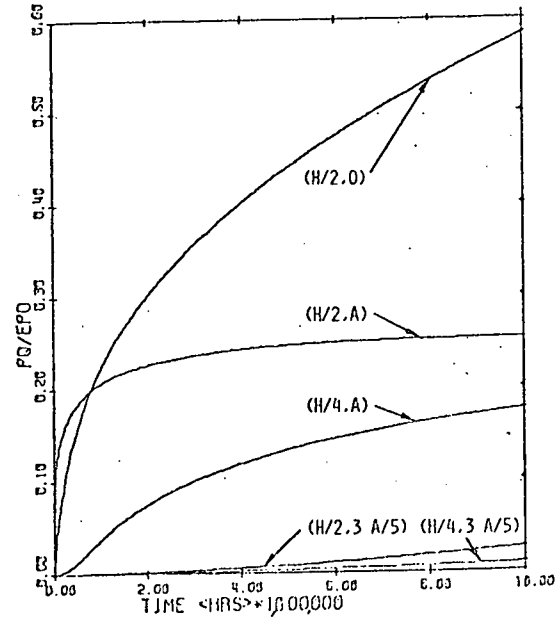

(d) STRAIN <PO/EPO> VS TIME

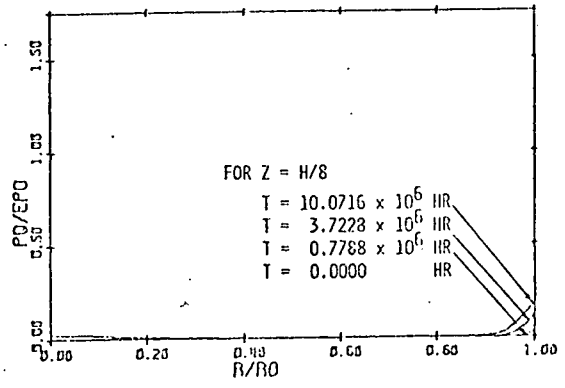

(c) PLASTIC STRAIN <PO> PROFILE

Figure 7. Plastic Strains